Addis Ababa University

Addis Ababa Institute of Technology

School of Mechanical and Industrial Engineering

Design, Development and Testing of Drop-weight Impact Test Machine

---

A thesis submitted for the partial fulfillment of MSc Degree in Mechanical Engineering, Mechanical Design specialization, in the School of Mechanical and Industrial Engineering, Addis Ababa Institute of Technology, Addis Ababa University, Ethiopia.

By

Dagmawe Tadesse

Advisors: Dr. Daniel Tilahun and Mr. Araya Abera

August 11, 2021

Declaration

This thesis work is my original work and has not been presented for a degree for any other university, and that all sources of material are duly acknowledged.

Name: **Dagmawe Tadesse**

Thesis title: **DESIGN, DEVELOPMENT AND TESTING OF DROP-WEIGHT IMPACT TEST MACHINE.**

Department: _____

Signature: _____

Advisor:_____

Signature: _____

Acknowledgment

I would like to express my sincere appreciation to my advisors, Daniel Tilahun (PhD.) and Mr. Araya Abera for their support and guidance throughout this thesis and throughout my education at Addis Ababa Institute of Technology. My appreciation also goes to Debre Berhan University mechanical engineering workshop personnel Mr. Surafel and all other crews for their help during prototyping process. Last but by no means least, I would like to thank my family for their full support and encouragement from the beginning of the project.

Abstract

The aim of this project is to design a drop weight impact test machine and conduct test with the prototype. The testing of materials under dynamic conditions needs an efficient and reliable equipment to experimentally examine and quantify the dynamic behavior of materials under low velocity impact loads.

Drop weight impact test machine designed and modeled is vertical, double column, simple, compact, inexpensive and easily transported to desired location. The development process includes conceptual design phase, detailed design phase prototyping and testing the intended testing machine. Both drop weight and height can be varied independently. The measurement system includes piezoelectric accelerometer connected to the drop weight and Model 485B39 digital ICP signal conditioner.

ASTM D7136/7136M standard testing method followed. The machine has a striker of fixed shape and known mass which has interchangeable 16 mm diameter hemispherical tup, two friction less guide rod assembly to freely fall the impact assembly, 1.2 m wide-flanged drop tower which used as a main support structure, a support bracket which attach the guide rod assembly to the drop tower and specimen fixture where standard flat rectangular test specimen (150 mm$\times$100 mm) sits on. It has maximum drop height of 0.62 m, standard mass of 5.5 Kg with increment of 0.45 and 0.5 Kg, and maximum impact energy and velocity of 33.5 J and 3.49 m/s respectively.

Contents

List of Figures

List of Tables

Chapter 1

Introduction

1.1 Overview of the project

Conventional metal alloys do not meet all the needs of the designer. There is the potential for aircraft and vehicle structures subjected to low-speed, high mass impact damage by dropped tools during assembly and maintenance operations, allowing the designers to use light weight, high strength materials such as polymer matrix composites reinforced with fiber of particles due to their excellent weight/strength, low specific density, high strength and modulus that increase efficiency and performance of vehicles [11].

It's important to know the amount of energy absorbed by the material until it fails, under different dynamic loading conditions. Thus, testing of materials becomes necessary. Test data show that the compression strength of composite materials can be significantly reduced by this kind of low-speed impact damage, even if the damage is not detectable by visual inspections [5, 12–14].

Impact testing which is the striking or collision between two objects, is an important measure of a material's failure properties. Properly testing both raw materials and molded components for their strength and durability can help engineers prevent failures, design lasting goods, and save lives [14]. One of the type of impact test is

drop weight, which is covered in this work.

Drop weight impact test is a type of testing where impactor assembly drops on to a specimen from a certain predetermined height [2, 12, 15–18]. The drop mass and impact velocity governs the impact energy in drop weight test. In this work, design of low velocity drop weight impact test machine for fibre reinforced composite laminates designed and a prototype developed.

The development process includes conceptual design phase, detailed design phase and finally prototyping the intended testing machine. Both drop weight and height (0.62 m) can be varied independently. The tester intended to be one-time expenditure to see damage on the composite specimen, the device is flexible enough to meet the anticipated future as well as current testing needs.

Drop weight impact test machine designed and modeled is vertical, double column, simple, compact, inexpensive and easily transported to desired location (total mass of 23.8 kg). It have the ability to employ standard masses of 5.5 kg, accommodate selected composite material of 150 $mm \times 100$ mm size according to ASTM D7136/7136M testing method.

1.2 Problem Statement

Composite materials in service and transportation, are open to low velocity impacts (i.e drop-weight impact), which corresponds to those usually introduced in the experimental procedures by mechanical test machines such as the drop-weight impact test technique, a=unlike to drop-weight impact test, static test is not representative of low velocity impact of fibre reinforce composite material [19, 20]. In low velocity impact, the contact period is such that the whole structure has time to respond to the loading, therefore dynamic structural response is important. The modes of impact damage induced ranges from matrix cracking and delamination through to

fibre failure and penetration, requiring several damage assessment techniques. Damage mode interaction must also be understood when attempting to predict initiation and growth of a particular form of damage [19, 21].

The low velocity impact response of random fibre/unidirectional composite laminate and impacts on complex geometry are less well studied in Ethiopia and haven't found any design and testing of such apparatus. Due to lack of the drop-weight impact test machine in the school of mechanical and industrial engineering in Addis Ababa University to conduct experimental analysis on fibre reinforce composite materials according to the ASTM-D7136 testing method, the following paper on the design, development and testing of drop weight impact test machine was necessary to see the damage phenomenon of such materials.

1.3 Research Scope and Objectives

General objectives

The main objective is design of low velocity drop weight impact test machine and conduct test with the prototype.

Specific Objectives

The project have the following specific objectives;

- Select test specimen which fulfill $ASTM\ D7136$ standard testing method
- Determine impact parameter i.e. impact velocity, drop height, impact energy and drop mass
- Determine suitable specimen fixture system
- Select and design different configurations of drop tower available
- Prototyping the intended machine on the institution workshop.
- Conduct test, generate results and discuss on those results.

Methodology

The objectives will be achieved by employing the following procedures. Generally, methods followed by the project illustrated in figure 1.1.

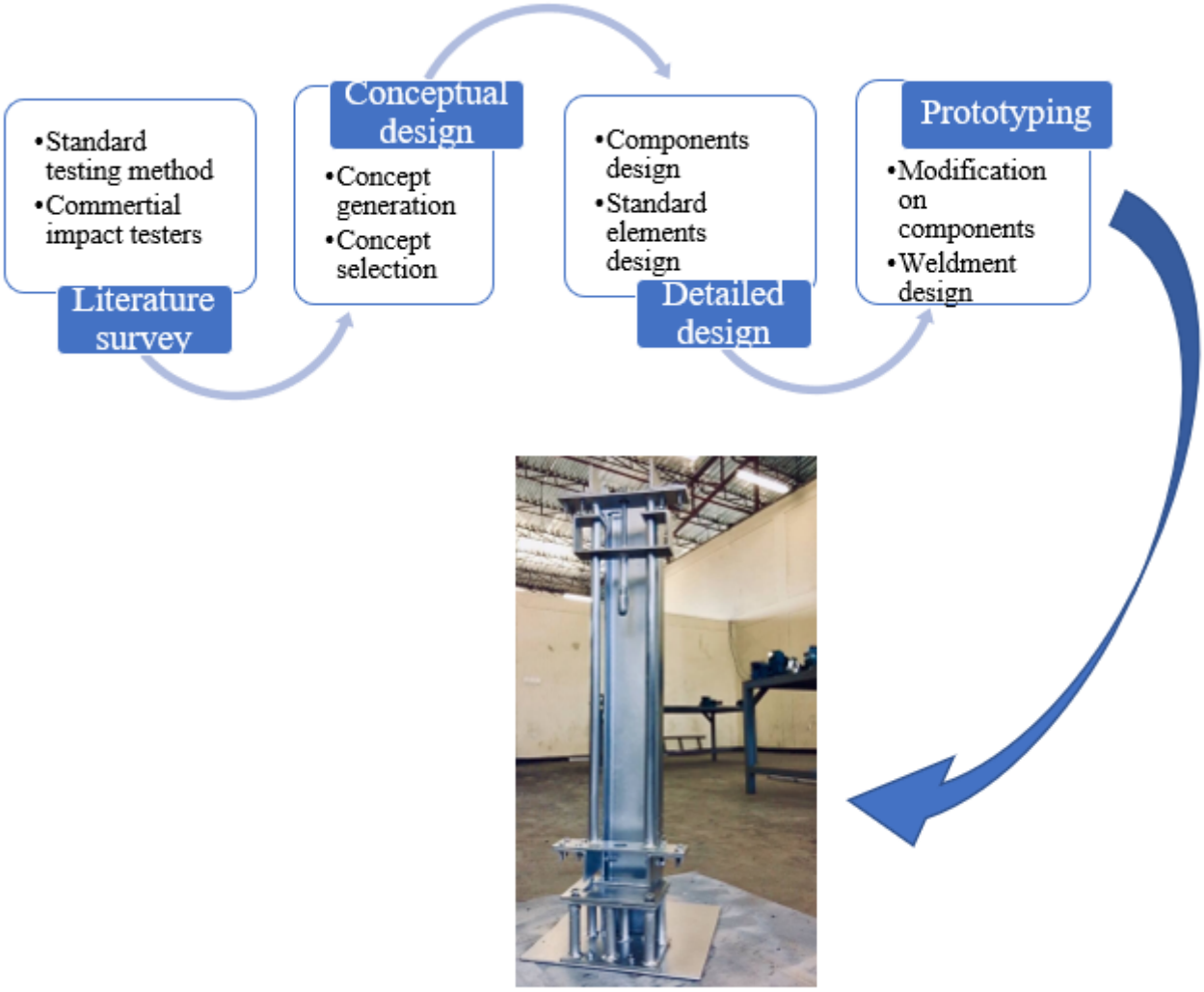

Figure 1.1: Schematic illustration of methods used in design and testing of drop weight impact machine

1.4 Outline of Thesis

The thesis divided in to the following chapters:

- **Chapter 2** presents the literature survey on composite materials, composite laminates under low velocity impact, impact test, dropped weight impact test

and on impact damages parameters.

- **Chapter 3** presents the preliminary design of drop weight impact apparatus, which is the conceptual design and detail design phases. The following points covered: Need assessment, market information gathered, customer requirements discussed, target specifications generated, finally concept generation and selection. The drop weight impactor consists of three major components: the impactor assembly, the drop tower and the specimen fixture. Each components further subdivided into sub-components and studied.

- **Chapter 4** presents the prototyping part of drop weight impact test machine. Modification made on components i.e drop tower, support bracket and foundation; and design for weldment summarized.

- **Chapter 5** presents the experimental investigation on the developed drop weight impact test machine. Impact instrumentation selected i.e. sensors, data acquisition method and analysis software (SpectralPLUS and Matlab).

- **Chapter 6** presents results and discussion of the experimental procedures conducted on selected composite material under drop weight impactor. Different plots results generated and studied in this chapter.

- **Chapter 7** outlines final conclusion and further works on drop weight impact testing machine.

Chapter 2

Literature Survey

2.1 Impact Test

'Toughness' in composite material is easy to demonstrate in specific situations but difficult to quantify in a manner relatable to different end-use conditions. The most commonly used measures of toughness involve the energy required to break a sample of defined geometry, often in the presence of a precisely specified crack. Most commonly, such toughness tests are done at high rates of loading and are then called impact tests [22].

Williams 1987 [23] defined impact as the striking or collision between two objects. This covers a very broad field and the current research has been confined to normal impact only, thereby reducing the complexity of test equipment required. Impact testing, regardless of the test machine used in the test, comes in two forms:

1. **General impact:** where the energy absorbed to cause damage, or in some cases, total failure is the only measurement.

2. **Fully instrumented impact:** where either, one or both, the load and displacement histories of the impacted body are monitored.

Impact testing of composite body is very material dependent, this is evident from the fact that most of the energy is absorbed through the degradation of the matrix

material.

It has been pointed out that the term 'Impact Strength' is not the correct description of the results generated from the impact test. 'Strength' normally implies the stress at failure (i.e. 'tensile strength') and it would be strictly correct to refer to the 'Energy absorbed by the specimen as it breaks'.

There are many different types of impact test and their results cannot in general be correlated with each other since their geometry and other factors are dissimilar [5, 12, 17, 19, 24–29] . This review considers some of the more commonly used examples and suggested classification under five headings as shown in table 2.1.

Table 2.1: Order of Magnitude Characteristics of Various Impact Tests [1]

Method	Order of magnitude of strain rate, S^{-1}	Impact velocity, m/s
Flexed beam		
•Charpy	10	3
•Izod	60	2.4
Falling weight	$10^{-1} - 10$	$1 - 4$
Conventional Tensile	$10^{-}3 - 10^{-1}$	$10^{-5} - 10^{-1}$
Pneumatic Gun	$10^{2} - 10^{4}$	20 - 140
Hydraulically operated	$1 - 10^{2}$	$10^{-3} - 4$

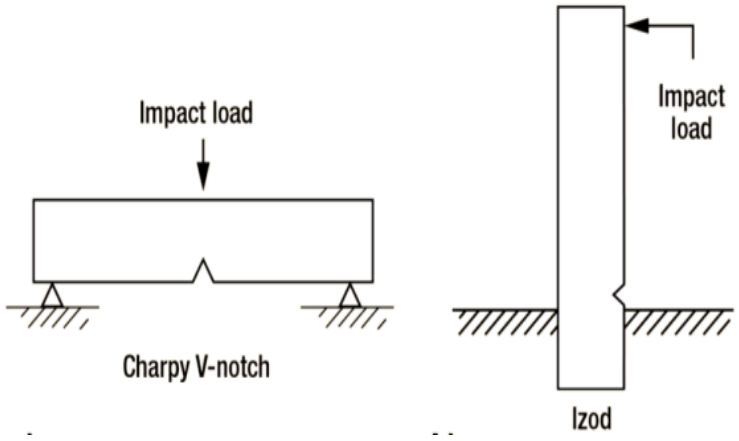

Figure 2.1: Standard Charpy and Izod Impact Test Loading Mechanism [1]

Cessna et al. [2] consider the impact problem from the point of view of the

designer and rank the different test methods in terms of their analytical usefulness, their simulation of real situations and the scale and cost involved.
Figure 2.2 shows the ranking, the direction of arrows indicate increasing quantities. Obviously a trade-off of criteria is required, the balance of which will be dependent upon the particular system.

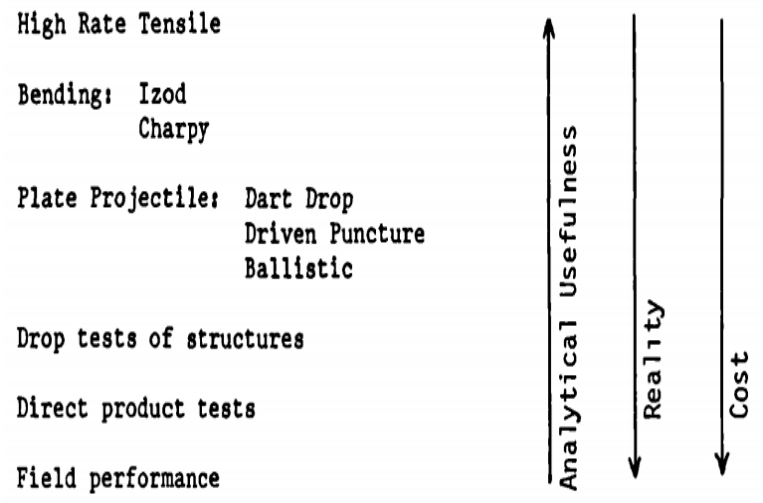

Figure 2.2: Rating of common impact tests [2].

In conclusion, this work focuses to design and prototype the drop weight impact test, and the procedure followed illustrated in chapter 3, chapter 4 and chapter 5.

2.2 Overview of Drop Weight Impact Test

The basic idea in a dropped-weight impact test machine (DWITM) is simply to drop an impactor or a weight of a given material and size onto a specimen from a given height to generate low-speed impact damage. It can be dropped vertically onto the specimen or swinging pendulum to impact the specimen. This work used these configurations and compared with design criterias in the conceptual design.

These variations depend on the intended application. The key feature, however, is that the striker must be equipped with a hemispherical tip of diameter $16mm$ and have a mass of 4.5–6.8 kg according to $ASTM\ D7136$ standard testing. The impact

drop height is adjusted to provide the required impact kinetic energy.

2.2.1 Theoretical aspects in drop weight impact test

In drop weight impact test accurate guidance is more important than accurate speed, since its easier to make allowances for speed variation in a test but variation in guidance totally affects testing may result wrong results.

Either varying the drop height (i.e. results in change in energy and velocity) or the mass of impactor (i.e. keeping velocity constant) determines the level of damage or energy absorbed [27].

The kinetic energy of the falling weight depends on its weight and the height of the fall. A falling weight acts as the impacting body (striker or tup), has the great advantage that the velocity at impact, v_0, can be varied easily by changing the drop height, applying the physics of motion results in equation 2.1 - 2.4. thus

$$v_o = \sqrt{2gh} \tag{2.1}$$

where, g is the acceleration due to gravity(m/s^2) and h is drop height (m)
The maximum energy that can be stored in the drop mass m is its potential energy (PE) which is given by:

$$PE = mgh \tag{2.2}$$

E_o and V_o can thus be varied independently from each other.

Total Energy

The energy is dissipated mainly in; deformation of the specimen, rebound of the striker assembly, elastic deformation of the drop weight machine [30]. In reviewed the literatures $\frac{1}{2}m{v_o}^2$ termed the impact energy without elaboration. By carrying

out the energy balance analysis when an impactor released from some predetermined height h as shown in figure 2.3.

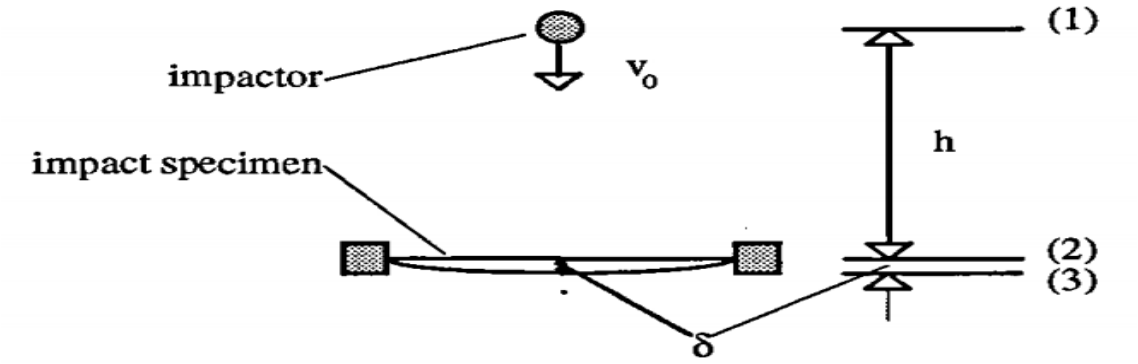

Figure 2.3: Energy balance of an impact event taking into account the deflection of the impact specimen

Assuming the deflection of the specimen δ, at heights (1) and (2):

(1)	$KE = 0$	(2)	$KE = \frac{1}{2}mv_o{}^2$
	$PE = mgh$		$PE = 0$
	$SE = 0$		$SE = 0$
	$Total = mgh$		$Total = \frac{1}{2}mv_o{}^2$

[where PE = potential energy, KE = kinetic energy, and SE = strain energy in the specimen].

Therefore the impact energy (IE) = mgh = $\frac{1}{2}mv_o{}^2$ and when the impactor comes to rest, then the strain energy in the plate is therefore given by equation 2.3:

$$SE = \frac{1}{2}K\delta^2 = mgh = \frac{1}{2}mv_o{}^2 \tag{2.3}$$

But, if the deflection of the plate is considered, an energy balance;

(1)	KE = 0	(2)	KE = $\frac{1}{2}mv_o{}^2$	(3)	KE = 0
	PE = mg(h+δ)		PE = mgδ		PE = 0

The strain energy absorbed by the plate is greater than the impact energy and therefore the total impact energy defined as [19]:

$$TIE = mg(h + \delta) = \frac{1}{2}m{v_o}^2 + mg\delta \tag{2.4}$$

2.2.2 Standard test methods

The standard procedure for conducting low velocity drop weight impact testing of FRP composites is defined in ASTM D7136/D7136M-15 [3]. Mainly the following components included in the standard, a drop tower with a rigid base, an impactor, a rebound catcher and a guide mechanism. The base of the tower consists of a support fixture that fix the test specimen in place.

On section 7 of the standard; [3],

- the specimen used is $150mm \times 100\ mm$ rectangular plate tightly attached onto a fixture base with a $125mm \times 75\ mm$ window cut-out as shown in figure 2.5
- the impactor used is a 5.5 kg mass with a 16-mm diameter smooth hemispherical tip
- If the desired energy cannot be achieved using the standard impactor mass dropped from a height of at least 300 mm, an impactor mass of 2.0 kg can be used

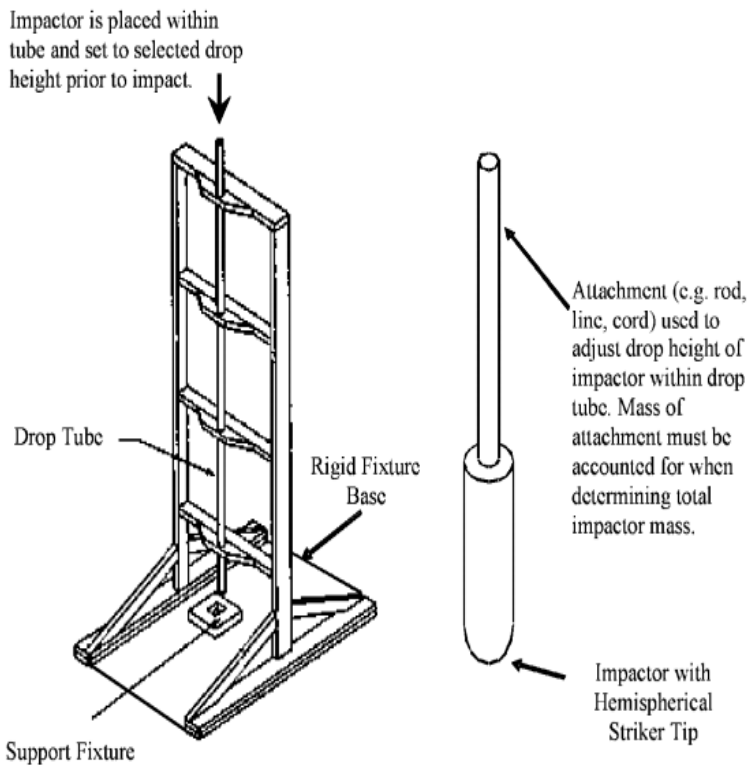

Figure 2.4: ASTM:D-7136 impact device with cylindrical impactor guide mechanism [3]

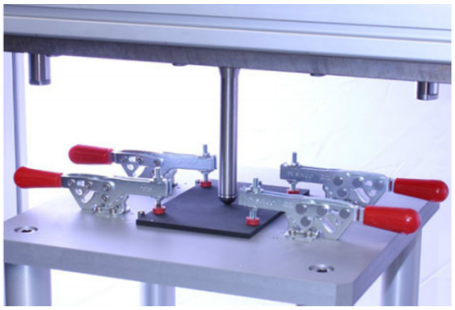

Figure 2.5: ASTM D-7136 specimen clamping method

Table 2.2: Common test standards adapted for composites

Method	**Impact Velocity**	**Striker**	**Support Conditions**
*ASTM D*7136		16 *mm* dia. hemispherical	specimen 150 $mm \times 100mm$, fixture base with a 125 $mm \times$ 75 *mm* window cut-out
BS 2780	3.46 m/s	12.7 mm dia.	50 mm I/D, 57 mm O/D ring clamped for specimens less than 0.89 mm thick. Specimens 60 mm diameter or square.
ASTM D 3029-FA	3.6 m/s	15.86 mm dia. hemispherical	76 mm I/D clamped specimen
ASTM D 3029-FB	3.6 m/s	12.7 mm dia. hemispherical	38.1 mm I/D ring, clamped specimen
ISO/DISS 6603/2	4.4 m/s	20 mm dia. hemispherical	40 mm I/D ring, specimen 60 mm dia. or square (clamping optional)

2.2.3 Commercial impact test machines

The major brands that produce drop weigh impact tester are **Instron, Imatek, and Zwick/Roell**. They offer different energy ranges for different types of materials. Medium energy towers, used for testing aerospace materials. Primarily, the parameters investigated are impact velocity, drop weight, and drop height, all of which contribute to impact energy.

The CEAST Drop Weight Machine

The machine consists of falling weight tower and instrumentation system.

- the drop tower consists of a cabinet (A) which is built around the of the drop tower and contains the specimen support pedestal (B)
- two vertical stainless steel guide bars (C) 2.5 m long are fixed to the base and guide the drop weight (D) on two adjustable vee blocks
- the drop weight impactor is attached to a carriage (E) by a fail safe ball-bearing latch which may only be released when the two red release buttons (F) on the control console are depressed simultaneously
- the striker (G) rigidly attached to the drop weight

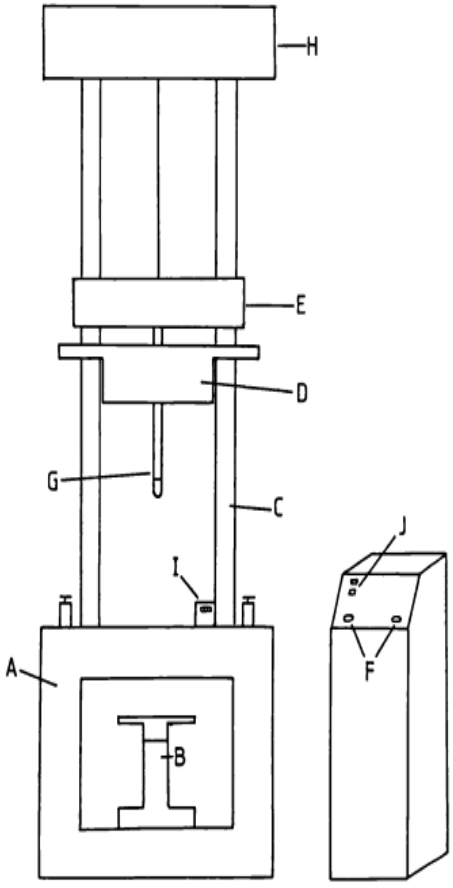

Figure 2.6: Schematic of Falling Weight Equipment

Generally, CEAST drop weight machines have the following specification listed in table

Table 2.3: Specification of CEAST Drop Weight Machines

Parameter	Value
Maximum drop height	2.2 m
Maximum impact velocity	6.5 m/s
Maximum falling weight	2 - 80 kg
Velocity measurement	electric flag device

These are the expected results from the test apparatus

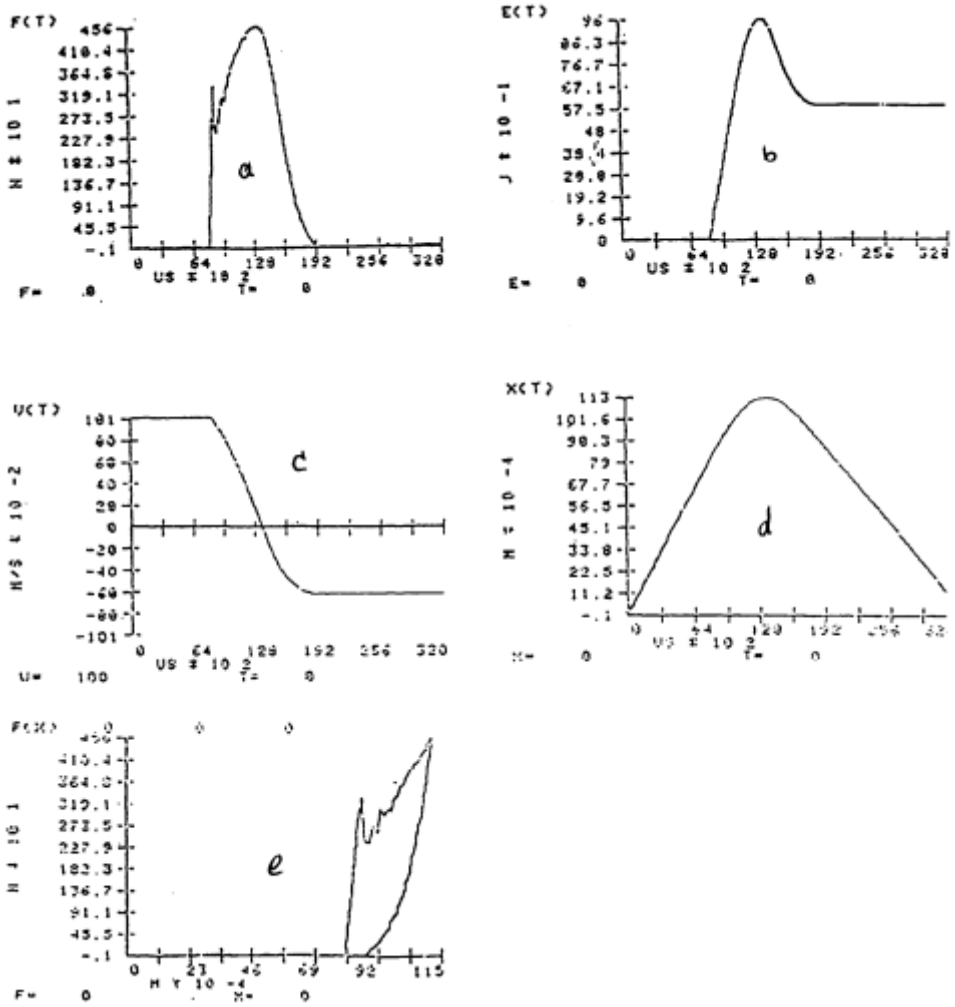

Figure 2.7: Typical curves of CEAST Drop weight machine

2.3 Parameters of Impact Test

These are some parameters which determine design of drop weight impactor and also the damage phenomenon in composite materials.

2.3.1 Geometrical and Material Parameters

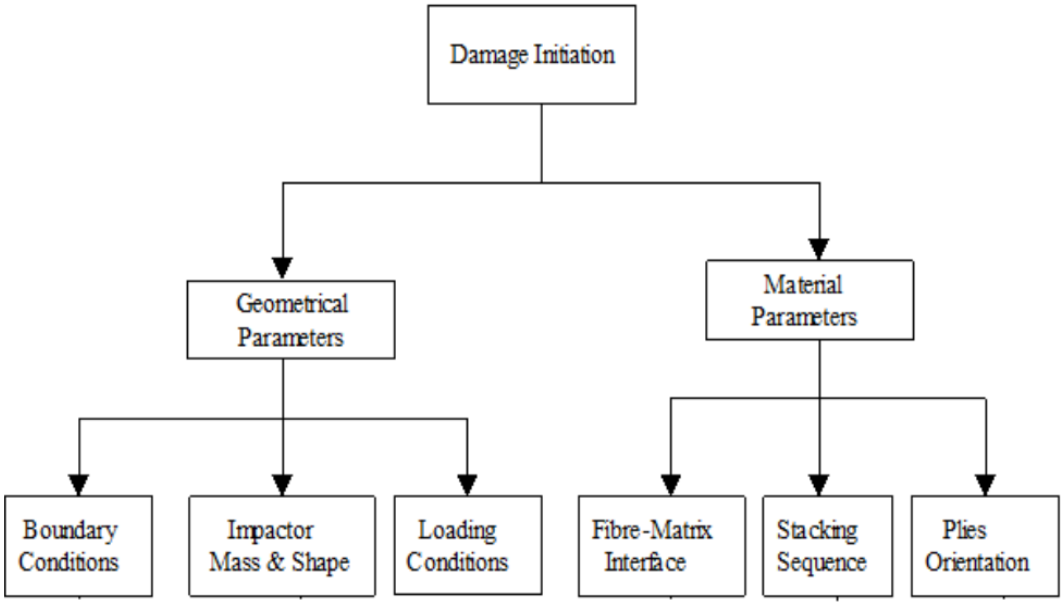

Figure 2.8: Effect of various parameters for damage initiation [4]

2.3.2 Thickness

The value of energy absorbed by the test specimen also controlled by the thickness. When fibre reinforced composite materials are subjected to low velocity impacts there is a pressure distribution around the area of contact which creates complex state of stresses.

2.3.3 Impactor Shape

The impactor shape is one of the crucial component in design of drop weight impact test machine. There is a relationship between factors like the mass, geometry of the impactor and target stiffness, geometry and rigidity.

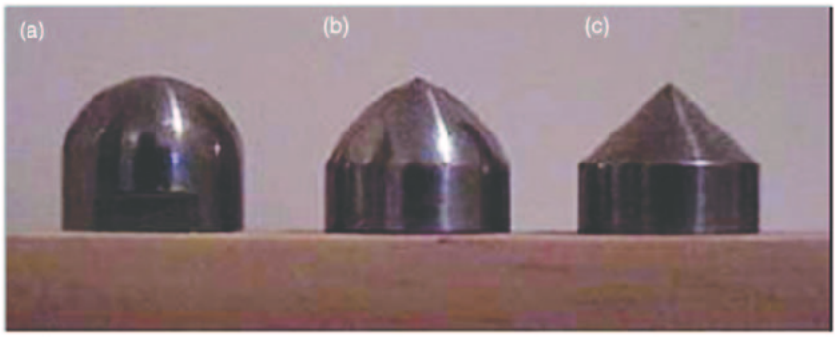

Figure 2.9: Impactor shapes: (a) hemispherical, (b) ogival, (c) conical

Mitrevski et al. [31] investigated the effect of different impactor shapes: flat, hemispherical, ogival and conical ended as shown in Figure 2.9. This research showed that *the hemispherical impactor* produced the largest peak force and shortest contact duration. Flat and hemispherical impactor produced similar energy dissipation and failure mechanisms within the composite specimens. The conical impactor absorbed the most energy and produced the largest penetration depth.

Based on the reviewed literatures and standard testing method, the work chooses hemispherical impactor.

2.4 Composite Materials under Low-velocity Impact

There is a complex failure mode when composite materials compared to conventional metallic materials. Generally the failure mechanisms of composite material classified into low-velocity impact damage or high-velocity impact damage [20, 32]. The low-velocity induced damage which is difficult to detect will be discussed below.

Carbon and glass composites of higher failure strength do well compared to composites with same type of reinforcement but lower failure strength in low-velocity impact tests [Sun].

2.4.1 Definition of Low-velocity Impact

Due to the uncertain transition between low-velocity impact and high-velocity impact the definition of low-velocity impact given by different researchers vary. On one hand, a commonly accepted one is suggested by Cantwell and Morton 2001 [33], under which the impact velocity is up to 10 m/s considering the height limit of test facility (such as drop-weight tower). On the other hand, Shen Z. 2015 [34], stated in his review book that, the impact speed of a low-velocity impact event should be less than 100 m/s.

Farooq et.al [12] insisted that the upper limit of low-velocity impact vary from 1 to 10 m/s depending on the material properties of target and the mass and stiffness of impactor. The research pointed out that, low-velocity impact event generates an entire structural response and in consequence more energy is absorbed elastically, as a result of a long enough impact duration.

Davies and Robinson [35] defined the low-velocity impact not only simply by a numerical limit, but by the material property, in which case the through-thickness stress wave effect on the stress distribution is negligible. A cylindrical zone under the impactor is considered to undergo a uniform strain, as the stress wave propagating through the plate, which gives the ultimate compressive strain.

Fanjing Yang [36] suggested that the type of impact can also be categorized by the existence of damage types. Low-velocity impact damage is characterized by delamination and matrix crack; whereas high velocity impact is dominated by fibre breakage and penetration.

In conclusion, considering the maximum impact velocity studied in this work is less than 10 m/s, and therefore the studied impact falls in the category of low-velocity impact.

2.5 Summary

Table 2.4: Summery of drop weight test from literatures

Investigator	**Impacting plate Dimensions, mm**	**Plate support dimensions and type of sopport**	**Diameter and shape impactor**
Williams 1987 [23]	200×125	560mm square steel frame	10mm-25mm hemispherical
Money 1988 [1]	88 dia	40 mm ID, 60 mm OD ring	5, 6.25,10 mm hemispherical
Madjidi 1994 [30]	102×140 and 560 dia.	580 mm square clamped	25 mm hemispherical
Wisheart 1996 [19]	135×85	60 mm ID, 80 mm OD ring	10 mm hemispgerical
Paran 1998 [25]	500×1000	100-300 mm clamped ring	
Lloyd 2002 [37]	40 or 120 dia.	200 mm, clamped simply supported	8-20 flat or hemispherical
Sofocleous 2008 [38]	100 mm dia.	140 mm, clamped	16 mm dia. hemispherical
Liu and Liaw 2009 [39]	100 square	70 mm dia, clamped	12.5 mm, hemispherical
Yang 2010 [36]	200×200	50, 100, 150, 200 mm dia. ring	5, 10, 15, 20 mm dia. hemispherical
Abessalam 2011 [40]	60×60	80×80 mm	20 mm dia. hemispherical
Gong 2011 [41]			30 mm hemispherical
Mouti 2012 [42]	80 long	60 mm square, clamped	10 mm hemispherical

Sevkat et al. 2013 [43]	101.6 square	76.2 mm clamped	
Ehrich 2013 [5]	150×100	160×110 clamped	16 mm hemispherical
Malhotra 2014 [44]	89×55	130×58 mm simply supported	20 mm hemispherical
Nash 2016 [45]	200×150	300×300 mm clamped	20 mm hemispherical
Rajput et al. 2018 [21]	150×100	ASTM D7136	
Zhang et al. 2017 [29]	100×100		40 mm cylinderical

Where, dia. stands for diameter.

Apart from standards, there are a wide variations of plate size and support dimensions listed in literatures, summarizes drop weight impact tests in Table 2.4. Only two researchers (i.e. Ehrich [5] and Rajput et al. [21]) used $ASTM\ D7136$ standard testing method, which this work mainly refer the work of those researchers.

Chapter 3

Preliminary Design of Drop Weight Apparatus

3.1 Conceptual Design

3.1.1 Identifying Needs and Gathering Information

The major purpose of the current work is to design an apparatus/machine that tests composite materials in impact. The device needs full interaction of the operator with the apparatus before testing begins. The operator needs to fix the specimen on the fixture. After testing begin the operator should withdraw himself/herself from the machine. The following guidelines should be addressed.

- The machine must allow free unobstructed fall.
- Standard striker and specimen size (i.e. based on ASTM D7136 [3])
- Maximum impact velocity in low velocity range according to [4] which is between 1 and 5 m/s.
- Minimum friction between impactor and guide mechanism.
- Total mass of the machine must not exceed 50 kg.

- The maximum dimension of the machine must not exceed 500 $mm \times 500\ mm \times 1500\ mm$.
- The device must be stand-alone unit.
- The plate fixture must be at least a factor of ten stiffer than the plate.
- There must be provision for sensors to measure at least the motion of the impactor and its incident velocity.
- The specimen should be in good condition when supplied to the machine (i.e not cracked, not pressed or twisted)

3.1.2 Market Information

The growth of global impact testing machine is directly proportional to the growth in manufacturing and construction sector. Over the past few years the global economy has seen several macro-economic turbulences, such as volatile oil prices and slowdown in construction industry and geopolitical instabilities. The mentioned factors are expected to have affected the growth of global impact testing machine market.

- Manufacturers are continuously investing on development and designing impact testing machine with electronic sensing instrumentation to analyses and compute & represent complete impact test rather than just a value. Also, with the increasing investment in R&D activities on material testing and development the demand for sophisticated testing equipment are increasing, this in turn will drive the demand for impact testing machine during the forecast period

Market Segmentation

On the basis of end-use,

- the market is separated into Construction, Automotive, Educational Institutions, and others. They lead the market income, mainly due to the research activities funded by government agencies to research scholars and universities

for the development of higher quality materials and greater efficiency machines at low price

On the basis of material,

- the market is separated into Metal, Plastics, Rubber and Elastomer, Ceramics and Composites. The demand for Composites in the aerospace and defense, automotive and construction industries, due to their advanced material properties, makes it the fastest growing material sector

Market key players:

Major companies playing their trade in material testing market include; Instron (US), Zwick Roell (Germany), MTS Systems (US), Shimadzu (Japan) are the leading shareholders of the global material testing market. This companies are majorly focused in the research and development of quality material at effective and efficient costs.

3.1.3 Customer Requirements

Three steps followed in preparing customer requirements according to [46, 47], these are.

1. *P*repare a list of design objectives
2. Order the list into sets of higher-level and lower-level objectives
3. *D*raw a diagrammatic tree of objectives

Design Objectives

Generally, the work has the following design objectives based on expected requirements from the product;

- Low damage (does not penetrate specimen)
- Can detect movement
- Can detect weight

- Ease of assembly disassembly
- Efficient
- Anti-rebound
- Ease of repair
- Least possible space utilization
- Noise free operation
- Precision
- Repeatable
- Minimum maintenance
- Safety
- Effectiveness
- Ease of use

Table 3.1: Mission statement: Low Velocity - Drop Weight Impact Test Machine (DWITM)

Product description	low velocity drop weight impact test machine for composite materials.
Benefit preposition	Provide significant information about the energy absorbed and the damage mechanism without complete failure in impact. Provide provision of a hardware for experimental data to validate numerical simulation of impact loads on specimen.
Assumptions	Drop weight principles Low velocity Power assisted Elevation and release at the certain height above the specimen.
Stakeholders	User/Operator School of Mechanical and Industrial Engineering Laboratories Production centers

Objective tree

The objective tree divided in to main heading and sub-heading.

Main Heading

As a main heading objectives, the intended drop weight impact test machine subdivided into performance, safety, appearance and inexpensiveness. These four objectives subdivided further as sub-headings.

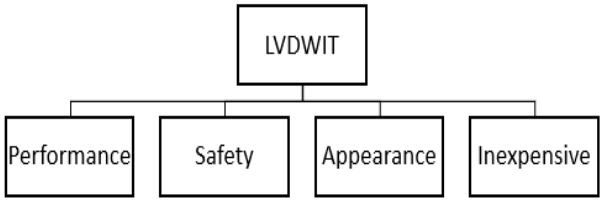

Figure 3.1: Main headings of DWITM

Sub-heading: performance, safety, appearance and inexpensiveness of the DWITM further divided as shown from Figure 3.2 to Figure 3.5.

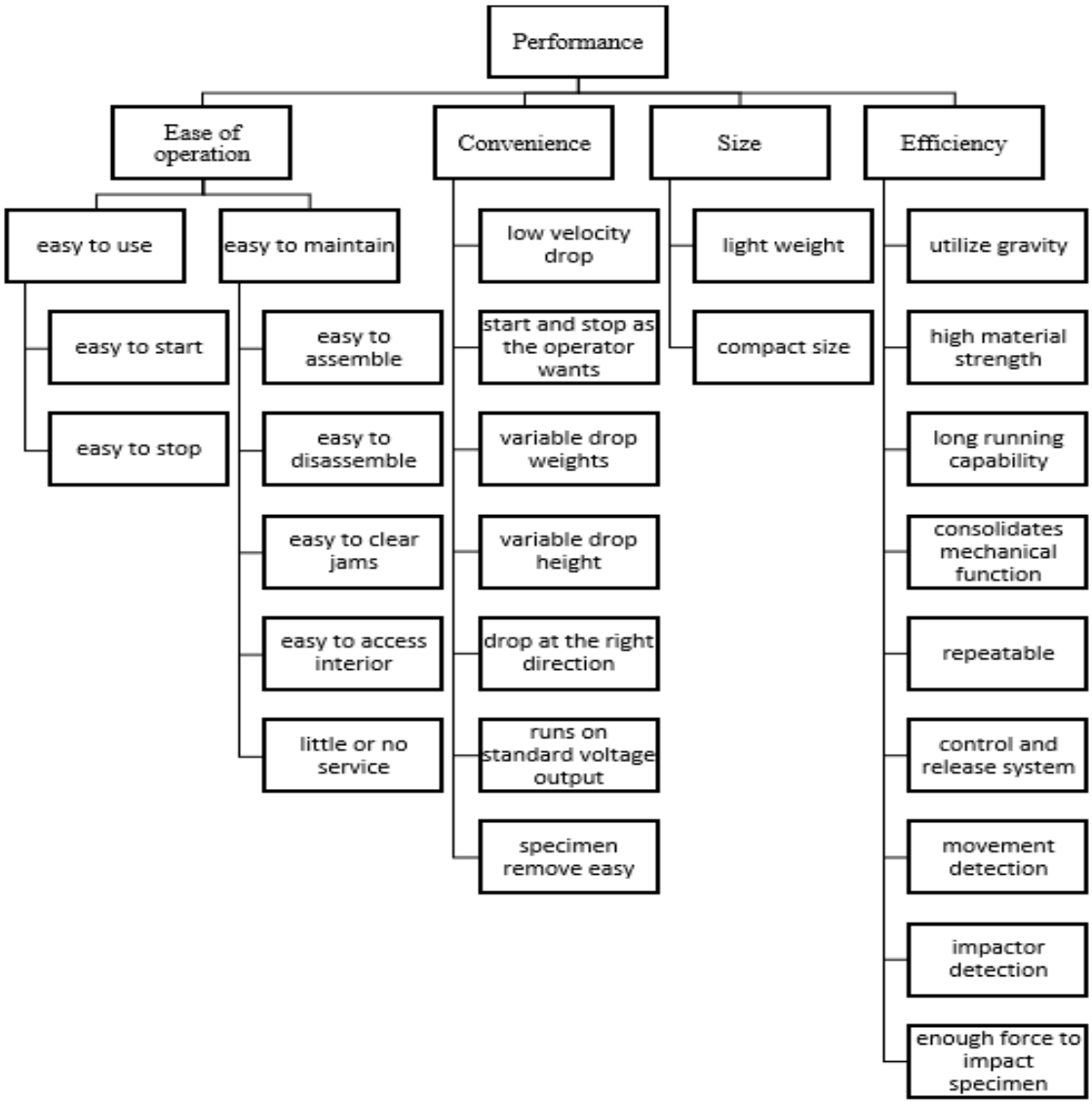

Figure 3.2: Performance of DWITM

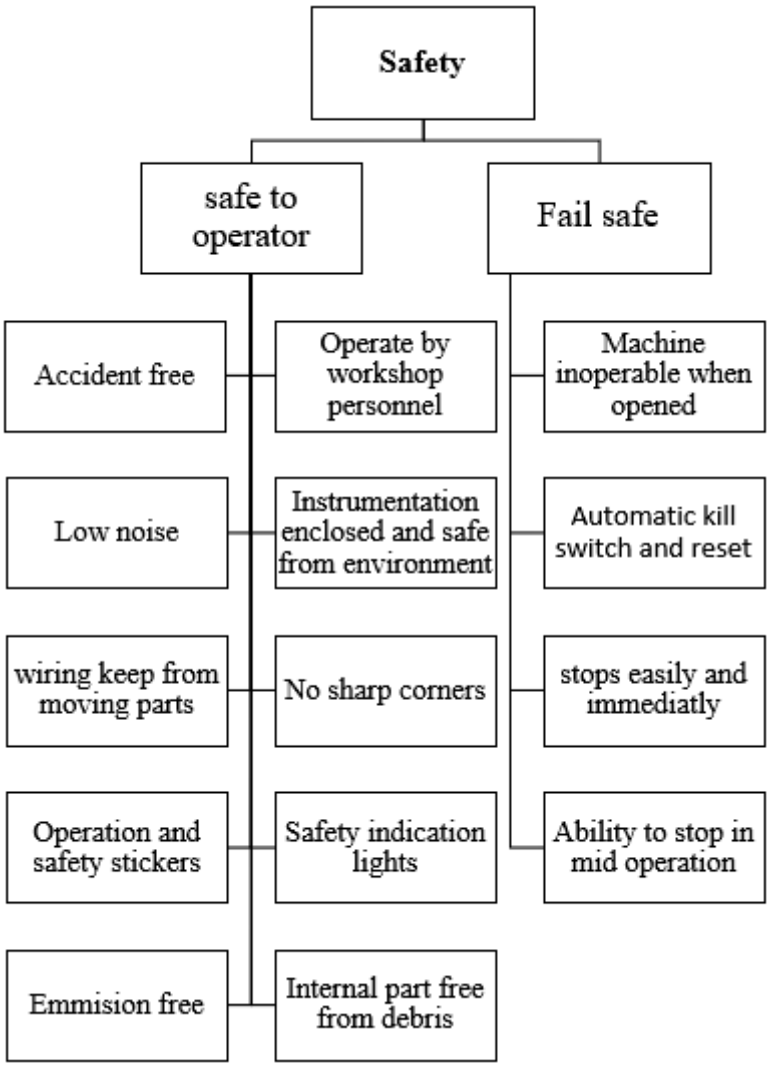

Figure 3.3: Safety of DWITM

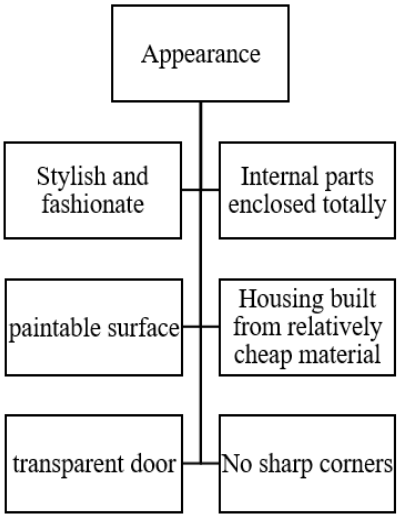

Figure 3.4: Appearance of DWITM

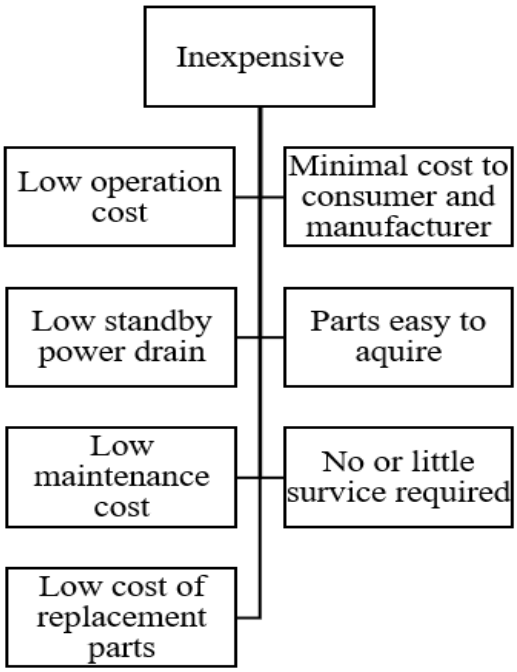

Figure 3.5: Inexpensiveness of DWITM

Functional Structures

The overall function of the machine is to convert input of impact force (energy) into an output of impact strength of the test specimen.

Black Box model of DWITM:

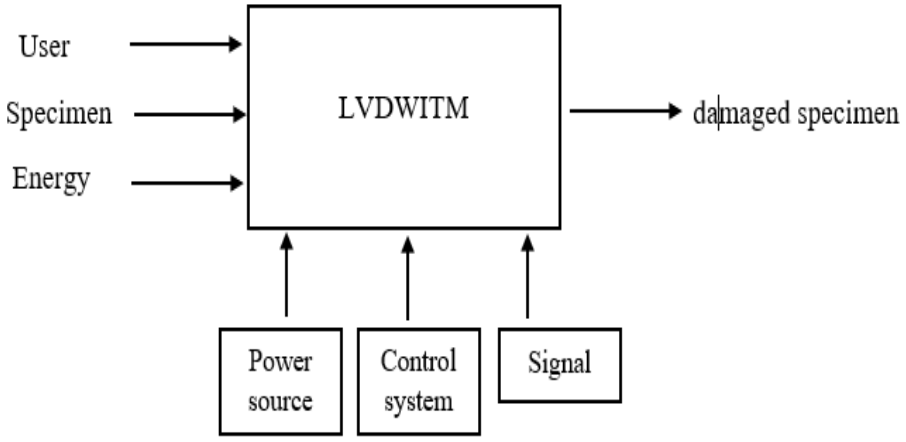

Figure 3.6: Black Box model of DWITM

Table 3.2: Esential sub-functions of the drop weight impact machine and means of achieving sub-functions

Essential sub-functions	**Means of achieving sub-function**
Fixed specimen	Using steel base
Impactor elevation and release	Rope/Chain/Motor/Actuator
Impactor geometry	Hemispherical
Impactor speed control	Using speed sensor
Impactor force control	Using force sensor
Energy absorption	Variable height control
Single impact condition	Anti-rebound mechanism

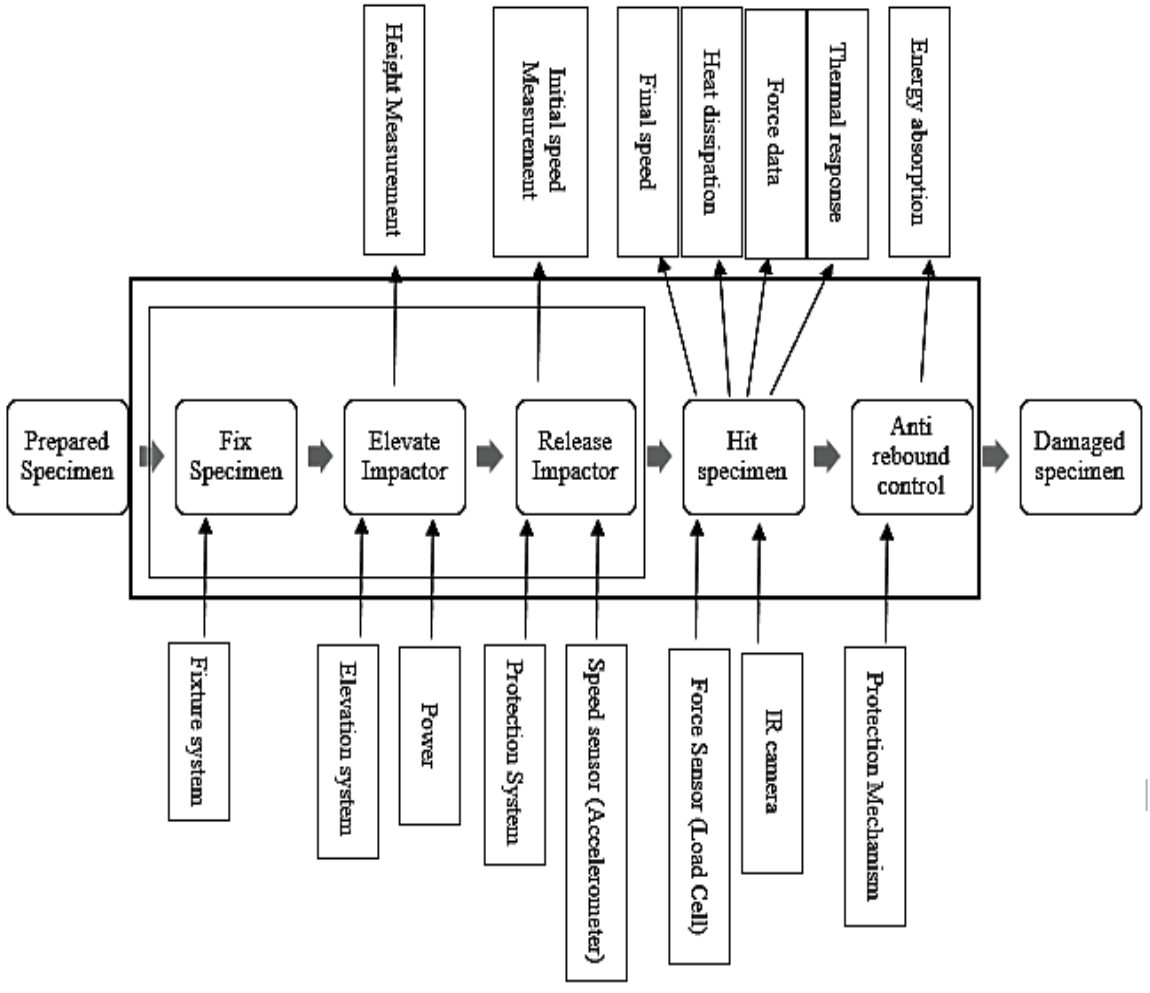

Figure 3.7: Block diagram showing interactions between sub-functions

3.1.4 Product Specification

Table 3.3: Customer need for the low velocity drop weight impact test machine and their relative importance

No.	The machine	Need	Imp.
1	DWIT	Allow easy elevation of impactor	5
2	”	Allow free fall of impactor at the center of the test specimen	5
3.	”	Allows falling masses with fixed shape and variable masses	4
4.	”	Prevent mass from falling off the apparatus	5
5.	”	Low friction carrier system	4
6.	”	Lightweight	3
7	”	Reduce vibration to the support system	3
8.	”	Able to conform ASTM-D7136	5
9.	”	Can be easily accessed for maintenance	3
10.	”	Last long time	3
11.	”	Affordable	5
12.	”	Easy release mechanism	4
13.	”	Single impact in all testing conditions	4
14.	”	Possibility of varying impact energy and velocity independently	5
15.	”	Able to capture the falling weight after the first impact	5
16.	”	Allow mounting of additional mass for adjustment	4
17.	”	Impactor able to transfer energy without complete deformability	4
18.	”	Able to replace the striker	4
19.	”	Able to measure energy absorbed by the specimen	5
20.	”	Able to measure deflection of the specimen	5
21.	”	Easy to install	4
22.	”	Accuracy of measurement (minimum possible error)	5
23.	”	Able to measure impactor travel distance	5
24.	”	Have a power supply	5

Customer need for the low velocity drop weight impact test machine and their relative importance with maximum value of 5 and minimum value of 1.

Process of establishing target specification

Prepare List of Metrics

List of metrics for the DWITM. The relative importance of each metric and the units for the metric are also shown. "Subj." is an abbreviation indicating that a metric is subjective.

Table 3.4: List of metrics for DWITM

No.	**Need No.**	**Metric**	**Importance**	**Units**
1.	1,2	Variable mass range of impactor	5	Kg.
2.	2,3,5,10	Minimum friction between impactor and guide	4	Subj.
3.	6	Overall dimension of the machine	4	mm.
4.	8,17	Specimen geometry and size	5	mm.
5.	8	Maximum test area	4	mm.
6.	16	Drop weight	5	Kg.
7.	4,15	Mass arresting(shock absorbers)	4	Subj.
8.	23	Drop height range	5	mm.
9	6	Total mass of the machine	3	Kg.
10.	7,9	Operation safety	3	Subj.
11.	8	ASTM:D-7136 standard test	5	Binary
12.	3,16	Mass increment	4	Kg.
13.	8,18	Striker/tup shape and size	4	mm.
14.	12	Control mechanism	5	Subj.
15.	14	Maximum impact energy	5	Joule
16.	14	Maximum velocity	5	m/s
17.	4,13,15	Anti-rebound mechanism	4	Subj.
18.	14,19,20	Capacity of force sensor	4	kN.
19.	21	Time to assemble and disassemble	3	Sec.
20.	24	Supply voltage range	2	Volt
21.	24	Supply current range	2	Ampere
22.	24	Compressed air supply	4	Bar.
23.	10,11	Unit manufacturing cost	5	Birr

Note: metrices define the overall performance of a product and should therefore be the dependent variables (i.e output variables).

Table 3.5: Need-Metric Matrix

	Metric	Variable mass range of impactor	Minimum friction between impactor and guide	Mass increment	Mass arresting/ shock absorbers	Anti-rebound mechanism	Total mass of the machine	Overall dimension of the machine	Operation safety	Maximum test area	ASTM-D7136 standard test	Specimen geometry and size	Striker shape and size	Unit manufacturing cost	Control and release mechanism	Maximum impact energy	Maximum velocity range	Weight of impactor/drop weight	Dynamic rated capacity of load cell	Time to assemble and disassemble	Drop height range	Supply voltage range	Supply current range	Compressed air supply
No	**Need**	1	2	3	4	5	6	7	8	9	10	11	12	13	14	15	16	17	18	19	20	21	22	23
1	Allow easy elevation of impactor	⊗																						
2	Allow free fall of impactor at the center of the test specimen	⊗	⊗																					
3	Allows falling masses with fixed shape and variable masses		⊗	⊗																				
4	Prevent mass from falling off the apparatus				⊗	⊗																		
5	Low friction carrier system		⊗																					
6	Lightweight						⊗	⊗																
7	Reduce vibration to the support system								⊗															
8	Able to conform ASTM-D7136									⊗	⊗	⊗	⊗											
9	Can be easily accessed for maintenance								⊗															
10	Last long time		⊗											⊗										
11	Affordable													⊗										
12	Easy release mechanism														⊗									
13	Single impact in all testing conditions					⊗																		
14	Possibility of varying impact energy and velocity independently															⊗	⊗		⊗					

15	Able to capture the falling weight after the first impact				⊗	⊗																	
16	Allow mounting of additional mass for adjustment			⊗														⊗					
17	Impactor able to transfer energy without complete deformability											⊗											
18	Able to replace the striker												⊗										
19	Able to measure energy absorbed by the specimen																		⊗				
20	Able to measure deflection of the specimen																		⊗				
21	Easy to install																			⊗			
22	Accuracy of measurement (minimum possible error)																						
23	Able to measure impactor travel distance																				⊗		
24	Have a power supply																					⊗	⊗	⊗

Based on those competitive benchmark's marginally and ideally acceptable target values generated.

Ideal values: the best result the team could hope for. *Marginally accepted values:* the values of the metric that would just barely make the product commercially viable.

Table 3.6: Competitive Benchmarking

Metric No.	Need No.	Metric	Imp.	Units	TMI Model:43-60	Instron CEAST 9310	Instron CEAST 9340	Instron CEAST 9350	Zwitch/ Roell HIT230F	Imatek IM10T-20	Imatek IMI-P
1.	1,2	Variable mass range of impactor	5	Kg.	0.5-16	0.5-3	1-37.5	2-70	23.5	2-5 and 50-100	10(fixed)
2.	2,3,5	Minimum friction between impactor and guide	4	Subj.	Bearing carrier system	Automatic lubrication ISO 6603	Automatic lubrication ISO 6603	Automatic lubrication ISO 6603	–	–	–
3.	6	Mass increment	5	Kg.	0.5	0.05	0.5	0.5	1	0.5 or 5	–
4.	8,17	Mass arresting	4	Subj.	Pneumatic	Pneumatic	Pneumatic	Pneumatic	Electrical	Electrical and pneumatic	Electrical and pneumatic
5.	8	Anti-rebound mechanism	5	Subj.	Pneumatic	Pneumatic	Pneumatic	Pneumatic	Pneumatic	Pneumatic	Pneumatic
6.	16	Total mass	4	Kg	270	38	340	550	400	2800	800
7.	4,15	Overall dimension (wxdxh)	4	mm	0.95×0.45×2.5	0.425 × 0.34 × 1.315	0.985 × 0.61 × 2.62	1.015×0.866× 2.7	1.0 × 0.6 × 2.6	1.42×0.76×4.5	1 × 0.8 × 3.0
8.	23	Maximum test area(wxdxh)	5	mm.	Not specified	0.25 × 0.15 × 0.145	0.49 × 0.45 × 0.565	0.7×0.72×0.55	Not specified	0.7×0.72×0.55	Not specified
9.	6	ASTM-D:7136 standard test	5	Binary	Pass	Pass	Pass	Pass	Pass	Pass	Pass
10.	7,9,10,11	Strkier shape and size	5	mm,Subj.	Hemi spherical	10-20 (hemispherical)	10-20 (hemispherical)	10-20 (hemispherical)	10-20 (spherical)	10-20 (hemispherical)	10-20 (hemispherical)
11.	8	Unit manufacturing cost	5	Birr							
12.	3,16	Control and release mechanism	4	Subj.	Solenoid	Pneumatic	Pneumatic	Pneumatic	Pneumatic	Pneumatic and servo	Pneumatic
13.	8,18	Maximum impact energy	5	Joule	Up to 314	0.15 - 20.4	0.3 - 4	0.59 - 757	Up to 230	2.5 - 588	24 - 118
14.	12	Maximum freefall velocity	5	m/s	up to 6.26	0.77-3.71	0.77-4.65	0.77-4.65	Up to 4.4	1-6.26	2.2-4.85
15.	14	Dynamic rated capacity of load cell	4	kN	±15	Not specified	Not specified	Not specified	±25	±60	±20
16.	14	Drop height range	5	m	2	0.03-0.7	0.03-1.1	0.03-1.1	0.11-1.0	0.05-2	0.25-1.2
17.	4,13,15	Time to assemble disassemble	2	Sec.	–	–	–	–	–	–	
18.	14,19,20	Supply voltage range	3	Volt	110 or 240	115/230	220-240	220-240	220-240	230	230
19.	21	Supply current range	3	mA	5-10	4-20	4-20	4-20	Not specified	16	5
20.	24	Compressed air supply	4	bar	7	5	5	5	8	10	5-8

Target specification

Table 3.7: Target specification

Metric No.	Metric	Imp.	Unit	Marginal value	Ideal value
1.	Minimum friction between impactor and guide	5	Subj.	Lubricant	Lubricant
2.	Variable mass range of impactor (drop weight)	5	Kg.	23.5-100	1-10
3.	Mass arresting/shock absorber	4	Subj.	Pneumatic	Pneumatic
4.	Overall dimension	4	m^3	1×0.9×2	0.5×0.2×1.2
5.	Maximum weight	3	Kg.	max. 60	max. 100
6.	Operation safety	3	Subj.	Closed	Closed
7.	Maximum test area	4	m^2	0.25×0.15×0.145	0.35×0.153×0.153
8.	ASTM-D7136 standard test	5	Binary	Pass	Pass
9.	Mass Increment	4	Kg.	max. 0.5	max. 1
10.	Striker shape and size	4	Subj./mm	Spherical, conical or round	Hemi spherical
11.	Control and release mechanism	4	Subj.	Solenoid/ pneumatic/ manual	Solenoid/ pneumatic/ manual
12.	Maximum Impact energy	5	Joule	230 - 600	Up to 50
13.	Maximum impact velocity	5	m/s	6.5	Up to 5
14.	Anti-rebound mechanism	4	Subj.	Manual	Electrical/ Pneumatic
15.	Maximum drop height	5	m	2	0.03-1.5

3.1.5 Concept Generation

A. Search externally

1. **Patents**

   The drawback of patent searches is that concepts found in recent patents are protected generally for two decades from the date of the patent implementation, so there may be a royalty involved in using them. However, patents are also useful to see what concepts are already protected and must be avoided or licensed. There are a lot of patents [48–52] which is hard to list every work, but most reviewed patents have common on the following points.

   - The should be enough space between guide columns with an impactor slidably mounted on and the main support.
   - A lifting mechanism slidably mounted on the guide columns above the impact hammer and can be raised by a hoist/chain/motor/fluid power to the top of the main support.
   - There should be a specimen fixture system where test specimen placed for testing.
   - While conducting test, to avoid vibration from transmitting from the specimen fixture to the frame, separate system followed.
   - In some literatures there is a means for tensioning the guide columns.
   - And different instrumentation techniques.

2. **Product Found in workshop** The following drop weight impactor shown in Figure 3.9 and 3.8, found in Debre Berhan University soil mechanics laboratory.

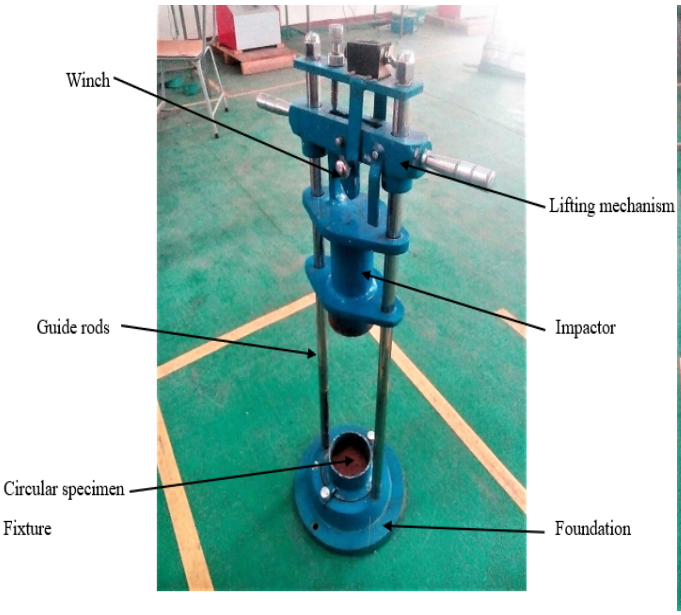

Figure 3.8: Drop height Position

Figure 3.9: Impact Position

The operator holds the handles of lifting system, which has a winch gripping the impactor at the desired drop weight position. When the desired position meet, the winch drops the impactor.

- The striker is constructed from circular 60 mm diameter stainless steel. Also the specimen fixture is 65 mm circular ring.

3. **Literature sources**

   The ASTM D7136/7136M standard testing method has a drop weight impact test machine shown in figure 3.10.

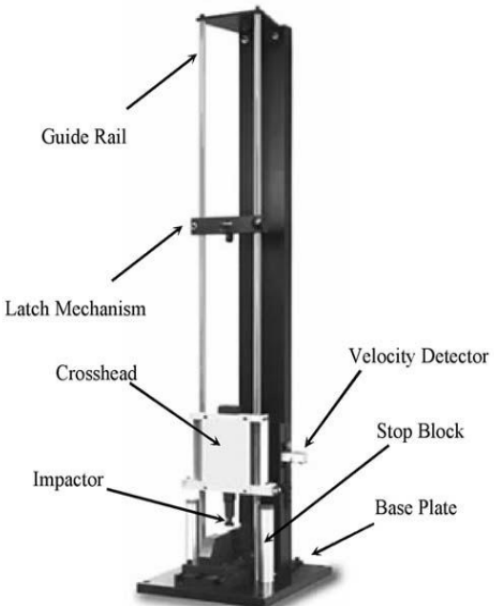

Figure 3.10: Machine Impact Norm. Source: (ASTM D7136/D7136M-07, 2005) [3]

Most literatures [2 - 10] come with slight modification to commercially available suppliers listed in table 3.6, this work divided these literatures based on instrumentation techniques and apparatus layout.

- **Drop Weight Impact Tester based on Apparatus Layout:** this method is based on machine layout i.e the impactor type and mass, drop tower and impact parameters (impact energy, drop weight, drop height and impact velocity). This work further divided and studied apparatus layout into drop weight type and swinging hammer type.
  - **Drop Weight Impact Type:**

Table 3.8: Literature sources based on apparatus layout

No.	**Articles**	**Energy (J)**	**Velocity (m/s)**	**Drop height (m)**	**Drop weight (Kg.)**
1.	**Francisco et al.**	20-90	11	0.6	
2.	**Gunawan et al. [53]**	7350	9.9	5	150
3.	Zhang et al.[54]	53.57	2.4	0.3	Aluminum hammer 18.6 and steel 60.55 – 315.55, increment 15
4.	**B.S.Sugun et al.**	3.5-15	1.2-2.4	-	5.42
5.	**Winkle and Adams [28]**	Energy to peak: E_m = 8.76, Total energy E_t = 21.65	Nominal 3.66	0.876	Rated maximum cross-head weight for the system is 32, in the present study, use was made of 15.88 kg cross-head.
6.	**Sevkat et al. [43]**	32	3.23	0.53	6.15
7.	**Aryal et al. [20]**	**Program 1** **Program 2**	17.13, 112.27 and 154.18 respectively 68.53, 68.52 and 68.3	2.5, 6.4 and 7.5 respectively 5, 4.14 and 3.16 respectively	5.5 5.5, 8 and 10.5 respectively
8.	**Ruiz-Herrero et al. [55]**	0.236-98.11	5.24 for maximum height	0.02-1.4	1.2-7.144

9.	**Ambur et al. [56]**	2.95 and 4.1	3.1	Total height of 1.6 m	1.0
10.	**Fukushima & Kurahara [48]**	56, 94, 132 and 189 respectively	2.2, 3.1, 3.7 and 4.4	0.3, 0.5, 0.7 and 1.0 m, respectively	18 (including impactor, load cell
11.	**Zoller et al. [22]**	2.58	4.8 max and nominal of 3.13	1.2 total and 0.5 drop height	0.1 and 2.5
12.	**Mitrevski et al. [31]**	At 4 and 6 (initial)	Not specified	Not specified	4.325
13.	**Robinson et al. [35]**	12	6		1.15-2.10
14.	**Money (1988) [1]**	-	6.5	2.2	19.063
15.	**Paran (1998) [25]**		4		
16.	**Lloyd (1987) [37]**	40	5.9		
17.	**Wisheart (1996) [19]**	Max 15	1.01		25.9
18.	**Madjidi (1998) [30]**	59	5.42	1.5	4
19.	**Yang (2010) [36]**	0.1-400	6.5	2	0.04-35
20.	**Abessalam (2011) [40]**	34.84	4.44	0.987	3.6
21.	**Mouti (2012) [42]**	3-12			
22.	**Rajput et al. [21]**	200	8	3.6	6

- **Swinging hammer type:** the second technique of conducting impact test on composite materials. In most literatures [57, 58] which use swinging hammer, the apparatus consists of a lever arm with a adjustable head and a housing which the specimen fixed on. This lever arm hinged to a heavy support to allow it to swing and to impact the specimen. The adjustable head designed to move along the lever arm creating smaller or larger impact energy. Sensors can be mounted on to either the adjustable head or the support.

- **Drop weight impactor based on instrumentation type and positioning**

  William (1988) [23], Ehrich (2013) [5]; used three different testing methods based on sensor and transducer orientation in

  (a) Drop weight-impactor with force sensor and a strain gauge.

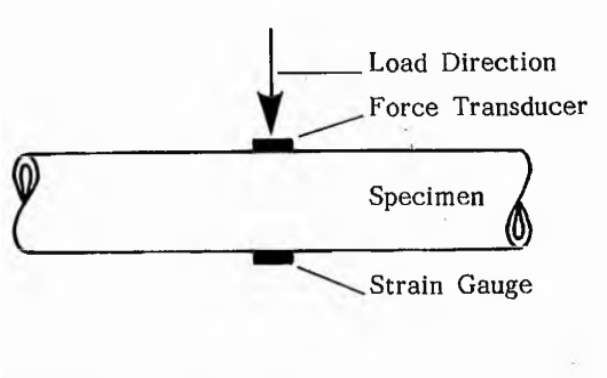

Figure 3.11: Drop weight impactor with force sensor and a strain gauge

  (b) Drop weight impactor with force sensor and accelerometer.

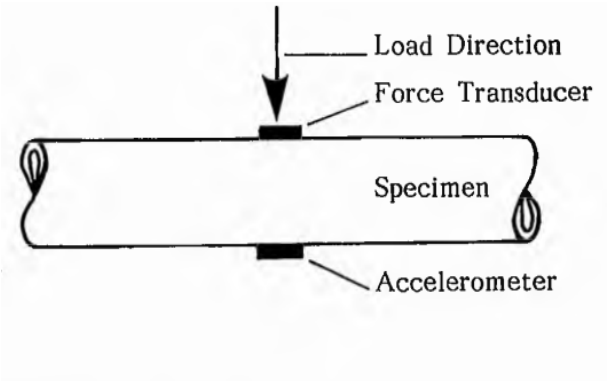

Figure 3.12: Drop weight impactor with force transducer and an accelerometer

(c) Drop weight impactor with only an accelerometer.

This method does not involve the provision of force sensors, since from a single accelerometer the acceleration data can be generated. If the impacting mass is known, the impact force can be found from Newton's second law of motion. The velocity and displacement data can be obtained from successive integration.

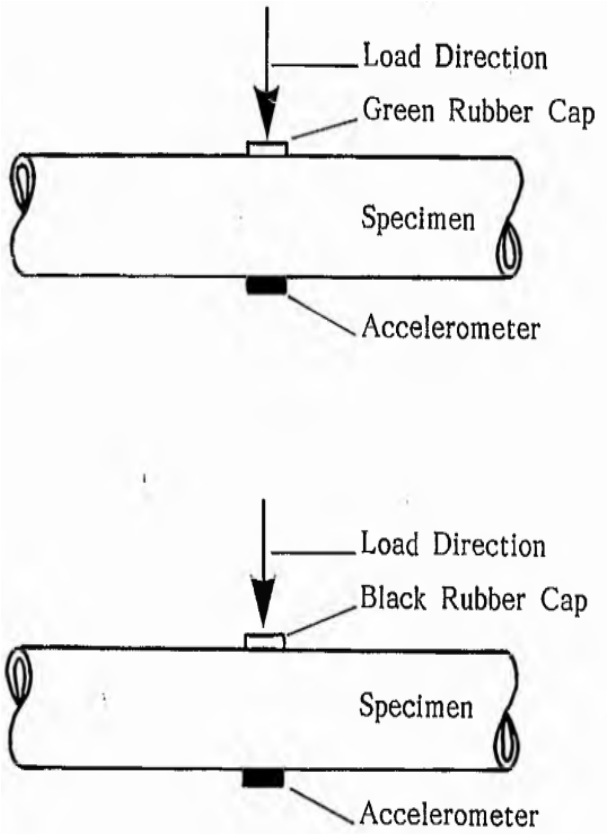

Figure 3.13: Drop weight impactor with only an accelerometer

Swinging hammer with different test arrangements.

(a) Spherical metal tip on hammer, Black rubber + Force transducer on specimen,

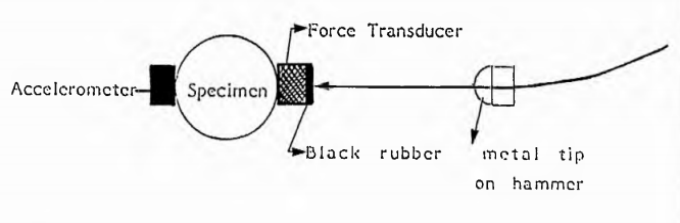

Figure 3.14: Transverse Section [Reza Maleki]

(b) Spherical metal tip + Force transducer on hammer, Black rubber on specimen.

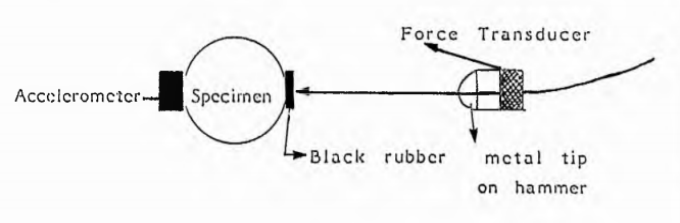

Figure 3.15: Transverse Section [5]

From external search of literatures, we can see on the graph below, the impact energy taken by various researchers varies greater when compared to other parameters i.e. velocity, drop height and drop weight.

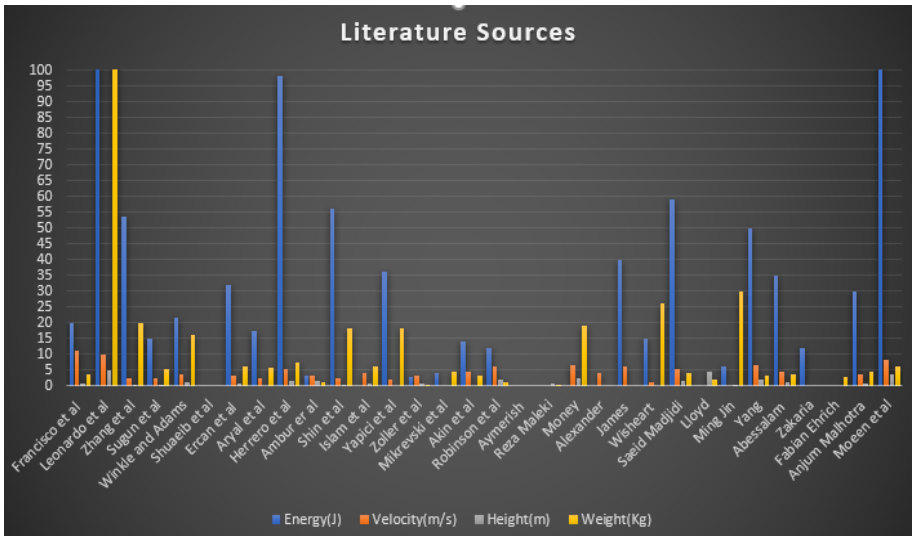

Figure 3.16: Literature source based on energy, velocity ,drop height and drop weight comparison

- Based on the drop weight requirement (<10 Kg.): articles 4, 8-11, 13, 15-20, 23, 26, 27, 29, 30, 32, 34 meet the requirement.
- Based on impact energy requirement (Max $50J$): articles 1, 4, 5, 8, 10, 11, 14-18, 23, 25, 28-31, 33 meet the requirement.
- Based on impact velocity requirement (Max 5 m/s): articles 3 ,4 , 5, 8-15, 17, 22, 23, 25, 26, 30, 33 meets the requirement.
- Based on drop height requirement (0.03-1.1 m): articles 1, 3, 5, 8, 10, 12, 13, 15, 20, 28, 30, 33 meet the requirement.

Remark: all basic requirements (energy, velocity, drop weight and height) are from target specifications.

Decisions

Dimensioning: Size of the base, the guide rail and drop weight assembly determined based on relevant ASTM standard as well as practical limitations. It should allow for transportation and fit through doorways. In addition the maximum drop height of the machine for the maximum velocity.

Foundation: depends on particularly the impacting mass and velocity. In general, the main criterion is the mass of the foundation and the damping capability. The choice depends on the size of the machine and degree of flexibility (possibility of repositioning or removing the foundation).

According to the standard, the reaction mass or the entire structure not including the drop weight, must be at least fifty times the mass of the drop weight. For our case, for drop weight of 10 kg (max), the reaction mass is 500 kg.

Instrumentation: all components of the instrumentation is within the drop tower or under specimen support. Load/or acceleration sensors either mounted on the striker (i.e. accelerometer) or beneath the test specimen (i.e. load cell).

Based on external searches the following concept found based on basic common components listed above.

Concept 1: Two column, motor operated impactor

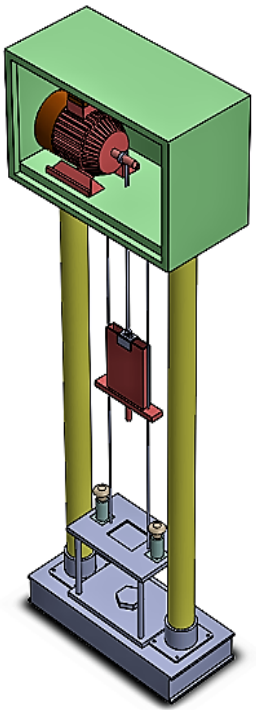

Figure 3.17: 3D model of concept 1

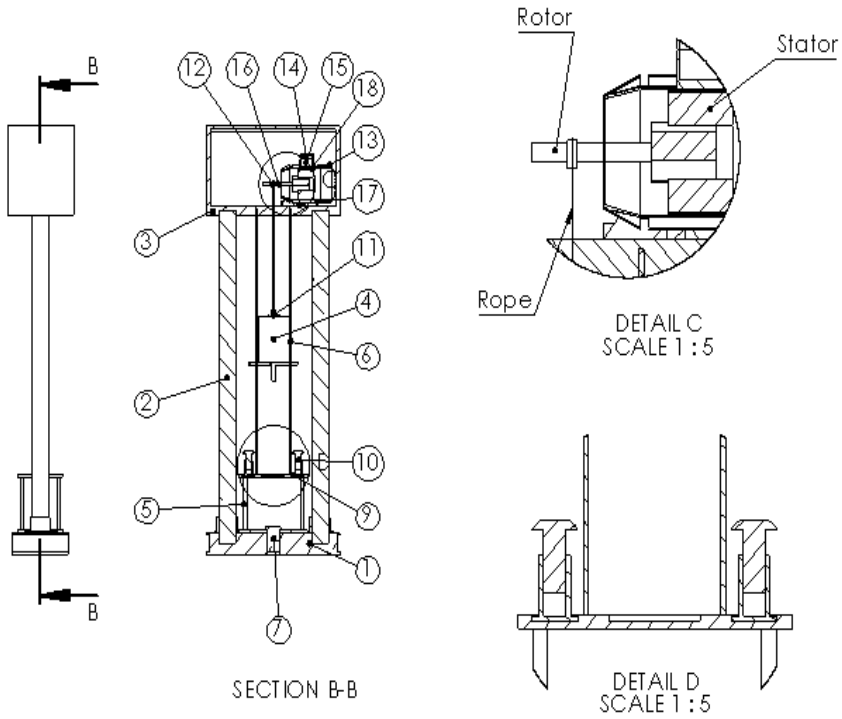

Figure 3.18: Sectional view of concept 1

The motor (i.e. 13, 14, 15 are motor covers , 16 is the rotor, 17 is the stand and 18 is the stator) used to elevate the impactor (4) where the impactor slides on the guide columns (2). The guide columns fixed on the foundation (1) and the motor housing (3). Supporting frames (2) which are fixed on the foundation help to hold the motor housing and additional support for the impactor.

Concept 2: Pendulum type impactor

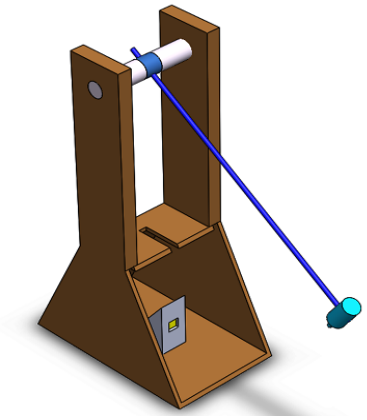

Figure 3.19: 3D model of Concept 2

The impactor (6) raised to some predetermined height using swinging pole (2) and impacted on the specimen which is fixed on the specimen fixture (5). The frame (1) contains the swing (3) which the swinging pole attached to the bearing (4).

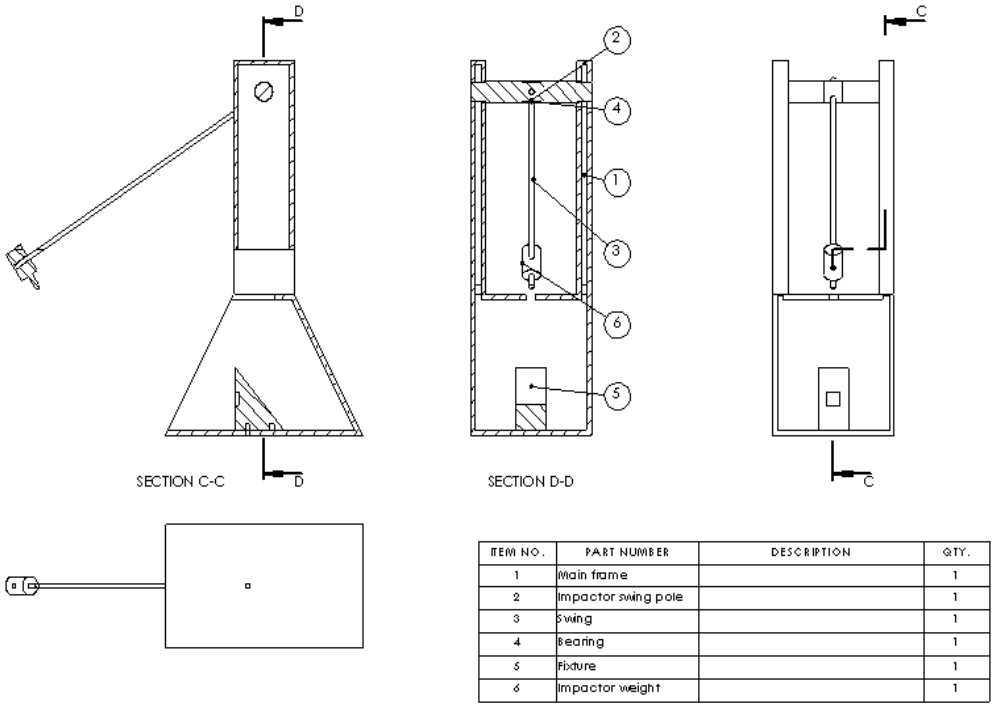

ITEM NO.	PART NUMBER	DESCRIPTION	QTY.
1	Main frame		1
2	Impactor swing pole		1
3	Swing		1
4	Bearing		1
5	Fixture		1
6	Impactor weight		1

Figure 3.20: Sectional view of Concept 2

Concept 3: One column pipe type impactor

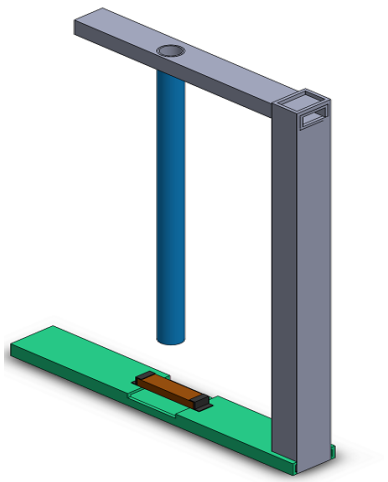

Figure 3.21: 3D model of Concept 3

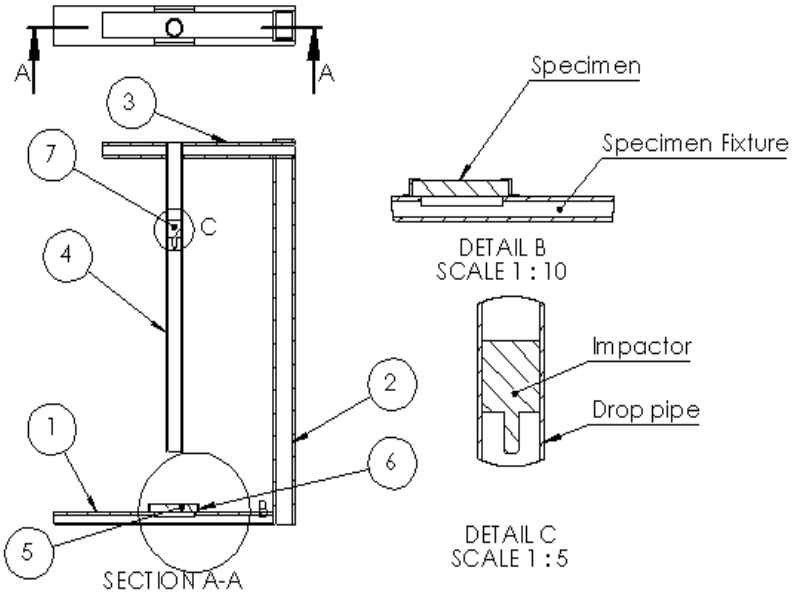

Figure 3.22: Sectional view Concept 3

1: Base of drop tower, 2: Tower, 3: Guide pipe beam 4: Drop pipe (impactor guide), 5: Specimen, 6: Specimen fixture 7: Striker.

In this concept, second impact prevented manually by stopping the impactor with a wood or metal insertion in the drop pipe. Pipe friction can be mentioned as the drawback of this concept.

B. Search internally

Te following two concepts generated internally which means the design used own knowledge and found nowhere.

1. **Concept 4: Roller Coaster type of impactor**

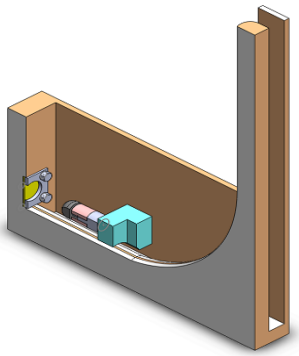

Figure 3.23: 3D model of Concept 4

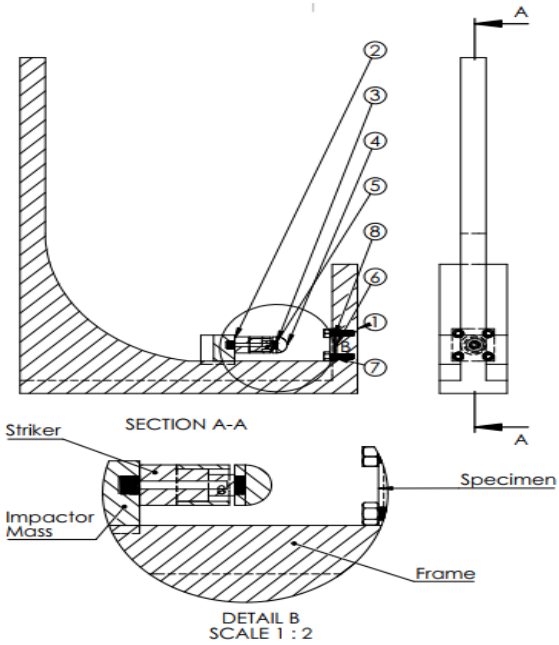

Figure 3.24: Sectional view of Concept 4

The impactor mass (2) which contains instrumented striker (3, 4 and 5) raised to predetermined height manually and released so that it follows the curved path of the frame (1). The specimen (6) fixed on the fixture (7) with a bolt (8).

Second impact prevented manually using a wood or metal insertion between impactor and specimen.

2. **Concept 5: Wide-flanged type of impactor**

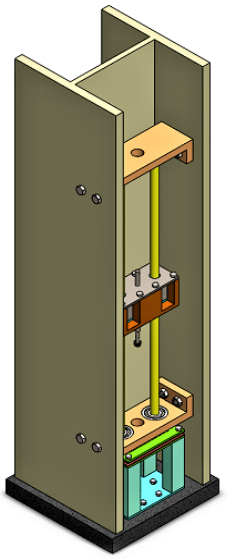

Figure 3.25: 3D model of Concept 5

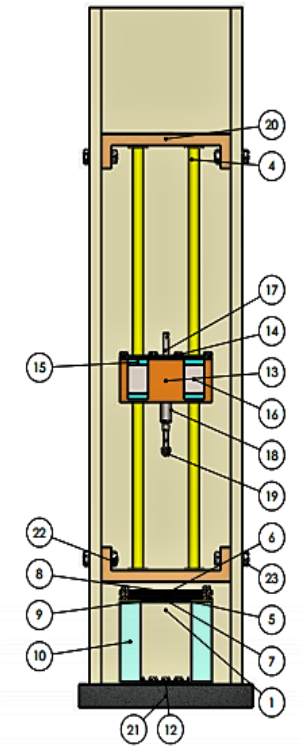

A standard specimen (5) ($150mm \times 100mm$) is clamped between on a given fixture ($6-9$) (i.e with a screw). The impact assembly ($13-17$) slides on

the friction less guide rods (4) again attached to support brackets (20) is then moved until the desired drop height met. The indentor assembly (18, 19), to which a variable mass is attached, is released from a drop height and hits the target specimen. Sensors attached to the striker tup and it intern attached to the data acquisition element which selected based in the experimental investigation phase.

3.1.6 Concept Evaluation

The $ASTM\ D7136/D7136M - 07$, 2005 in figure 3.10 used as a reference concept which other concepts screened and scored relative to this reference concept.

Concept screening

Table 3.9: The concept screening matrix

Concepts						
Selection criteria	REF	1	2	3	4	5
Physical Requirements:						
• Portable	0	0	+	−	+	0
• Lightweight	0	0	+	−	+	+
• Material strength	0	0	-	0	0	+
• Durable	0	-	-	-	0	+
• Space utilization	0	0	+	0	+	0
Performance						
• Convert energy efficiently	0	0	-	-	-	0
• Low noise	0	0	+	-	-	0
• Low energy dissipation	0	0	0	-	-	0
• Low friction between impactor assembly and guide	0	+	+	-	-	0
• Low vibration	0	-	+	-	0	0
• Ease to raise/lower impactor assembly	0	+	0	0	-	0
• Ease of impactor control	0	0	-	-	+	+
• Aesthetically appealing	0	0	-	0	-	+
Assembly						
• Ease to assemble	0	-	+	-	+	0
• Ease to disassemble	0	-	-	-	+	0
• Moderate assembly time	0	0	+	-	+	0
• Not too many parts	0	0	+	-	+	0
• Interesting to built	0	0	-	-	-	+

Cost						
• Low replacement of parts	0	0	0	-	0	0
• Inexpensive to built	0	0	+	-	+	+
• Retails for less than the competitors	0	0	+	0	+	+
Safety						
• Low pollution	0	0	0	-	0	+
• No sharp corner	0	0	0	0	0	0
• Safe to operation	0	0	-	-	-	0
Sum +'s	0	2	10	6	10	9
Sum 0's	24	18	5	6	6	15
Sum −'s	0	4	8	18	7	0
Net score	0	-2	2	-12	3	9
Rank	**4**	**5**	**3**	**6**	**2**	**1**
Continue ?	No	No	Yes	No	Yes	Yes

Concept Scoring

Table 3.10: The concept-scoring matrix.

Concepts									
		REF		**2**		**4**		5	
Selection criteria	**Weight %**	**Rating**	**Weighted score**	**Rating**	**Weighted score**	**Rating**	**Weighted score**	**Rating**	**Weighted score**
Portable	5	3	0.15	4	0.20	3	0.15	3	0.15
Lightweight	4	3	0.12	4	0.16	2	0.08	3	0.12
Material strength	4	3	0.12	2	0.08	3	0.12	4	0.16
Durable	5	3	0.15	2	0.10	3	0.15	3	0.15
Space utilization	4	3	0.12	4	0.16	3	0.12	4	0.16
Convert energy efficiently	6	3	0.18	2	0.12	3	0.18	3	0.18
Low noise	3	3	0.09	3	0.09	2	0.06	3	0.09
Low energy dissipation	6	3	0.18	2	0.12	3	0.18	3	0.18
Low friction between impactor assembly and guide	5	3	0.15	4	0.20	3	0.15	4	0.20
Low vibration	4	3	0.12	2	0.08	3	0.12	3	0.12
Ease to raise/lower impactor assembly	5	3	0.15	4	0.20	3	0.15	4	0.20
Ease of impactor control	4	3	0.12	2	0.08	3	0.12	3	0.12
Aesthetically appealing	2	3	0.06	2	0.04	2	0.04	3	0.06
Ease to assemble	5	3	0.15	4	0.20	2	0.10	4	0.20
Ease to disassemble	5	3	0.15	2	0.10	2	0.10	4	0.20
Moderate assembly time	3	3	0.09	4	0.12	2	0.06	3	0.09
Not too many parts	4	3	0.12	4	0.16	2	0.08	4	0.16

Interesting to built	2	3	0.06	2	0.04	3	0.06	4	0.08
Low replacement of parts	4	3	0.12	2	0.08	3	0.12	3	0.12
Inexpensive to built	6	3	0.18	4	0.24	3	0.18	4	0.24
Retails for less than the competitors	3	3	0.09	4	0.12	3	0.09	3	0.09
Low pollution	3	3	0.09	3	0.09	3	0.09	3	0.09
No sharp corner	4	3	0.12	2	0.08	2	0.08	2	0.08
Safe to operation	4	3	0.12	2	0.08	4	0.16	3	0.12
Total score		3		2.94		2.97		3.27	
Rank		2		4		3		1	
Continue ?		No		No		No		Develop	

3.2 Detail Design

3.2.1 Introduction

Two points examined in the literature review. First, the nature of composite material under low velocity impact and the key forces and the nature of results to be obtained identified. Second, existing drop weight impactors were reviewed and key design features were assessed. Third, the drop weight impactor designed in this chapter to satisfy the features identified in the literature review.

The type of impact machine used is defined through product development process and citing examples of other configurations. The designed drop weigh impact-testing machine consists of three major components: the impactor assembly with striker of known mass and fixed shape, the drop tower, the specimen fixture which holds the specimen. Each of these major components are further subdivided into sub-assemblies depending on function or purpose.

Computer-aided-design (CAD) software used for the solid modelling and drafting processes. The final drawings of the DWITM are given in Appendix B.

3.2.2 Test Specimen Design

In this work any available, constructed composite material listed in Table A.1, which found in the institute's laboratory can be used. The most important is the geometries of the specimen and theoretical strength/or stiffness on the test specimen.
The test specimen selected is flat rectangular according to ASTM D7136/7136M standard.

Flat Rectangular specimen

The standard [3] required the rectangular drop-weight impact test specimen (150mm ×100mm) with the longitudinal axis in the 0° direction. Moreover, the prepared specimens impacted under various impact energy levels. The work chooses the specimen illustrated in figure 3.26.

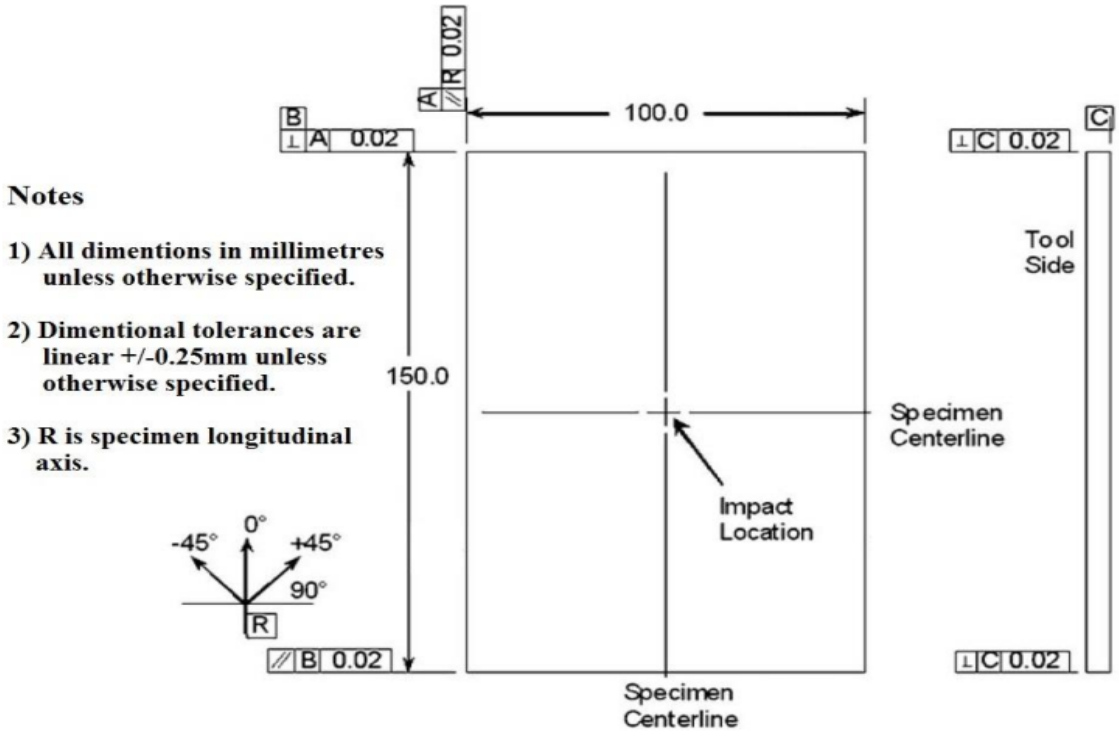

Figure 3.26: Standard Test Specimen per ASTM D7136/D7136M-05 [3]

Theoretical reduction in strength

Hence, knowing the imparted energy (E_I), tensile strength, constant K_1, and $W_2(A_d)$ the residual strength of an impacted specimen maybe evaluated. All calculation steps found in appendix D.1.

$$\sigma_{ds} = \sigma_{us}\left[1 - \frac{1}{K_I W_{us}}\left[E_I - W_2(A_d)\right]\right]^{1/2} \tag{3.1}$$

Where, σ_{ds} is maximum applied stress in the damaged specimen.

Theoretical Reduction in Stiffness

Stiffness, measure of load required to create a deformation in the test material [9]. Theoretically calculations to find the material stiffness and toughness of damaged specimen are found in Appendix D.1.

$$E = \frac{d(\sigma)}{d\epsilon} = \frac{3}{2}\frac{\sigma_m}{\epsilon_m}\left(1 - \frac{\epsilon}{\epsilon_m}\right)^{1/2} \tag{3.2}$$

At $\epsilon = 0$

$$\boxed{E = \tfrac{3}{2}\tfrac{\sigma_m}{\epsilon_m}} \tag{3.3}$$

where, σ_m =maximum stress, ϵ_m =maximum strain

The material toughness will be theoretically computed, if the area under the Load Extension curve is evaluated (provided the end points of the curve are known). Toughness of damaged specimen is given as:

$$\Rightarrow \quad \boxed{W_{ds} = \tfrac{3}{5}\sigma_m\epsilon_m} \tag{3.4}$$

3.2.3 Test Ranges

For comparison screening of the drop-weight impact damage resistance of the selected composite material, the standard specimen thickness shall be 4.0 to 6.0 mm with a target thickness of 5.0 mm [3].

In order to properly define a test procedure in which sets of results could be compared it was necessary to understand the effect of specimen thickness on the impact response. Using these thickness ranges, calculate the impact energy level using equation 3.5 unless otherwise specified.

$$E = C_E h \tag{3.5}$$

Where:

E = potential energy of impactor prior to drop, J

C_E = specified ratio of impact energy to specimen thickness, 6.7 J/mm, and

h = nominal thickness of specimen, mm.

According to the standard [3] at section 7.3.1 the impactor shall have a mass of 5.5±0.25 kg and a hardness of 60 to 62 HRC and also must permit a minimum drop height of 300 mm. Table 3.2.3 illustrates the energy and drop height levels using the given impactor mass and specimen thickness.

Table 3.11: Drop weight impact parameters

Thickness (mm)	C_E (J/mm)	Energy (J)	Mass (kg)	Height (m)	Velocity (m/s)
4	6.7	26.8	5.5	0.496710221	3.121771059
4.25	6.7	28.475	5.5	0.52775461	3.217847954
4.5	6.7	30.15	5.5	0.558798999	3.311138228
4.75	6.7	31.825	5.5	0.589843388	3.401871143
5	6.7	33.5	5.5	0.620887777	3.490246149
5.25	6.7	35.175	5.5	0.651932166	3.576438045
5.5	6.7	36.85	5.5	0.682976555	3.660601044
5.75	6.7	38.525	5.5	0.714020943	3.742872013
6	6.7	40.2	5.5	0.745065332	3.823373094

For target thickness of 5 mm based on the ASTM D7136 standard, the impact parameters can be found,

- the maximum potential energy level is 33.5 J.

Using equation 2.1 and 2.3 with a mass of 5.5 kg;

- maximum drop height of 0.62 m
- maximum velocity of 3.49 m/s

3.2.4 Floor plan of workspace (Foundation)

As we can see in Figure 3.27, the guide columns, specimen fixture, and guide rails of impacting body fit in the area of 25.4 $cm \times 15.4$ cm of the $W310 \times 143$ wide flanged steel column. Since no additional area is required, the total working area have the area of the wide flanged steel column support with additional clearances. Taking a clearance of 0.9 cm and 2 cm in the x and y directions respectively. Which finally compacts the total area of the machine to a square dimension of 34 $cm \times 34$ cm (length$\times$width).

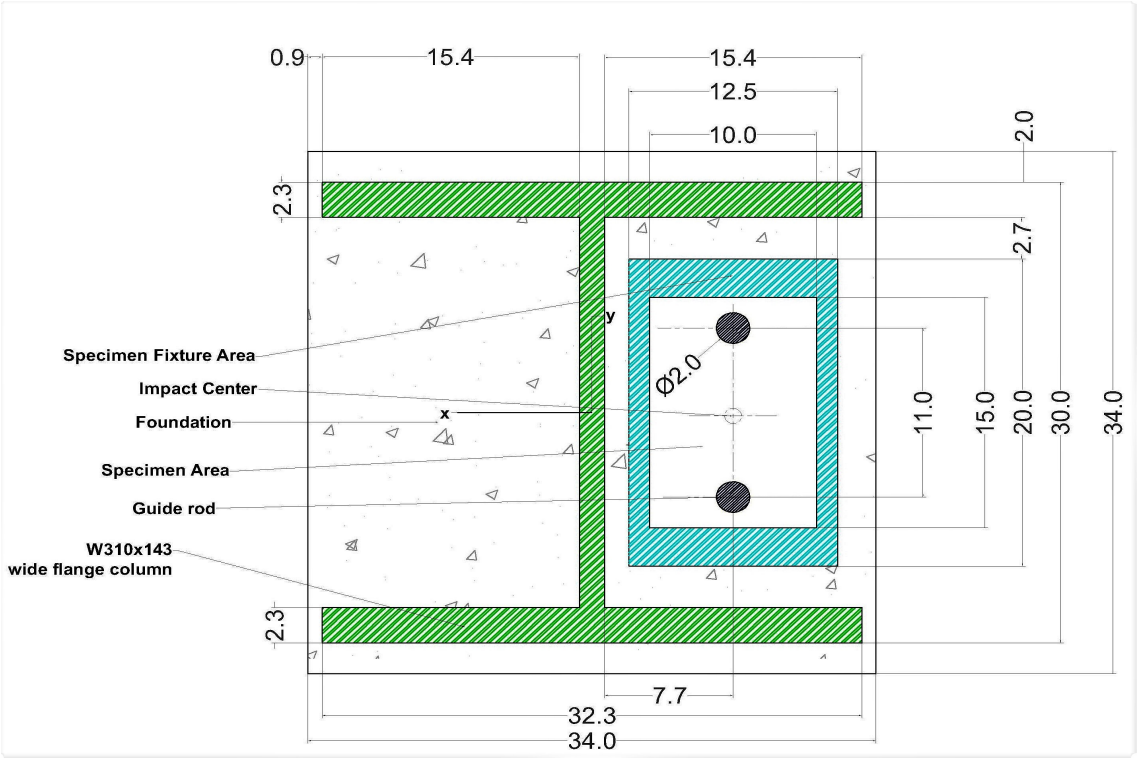

Figure 3.27: CAD model of working area of DWITM, where all dimensions are in cm.

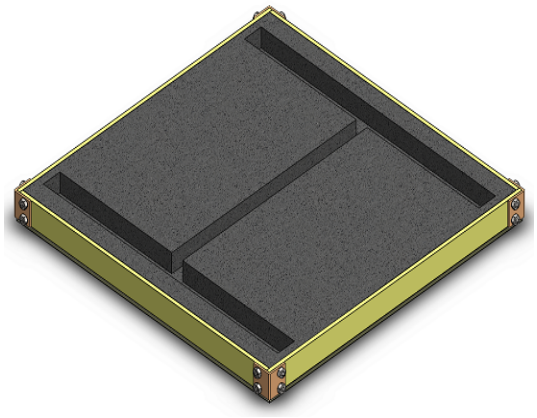

Figure 3.28: CAD model of foundation

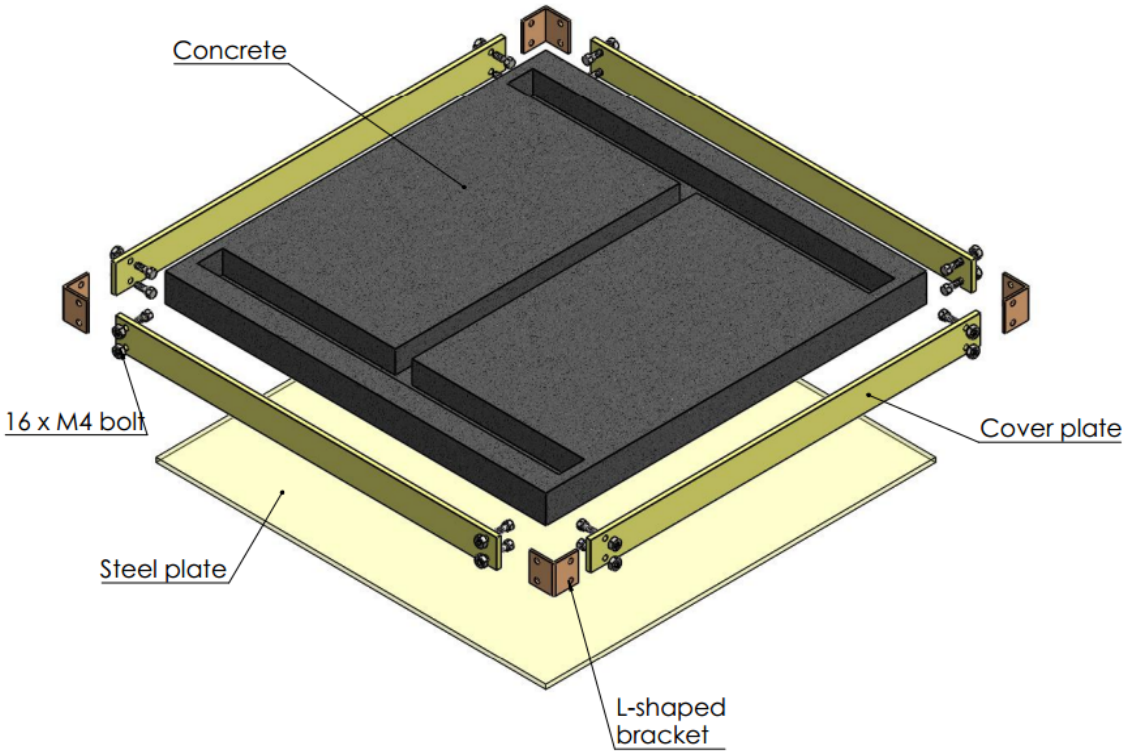

Figure 3.29: Exploded view of foundation

3.2.5 Specimen Support (Fixture)

The ASTM D 7136 standard lists basic requirements which affect the design of the specimen fixture. These requirements are given on the application section in the standard.

Section 7.2 [3] of the standard requires,

- The exposed specimen surface underneath the specimen be a 76.2 mm by 127 mm rectangular area centered with respect to the specimen.
- The specimen be clamped to the surface of the support structure by a minimum of 890 N.
- The fixture contact the upper surface of the specimen using neoprene rubber of $(211mm \times 125mm \times 2.5mm)$.
- Guide pins be placed on the support fixture in order to locate the specimen centrally over the 76.2 mm by 127 mm exposed area underneath the specimen.
- The length of specimen fixture must be shorter than 283 mm. The width must be shorter than 153 mm to fit between the guide rails. The specimen must sit at a height of 153 mm or higher. All components of the specimen fixture must fit within this volume.

Relation between specimen fixture area and total dimension of the machine (from target specification),

i . the fixture length should be less than 283 mm and the length of the machine should be less than 340 mm.

ii . the fixture width should be less than 153 mm and total width of the machine should be less than 340 mm

Based on this information the following table developed where the minimum length of the fixture should be the specimen length which is 150 mm and the minimum width of the fixture should be the specimen width which is 100 mm.
The factor for length table 3.12,

$$Factor_{length} = \frac{283}{150} = 1.89 \tag{3.6}$$

Based on Table 3.12, the length of specimen fixture is then 180 mm.

- Assume that the ratio of length to width of the specimen equals to the ratio of length to width of the specimen fixture.

Table 3.12: Specimen fixture length iteration table

length of specimen fixture (mm)	Total length of the machine (mm)
150	283.5
152.5	288.225
155	292.95
157.5	297.675
160	302.4
162.5	307.125
165	311.85
167.5	316.575
170	321.3
172.5	326.025
175	330.75
177.5	335.475
180	340.2
182.5	344.925
185	349.65
187.5	354.375
190	359.1
192.5	363.825
195	368.55
197.5	373.275
200	378

Now, take the ratio of specimen $\frac{length}{width} = \frac{150}{100}$ which is 1.5. Then the ratio of specimen fixture $\frac{lenght}{width} = 1.5$, this gives the width of specimen fixture;

$$Width_{(fixture)} = \frac{Length_{fixture}}{1.5} = \frac{180}{1.5} = 120mm \tag{3.7}$$

The specimen fixture fixed onto the foundation by fixing bolts ($6 \times M8$) which can be disassemble from the foundation when needed. By varying the cut-out window of specimen fixture, different test specimens can be tested. The maximum allowable size of the specimen fixture is has a length of 180 mm, width of 120 mm and total height of 165 mm including the test specimen.

Material Selection

In most literatures, material for the fixture plate is low carbon steel. Based on this $SAE/AISI$ 1006 low carbon steel selected as a first trial which is mainly soft, ductile and cheap; and has the following mechanical properties.

- $Tensile\ strength(S_{ut}) = 300$ MPa.
- $Yield\ strength(S_y) = 170$ MPa

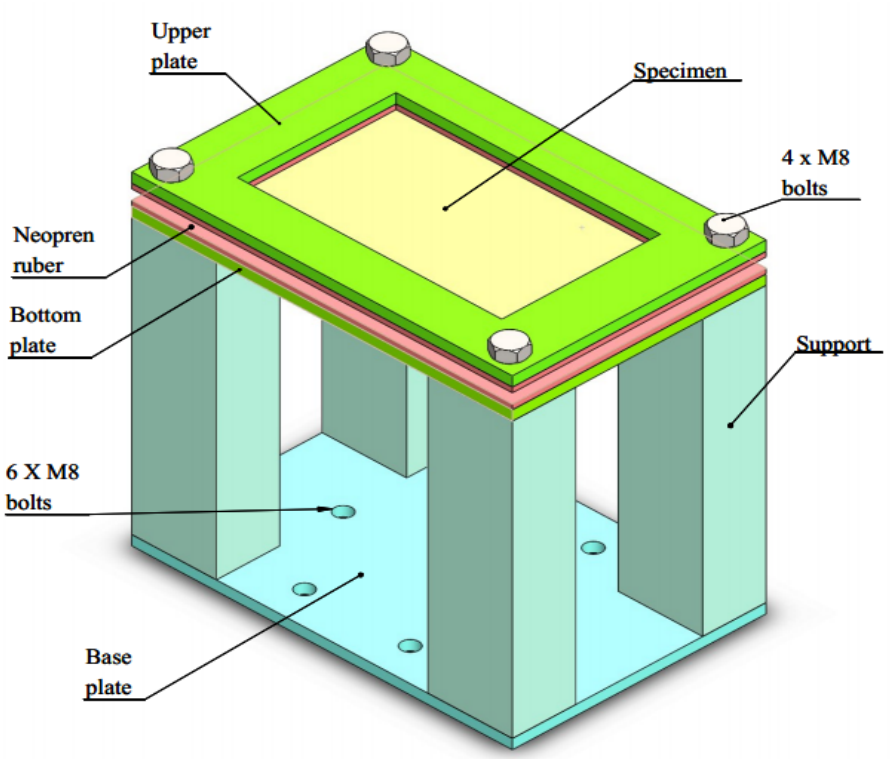

Figure 3.30: CAD Modelling of Specimen Fixture

Plate Design

The plate is subjected to impact load which makes this component critical to design. The calculations of the base plate of the machine are carried out by simulating it with a mass-spring system. After calculating spring constant of plate, its deflection is calculated and finally the stress is obtained. Detail calculations found in Appendix D.2.

Stress on the plate for concentrated force acting found as:

Givens: $m = 5.5kg, g = 9.81m/s^2, h = 0.62m, t = 20mm, E = 210GPa, v = 0.3$

$$\sigma_x = \frac{6M_y}{at^2} = 257MPa \tag{3.8}$$

$$\sigma_y = \frac{6M_x}{at^2} = 419MPa \tag{3.9}$$

Let $\sigma_x = \sigma_A$, $\sigma_y = \sigma_B$ and $\sigma_3 = 0$, the von Mises stress ($\sigma^{'}$)

$$\sigma^{'} = \left(\sigma_A^2 - \sigma_A\sigma_B + \sigma_B^2\right)^{1/2} = 366MPa \tag{3.10}$$

$$SF = \frac{S_y}{\sigma^{'}} = \frac{170MPa}{366MPa} = 0.46 \tag{3.11}$$

Which fails based on the selected material.

Lets selected more stronger material, where it's yield strength is greater than the von Mises stress. Based on this from Table A, $SAE/AISI$ No. 1045 CD selected which have;

- Tensile strength (S_{ut}) = 630 MPa
- Yield Strength (S_y) = 530 MPa

Then, the safety factor;

$$SF = \frac{530}{366} = 1.45 \tag{3.12}$$

Which is safe against impact loading.

3.2.6 Drop Tower

In designing the drop tower, this work had two primary concerns;

1. the strength of the structure, i.e., its ability to support a load without experiencing excessive stress;
2. the ability of the structure to support a specified load without undergoing unacceptable deformations.

In order to meet these requirements, the proposed tower consists of two separate structures i.e. two vertical guide rods which the impactor slides on and a supporting frame (Wide flanged-beam). The purpose of separating is for assembly disassembly.

The drop weight tower consists of Wide flanged section steel beam and two steel

guide columns where the frames directly attached to the foundation, having a total height of 1.2 m; and the guide columns which are circular with a diameter and height of 20 mm and 77 mm respectively. The guide rods directly attached to the hole created on support brackets.

Wide Flanged Frame

Wide-flange W310×143 selected for the purpose of attaining vertical guidance system for the impactor and easy assembly and disassembly between guide columns and the frame, in addition it makes the whole machine simple and compacted where all components of the machine incorporated in the section steel frame. Its detail geometry listed in Appendix A.

Material selection

Material selection for the frame started from inexpensive and easily available material. Based on these requirements ASTM A36 steel section selected which its specification covers carbon steel shapes, plates, and bars of structural quality for use in riveted, bolted, or welded construction of bridges and buildings, and for general structural purposes. It has the following mechanical properties;

- Yield strength = $250MPa$
- Modulus of elasticity, $E = 210,000N/mm^2$
- Shear modulus, $G = E/[2(1 + v)]N/mm^2$, often taken as $81,000N/mm^2$
- Poisson's ratio, v = 0.3
- Coefficient of thermal expansion, $\alpha = 12 \times 10^{-6}/^{\circ}C$ (in the ambient temperature range).

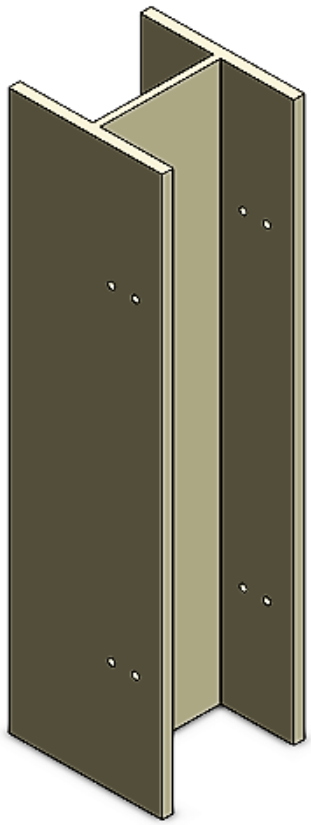

Figure 3.31: CAD model of Wide Flanged support (W310×143)

Guide Rods

There are two guide rods which the impactor slide on and impact the specimen.

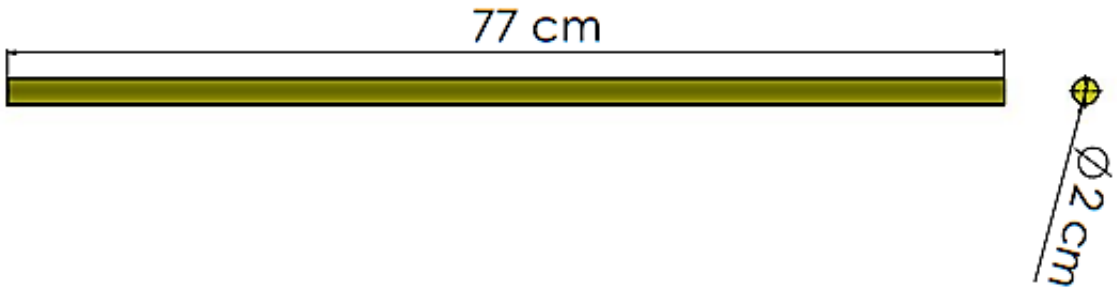

Figure 3.32: CAD Model of Guide rod

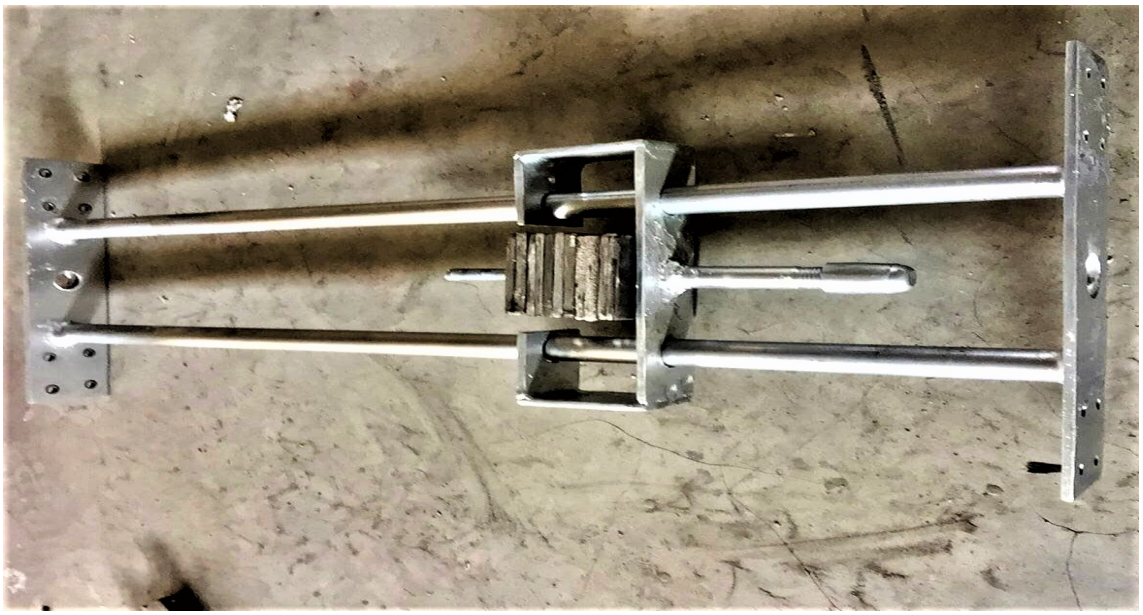

Figure 3.33: Guide Rods with impacting mass (after prototyping)

Material selection:

Stainless steel is a highly corrosive resistant material that can be used structurally, particularly where a high-quality surface finish is required (minimum friction between impactor and guide rod). From *Shigley's Mechanical Engineering Design* 9^{th} *Edition Textbook*, $AISI$ 304 annealed stainless steel selected with mechanical properties listed in Appendix A.

- Yield strength $(\sigma_y) = 273MPa$
- Ultimate Tensile strength $(\sigma_{ut}) = 568MPa$

Design of columns under load

The main criterias listed in the beginning paragraph relate chiefly to columns, i.e., to the analysis and design of wide flange steel section (main support structure) and AISI 340 stainless steel guide columns.

The formulas most widely used for the allowable stress design of steel columns under a centric load are found in the Specification for Structural Steel Buildings of the American Institute of Steel Construction. An exponential expression is used

to predict σ_{all} for columns of short and intermediate lengths, and an Euler-based relation is used for long columns [6].

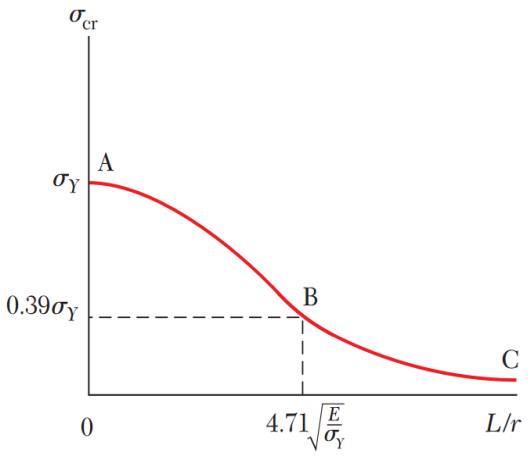

Figure 3.34: Steel column design[6]

The design relations are developed in two steps:

1. First a curve representing the variation of critical stress (σ_{cr}) with slenderness ($\frac{L}{r}$) is obtained (Fig. 3.34. It is important to note that this curve does not incorporate any factor of safety. The portion AB of this curve is defined by the equation

$$\sigma_{cr} = \left[0.658^{\frac{\sigma_Y}{\sigma_e}}\right] \sigma_Y \tag{3.13}$$

$$Where, \sigma_e = \frac{\pi^2 E}{(L/r)^2} \tag{3.14}$$

The portion BC is defined by the equation

$$\sigma_{cr} = 0.877\sigma_e \tag{3.15}$$

Note that when $L/r = 0$, σ_{cr}=σ_Y in Eq. 3.13. At point B, Eq. 3.13 joins Eq. 3.15. The value of slenderness L/r at the junction between the two equations is

$$\frac{L}{r} = 4.71\sqrt{\frac{E}{\sigma_Y}} \tag{3.16}$$

If L/r is smaller than the value in Eq. 3.16, σ_{cr} is determined from 3.13,

and if L/r is greater, σ_{cr} is determined from Eq. 3.15. At the value of the slenderness L/r specified in Eq. 3.16, the stress $\sigma_e = 0.44\sigma_Y$. Using Eq. 3.15, $\sigma_{cr} = 0.877(0.44\sigma_Y) = 0.39\sigma_Y$.

2. A factor of safety must be introduced to obtain the final AISC [1]design formulas. The factor of safety specified by the specification is 1.67. Thus

$$\sigma_{all} = \frac{\sigma_{cr}}{1.67} \tag{3.17}$$

For the Guide rods

The guide rods are fixed at both ends with a bearing that no rotation can occur.

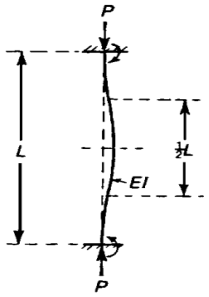

Figure 3.35: Buckling of guide rod with fixed ends

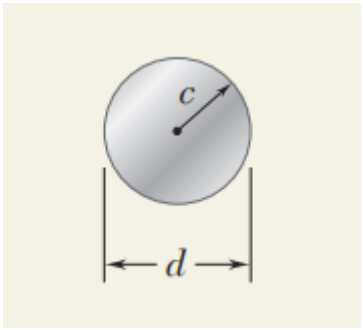

Figure 3.36: Cross section of guide rods

For the cross section of AISI 304 stainless steel guide rods (solid circular rod), we have $c = 10mm, E = 193Gpa$, $\sigma_Y = 273MPa$

[1]The American Institute of Steel Construction (AISC) is a not-for-profit technical institute and trade association for the use of structural steel in the construction industry of the United States.

$I = \frac{\pi}{4}c^4 = 7.854 \times 10^{-9}m^4$, $A = \pi c^2 = 3.14 \times 10^{-4}m^2$

$r = \sqrt{\frac{I}{A}} = \frac{c}{2} = 0.005m$

Slenderness, $\frac{L}{r} = \frac{0.77m}{0.005} = 154$ and $4.71\sqrt{\frac{E}{\sigma_Y}} = 4.71\sqrt{\frac{193\times10^9}{273\times10^6}} = 127.5$

which $\frac{L}{r} > 4.71\sqrt{\frac{E}{\sigma_Y}}$, therefore we will use equation 3.15 to calculate the critical stress on the guide rod.

$\sigma_{cr} = 0.877\sigma_e = 0.877(\frac{\pi^2 E}{(L/r)^2}) = 80.3MPa$

Thus the allowable stress,

$\sigma_{all} = \frac{\sigma_{cr}}{1.67} = 48.1MPa.$

Finally, the allowable load which the guide rod can support is given as;

$\sigma_{all} = \frac{P_{all}}{A}, P_{all} = \sigma_{all} \times A$

$P_{all} = 15.1kN$

The buckling load (see figure 3.35) is therefore can be calculates as;

$$P_{cr} = \frac{\pi^2 EI}{(L/2)^2} = 4\pi^2\frac{EI}{L^2} = 4\pi^2\frac{193 \times 10^9 \times 7.854 \times 10^{-9}}{0.77^2} = 101kN \qquad (3.18)$$

Always the allowable load must be smaller than the critical load, which is satisfied.

For the W310×143 Support (vertical cantilever)

When a vertical load P (due to the mass of the guide columns) is applied to the

free end of a vertical cantilever beam (W shaped steel support, ABC), at the lowest critical load the laterally deflected form of column is a sinusoidal wave length of 2L.

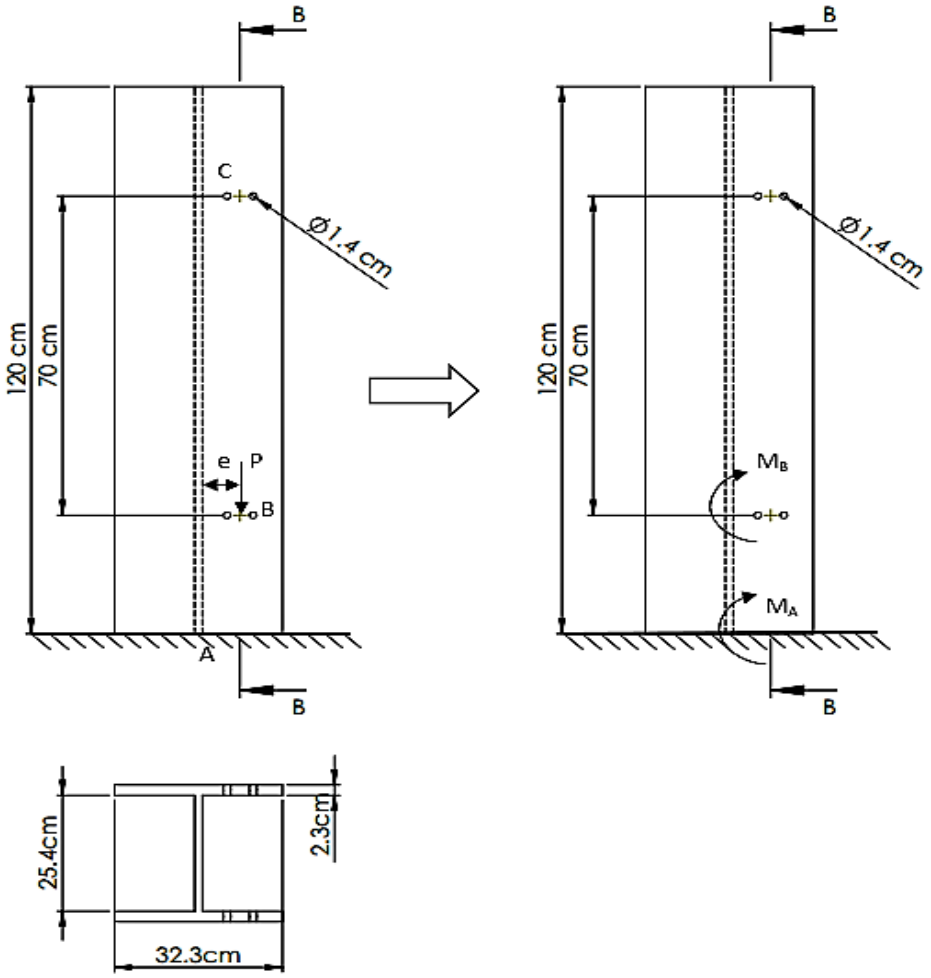

Figure 3.37: Applied force on the wide flanged beam

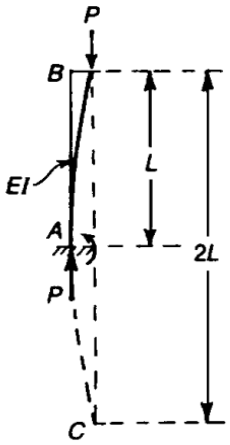

Figure 3.38: Buckling of column with one end free and the other built-in[6]

The buckling load is given as [6];

$$P_{cr} = \frac{\pi^2 EI}{(2L)^2} = \frac{\pi^2 EI}{4L^2}, where L_e = 2L \tag{3.19}$$

Given data:

$d = 323mm, b_f = 310mm, t_f = 23mm, t_w = 14mm, I_x = 343 \times 10^6 mm^4, I_y = 112 \times 10^6 mm^4, r_x = 138mm, r_y = 78.5mm, eccentricity(e) = 80mm$, total length of the column $(L) = 1200mm$. The effective length of the column is,$L_e = 2(1200) = 2400mm = 2.4m$.

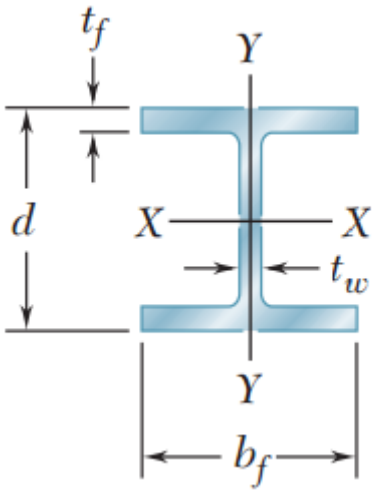

Figure 3.39: Cross section of W310×143 support structure (see Appendix A)

The largest slenderness ration of the column $\frac{L}{r_y} = \frac{2.4m}{78.5\times10^{-3}m} = 30.6$

Using equation 3.16 with $E = 210GPa, \sigma_Y = 250MPa$

$\frac{L}{r} = 4.71\sqrt{\frac{E}{\sigma_Y}} = 136.5.$

Thus using equation 3.13 and 3.14, the critical stress

$\sigma_{cr} = 0.877\sigma_e = 0.877[\frac{\pi^2 E}{(L/r)^2}] = 97.6MPa$

Using equation 3.16, the allowable stress is

$(\sigma_{all})_{centric} = \frac{\sigma_{cr}}{1.67} = \frac{97.6MPa}{1.67} = 58.44MPa$

Based on the allowable stress method for an eccentrically loaded columns is the same as if the column were centrally loaded.

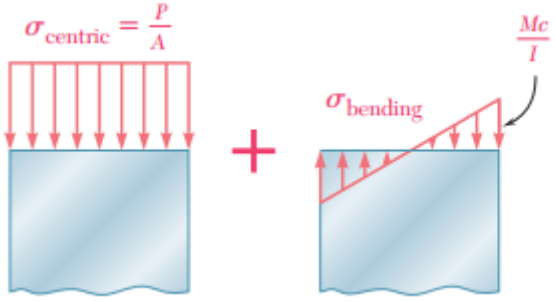

Figure 3.40: Stress on column transverse section [6]

The normal stress due to the eccentric load **P** can be expressed as;

$$\sigma = \sigma_{centric} + \sigma_{bending} \tag{3.20}$$

The maximum compressive stress in the column is given as (*refer section 4.12 of Beer Johnston Mechanics of Material* 6^{th} *Edition Textbook [6]*)

$$\sigma_{max} = \frac{P}{A} + \frac{Mc}{I} \tag{3.21}$$

In a properly designed column, the maximum stress defined by Eq. 3.21 should not exceed the allowable stress for the column. Therefor, $\sigma_{max} \leq \sigma_{all}$, thus equation 3.21

$$\frac{P}{A} + \frac{Mc}{I} \leq \sigma_{all} \tag{3.22}$$

$$\frac{Mc}{I} = \frac{M}{S_x} \tag{3.23}$$

$\frac{P}{18200\times10^{-6}} + \frac{P(0.08)}{2150\times10^{-6}} \leq 58.44MPa$

The largest load P that can be safely carried by a W310×143 steel column of 2.4-m effective length is;

$\rightarrow$ **P = 633 kN**

3.2.7 The Striker

The main design objective behind the construction of the striker head was to ensure that only the vertical component of the load on the striker head is measured. The striker rod is attached rigidly to the drop weight, which has a standard hemispherical tup of 16±1 mm diameter and a hardness of 60 to 62 HRC in accordance of ASTM-D 7136[3].

The impactor shape chosen so as to limit their deformability as much as possible and to assure their main function of transferring energy to the specimen without absorbing or dissipating it by elastic deformation or excessive oscillation (see Sec. 2.2.1 and 2.3.3).

- The tup can be replaced, which able to study the influence of impact parameters like size and shape of the impactor on the impact (not covered in this work).

Material selection

Bayer et al. [18] conducted a test on four different materials (Makrolon , titanium, aluminum and stainless steel) used to build up a suitable impactor for conducting a test. The research found out the following points.

- Stainless steel considered the least suitable material due to large errors even if coated with TiN,
- Aluminum results moderate deviation,
- Only titanium and Makrolon were proven to be widely suitable impactor materials

But titanium and Makrolon are not widely available and relatively expensive which this work not able to use those materials. Stainless steel widely used for its relative minimum cost and availability.

The striker shaft can be built from stainless steel material, but the tup which directly impact the test specimen should hardened material.

Instron Tups

Instron provides tup and inserts which comes in different shapes, sizes and weights. Most tups can be purchased with sensors to perform instrumented impact tests, as well as interchangeable inserts (the head of the tup). The required capacity depend on the application and based on the expected maximum load, not the machine's energy capacity.

It comes into two forms; strain gauge (for load values $> 5\ kN$) and piezoelectric (for testing light-load materials) types.

From Appendix A type 1 tup insert for strain gauge which accommodates ASTM D7136 standard testing method is 7529.322 (catalog number) with 16 mm Hemispherical selected.

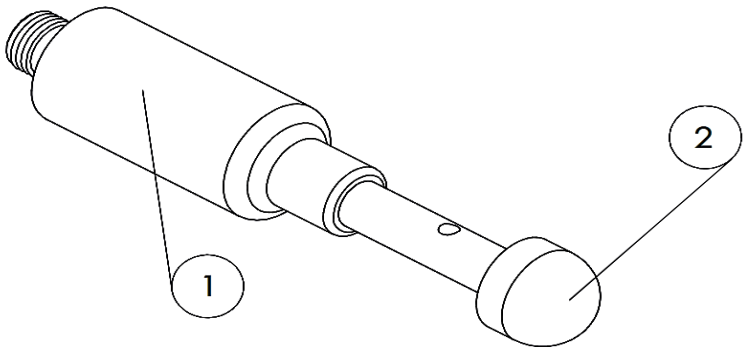

Figure 3.41: Exploded CAD view of striker assembly

Figure 3.42: Actual Prototype of striker assembly

Interchangeable tup design

The interchangeable tup which is non-instrumented shown in figure 3.41. Where the striker shaft (1) made of AISI 1020 steel attached to the impacting mass, the tup (2) which is AISI Type A2 tool steel, intern attached to (1).
The striker tup is 16-mm diameter hemispherical according to ASTM D7136 [3].

Figure 3.43: Modeled interchangeable hemispherical tup

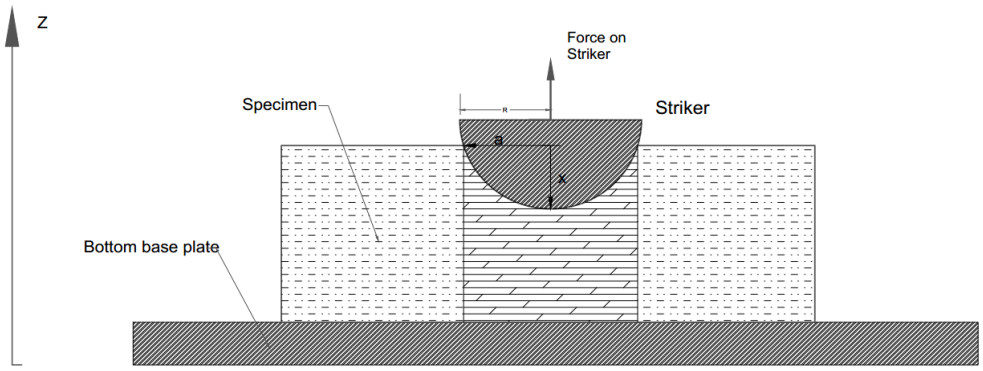

Figure 3.44: CAD model of parallel path model with a vertical compressive stress in the yielded zone

The parallel path model [59] shown in figure 3.44, the central deflection x is much smaller than the radius R of the hemispherical striker, the x^2 term can be ignored in the relationship between the contact radius a and x. Where $R = 8mm$,

$$a^2 = 2Rx - x^2 = 16x - x^2 \tag{3.24}$$

$$x^2 + 2Rx - a^2 = 0 \longrightarrow x^2 + 16x - a^2 = 0 \tag{3.25}$$

Equation 3.25 predicts the relation between contact radius's a and x. If the composite material has a constant compressive yield stress σ_y, the force F varies according to

$$F = 2\pi R\sigma_y x = 16\pi\sigma_y x \tag{3.26}$$

Where, the contact area is a function of x (i.e. $2\pi Rx$). The theory assumes that the only significant stress in the composite material is the compressive stress in the vertical (z) direction, which does not vary with the z coordinate, and is determined by the compressive strain in the z direction. No account is taken of shear strains at the sides of the indentation.

3.2.8 Impactor Assembly

From the point of view of strength, the impactor was the most critical element to design, since it is greatly stressed by the contact force during the impact and, at the same time, it must allow the mounting of fixed shape and variable mass. Based on the standard [3], the total mass of the impact assembly is 5.5 Kg (i.e. include the striker).

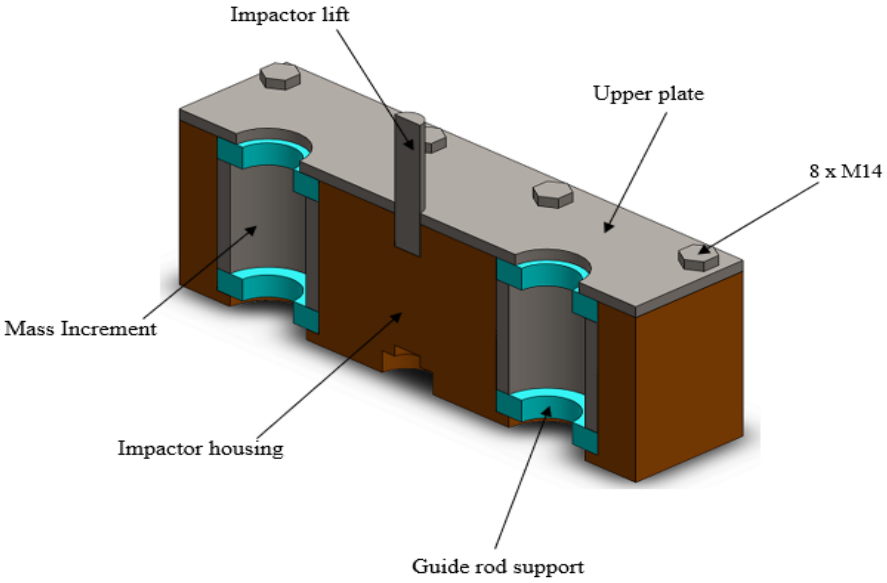

Figure 3.45: CAD Model of impactor assembly

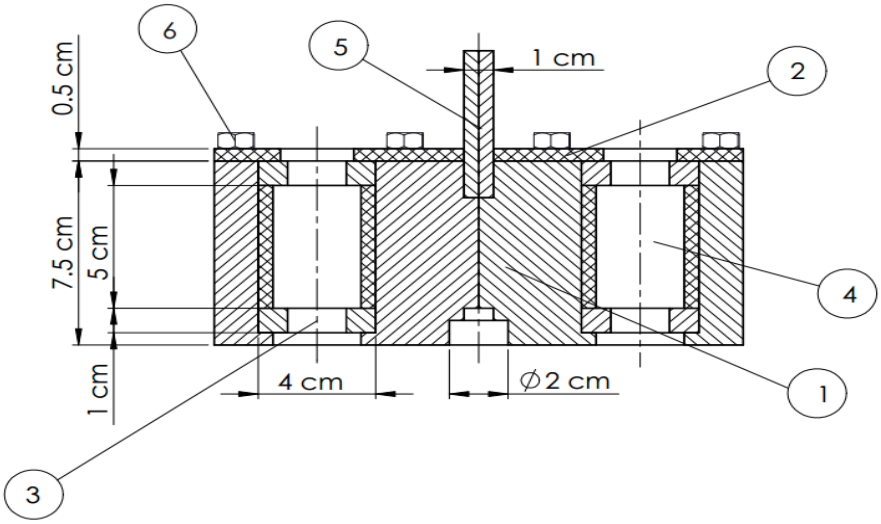

Figure 3.46: Sectional view of Impactor assembly

The impactor assembly composed of impactor housing (1), upper plate (2), guide rod holder (3), mass increment (4), lifting rod (5) and $8\times M6$ fixing bolts.

It should fit in the area of the wide flanged frame (see section 3.2.4) and between guide columns. Allowing a clearance of 2 mm between impactor assembly and drop tower, the total dimension of impactor assembly is then $18cm \times 8.5cm \times 8cm$.

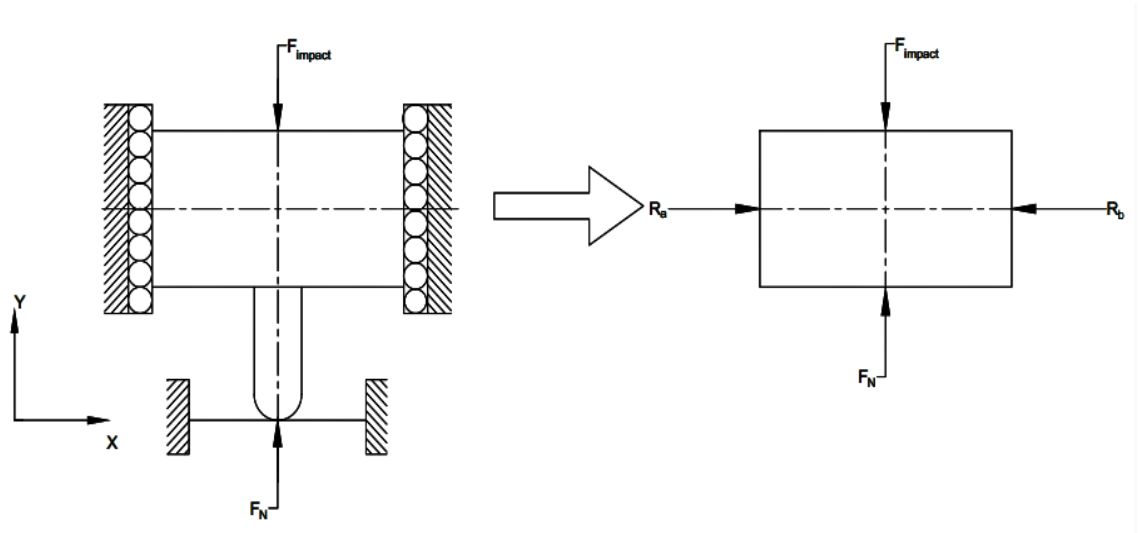

Figure 3.47: Schematic illustration of impact event and system of forces

Strength analysis on impactor assembly

The main requirement in designing impactor assembly is minimum friction between guide rods and impactor, which means the contact area between the impactor and guide rods should be minimum at the same time keeping verticality. Due to this guide rods inserted (3) as shown in figure 3.46 to fulfill this requirement. By considering these requirements the work come up with impactor assembly configuration shown in Figure 3.45.

Material Selection

For impactor assembly, starting from low carbon steel AISI 1006 HR with;

- Tensile strength (σ_{ut})= 300 MPa
- Yield strength (σ_y)=170 MPa

As we can see in figure 3.47, there are 4 (four) forces at the moment of impact i.e.

- F_I = Impact force of impactor
- F_N = Normal force from specimen support

$$\sum F_y = 0 \longrightarrow F_N = F_I \tag{3.27}$$

The impactor has a $(b \times h)$=$8.5 \times 8cm = 6.8 \times 10^{-3}m^2$ rectangular cross section, the centroidal moment of inertia of rectangular cross section is;

$$I = \frac{1}{12}bh^3 = \frac{1}{12}(0.085)(0.08)^3m^4 = 3.63 \times 10^{-6}m^4 \tag{3.28}$$

Assuming a factor of safety $(F.S)$ of 3, the allowable stress

$$\sigma_{all} = \frac{\sigma_{ut}}{F.S} = \frac{300}{3} = 100MPa \tag{3.29}$$

The largest moment that can be applied to the impactor (assumed as a beam) neglecting effects of fillet is

$$M = \frac{\sigma_{all}I}{c} = \frac{100 \times 10^6(3.63 \times 10^{-6})}{0.04} = 9kN.m \tag{3.30}$$

The largest force acting at the centroidal axis $(y^* = \frac{8}{2} = 4cm)$ on the impactor is

$$F = \frac{My^*A}{I} = \frac{9000 \times 0.04 \times 6.8 \times 10^{-3}}{3.63 \times 10^{-6}} = 674.4kN \tag{3.31}$$

The impactor can support maximum of 674.4 kN reaction force when the impactor falls on the specimen.

3.2.9 Design for bolt strength

Bolt strength is specified by stating SAE or ASTM minimum quantities:

i Minimum proof strength or minimum proof load: - maximum load (force) that a bolt withstand without permanent set.

ii Minimum tensile strength: the quotient of the proof load and tensile – stress area.

Bolts at the support bracket are subjected to maximum load, which makes them critical to design. The load P supported by bolts, is the weight of the guide rods and impactor assembly, lets take the allowable buckling load that the guide rods can support, which is 15.1 kN.

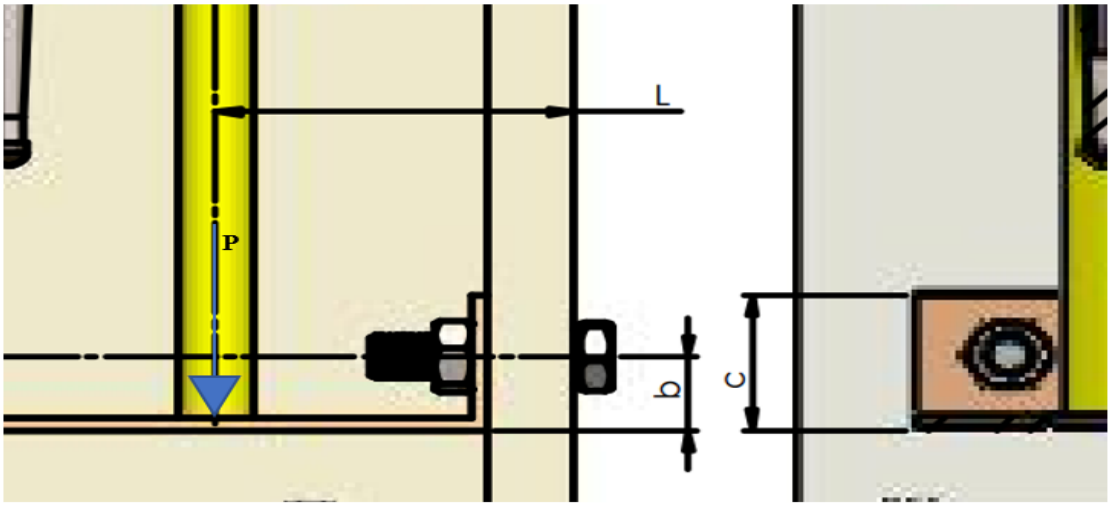

There are 4 bolts, the direct shear load on each bolt,

$$V = \frac{P}{n} = \frac{15.1}{4} = 3.775kN \tag{3.32}$$

Since the load P will try to tilt the support bracket in the clockwise (if the left half considered) and counterclockwise (if the right half considered) directions about the lower edge, which means the bolts will be subjected to tensile load due to turning moment. All bolts support equal loads due to their alignment.
The maximum tensile load, where L =95 mm, b =24 mm, c =44 mm.

$$P_t = \frac{P.L}{4b} = \frac{15.1 \times 95}{4 \times 24} = 14.94kN \tag{3.33}$$

Also, the bolts are subjected to shear load as well as tensile load, the equivalent tensile load,

$$P_{eq} = \frac{1}{2}\left[P_t + \sqrt{(P_t)^2 + 4(V)^2}\right] = \frac{1}{2}\left[14.94 + \sqrt{(14.94)^2 + 4(3.775)^2}\right] = 15.84kN \tag{3.34}$$

Size of the bolt

Let, d = core diameter of the bolt. Using load-stress relationship, the core diameter can be determined.

Property Class	Size Range, Inclusive	Minimum Proof Strength,† MPa	Minimum Tensile Strength,† MPa	Minimum Yield Strength,† MPa	Material	Head Marking
4.6	M5–M36	225	400	240	Low or medium carbon	
4.8	M1.6–M16	310	420	340	Low or medium carbon	
5.8	M5–M24	380	520	420	Low or medium carbon	
8.8	M16–M36	600	830	660	Medium carbon, Q&T	
9.8	M1.6–M16	650	900	720	Medium carbon, Q&T	
10.9	M5–M36	830	1040	940	Low-carbon martensite, Q&T	
12.9	M1.6–M36	970	1220	1100	Alloy, Q&T	

Figure 3.48: Metric Mechanical-Property Classes for Steel Bolts, Screws, and Studs [7]

Lets assume as first trial that the size of the bolt lies in property class 4.6 ($M5 - M36$), then from figure 3.48, minimum tensile strength σ_t=400 MPa. The core

diameter can be calculated from bolt area,

$$A_{bolt} = \frac{\pi}{4}d^2 = \frac{P_{eq}}{\sigma_b} = \frac{15.84kN}{400MPa} = 3.96 \times 10^{-5}m^2 \tag{3.35}$$

$$d = \sqrt{\frac{4A_{bolt}}{\pi}} = 7.1mm \tag{3.36}$$

The standard core diameter is 9.026 mm and the corresponding size of the bolt is $M10$

3.2.10 Support Bracket

Support bracket which directly fixed to the drop tower subjected to loads exerted by the weight of guide rod assembly. Since forces applied symmetrically, analyzing half of the support bracket is enough. Maximum load acted at the bottom support bracket, which makes it critical for failure compared to the upper bracket.

Given values: d $(thickness)$=4 mm, F (applied force = due to weight of guiding arms and top support bracket) = 70 kN, b (moment arm) = 72 mm.

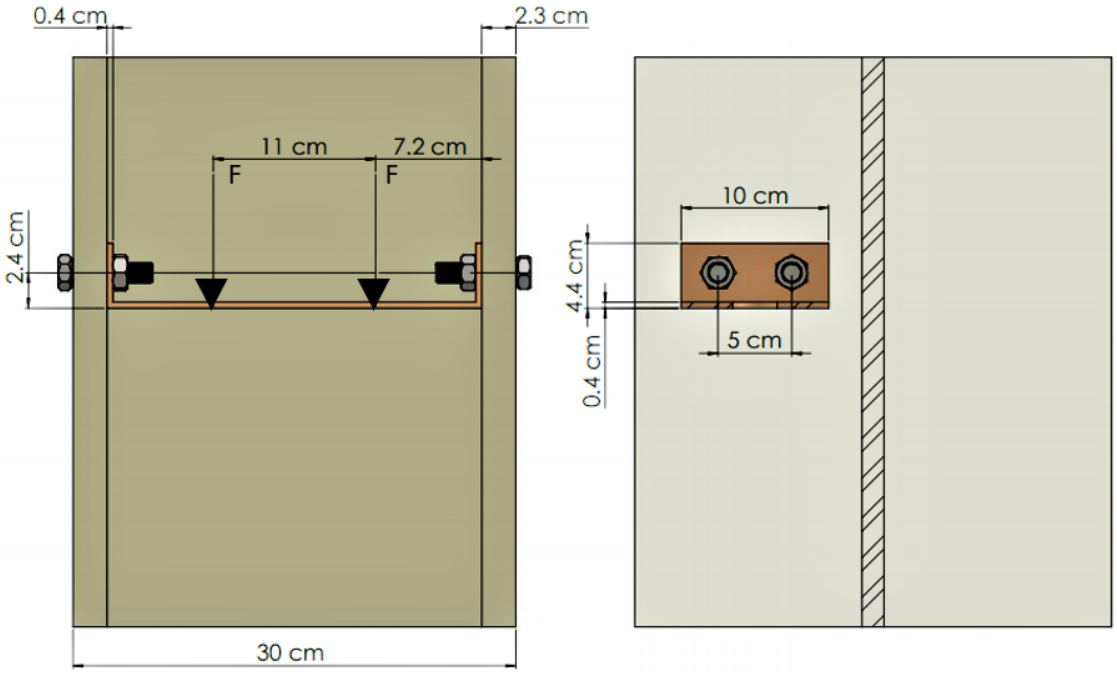

Figure 3.49: Support bracket under load

1. Maximum bending moment Let's consider our case as a cantilever beam (though it is not a proper cantilever beam but for the initial analysis we are considering this as a cantilever beam).

   Net area moment of inertia: rectangular section

$$I = \frac{bd^3}{12} = \frac{72mm \times (4)^3}{12} = 384mm^4 \tag{3.37}$$

   • Maximum bending moment occur at the corner of the bracket (point of stress concentration), then:

$$M = F.L' = F(L - d) = 70(72 - 4) = 4760N - mm \tag{3.38}$$

2. Bending stress: the formula for determining the bending stress in the member is:

$$\sigma_b = \frac{My}{I} = \frac{Md}{2I} = \frac{4760 \times 4}{2 \times 384} = 24.8MPa \tag{3.39}$$

   Material selection

   starting with $AISI$ 1006 steel with yield strength (S_y) of 170 MPa and tensile strength (S_{ut}) of 300 MPa. The We have to reduce the thickness of the support bracket since the material is enough to support the given load.

   First trial of $thickness = 4\ mm$, $I = 384\ mm^4$, $M = 70(72-4) = 4760$ N-mm, then bending stress:

3. Shear stress:

   Shear area, $A_{shear} = d(L - 2d')$, where d' is diameter of the bolt which is 10 mm ($M10$).

$$\tau = \frac{F}{A_{shear}} = \frac{F}{d(L - 2d')} = \frac{70}{4 \times (10 - 2)} = 2.2MPa. \tag{3.40}$$

Von Mises stress, σ'

$$\sigma' = \left(\sigma_1^2 + 3\tau_{xy}^2\right)^{\frac{1}{2}} = \left(24.8^2 + 3 \times 2.2^2\right)^{\frac{1}{2}} = 25.1MPa \tag{3.41}$$

4. Safety factor:

$$S.F = \frac{S_y}{\sigma'} = \frac{170}{25.1} = 6.7 \tag{3.42}$$

The support bracket is safe for bending with a thickness of 4 mm.

3.2.11 Design summary

Table 3.13: Design Summary, where dimensions are in *length* × *width* × *height*

Components	**Quantity**	**Material**	**Parameter**
Test specimen	1	Fibre reinforced composite	Dimension=150 mm×100 mm×5 mm, $E = \frac{3\sigma_m}{\epsilon_m}$, $W_{ds} = \frac{3}{5}\sigma_m\epsilon_m$
Floor Plan (Foundation)	1	Concrete and $AISI$ 1006 steel	Dimension=340mm×340mm×25mm
Specimen fixture	1	$AISI$ 1030 CD steel	Dimension=180mm×120×6mm
Drop tower	1	$ASTM$ $A36$ steel	Dimension=300mm×323mm×1200mm, $P_{cr} = 633\ kN$, σ_{cr}=97.6 MPa
Guide rod	2	$AISI$ 304 stainless steel	Diameter=20 mm, length= 770 mm, $\sigma_{cr} = 80.3\ MPa$, $\sigma_{all} = 48.1\ MPa$, $P_all = 15.1\ kN$
Striker	1	Stainless steel	Diameter= 20 mm, length= 108 mm
Interchangeable tup	1	$AISI$ $Type$ $A2$ steel	Diameter=16 mm, Hemispherical in shape
Impactor Assembly	1	$AISI$ 1006 HR steel	Dimension=180mm × 85mm × 75mm, $\sigma_{all} = 100\ MPa$, reaction force ($F_r = 674.4kN$)
Support bracket	2	$AISI$ 1006 steel	Dimension=254mm × 100mm × 44mm, thickness= 4mm, $\sigma_b = 24.8\ MPa$, $\tau = 2.2\ MPa$
$M10$ bolt	8	Low carbon steel	Fixing bolts at the support bracket
$M8$ bolt	28	Low carbon steel	Fixing bolts at the impactor assembly, specimen fixture and foundation

3.2.12 Final Specification

Table 3.14: Specification of drop weight impact test machine

No.	**Parameter**	**Value**
1.	Maximum drop weight of impactor	5.5 Kg.
2.	Maximum drop height	0.62 m
3.	Mass increment	0.45 and 0.5 Kg
4.	Striker shape and size	16 mm dia. hemispherical
5.	Release mechanism	Free fall (manual)
6.	Maximum impact energy	33.5 J
7.	Maximum impact velocity	3.49 m/s
8.	Acceleration measurement	352B PCB Accelerometer
10.	Data acquisition and manipulation	Model 485B39 digital ICP signal conditioner
9.	Operating temperature	room temperature
10.	Anti-rebound control mechanism	manual
11.	Test specimen dimension (l×w×t) as per ASTM D7136	150 mm×100mm×5mm
12.	Overall dimension (l×w×h)	340mm×340mm×1200
13.	Standard testing method	ASTM D7136

Chapter 4

Prototyping of drop weight-impact test machine

4.1 Prototyping

4.1.1 Introduction

Prototype is an early sample, model, or release of a product built to test a concept. Some editing on components was necessary due to unavailability of material in local market, but without violating the basic working principle of the concept.

In this chapter for prototyping the drop weight impactor (DWITM) some components concept i.e drop tower, guide rod assembly, support bracket modified, other modification occurred in geometry. Design for weldment on components and assembly disassembly of final concept (prototype) explained.

4.1.2 Modified components

Modification on the drop weight impact tester components is made for prototyping. Resizing the drop tower affects the following components listed in each sub-sections.

Drop tower

Due to the unavailability of the selected Wide-Flanged drop tower (W310×143), the work used smaller wide flanged (shown in figure below)

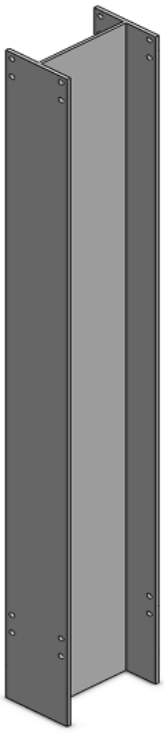

Figure 4.1: CAD model of modified drop tower

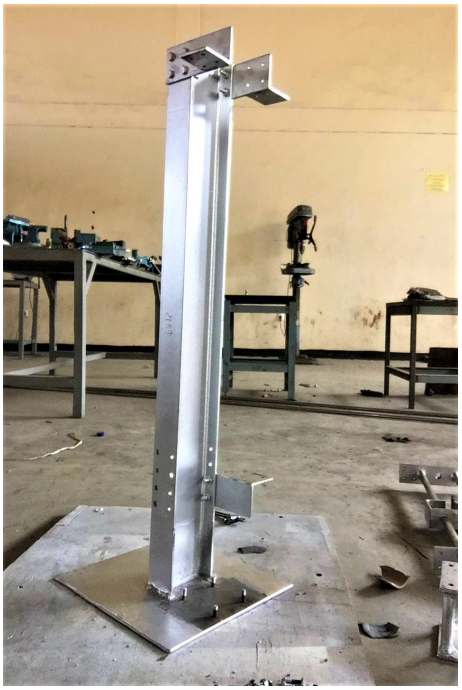

Figure 4.2: Drop tower with foundation

The work uses similar shape with the conceptual drop tower only differ in size. The modified drop tower has a total height of 92.5 cm. Other details shown in figure 4.3.

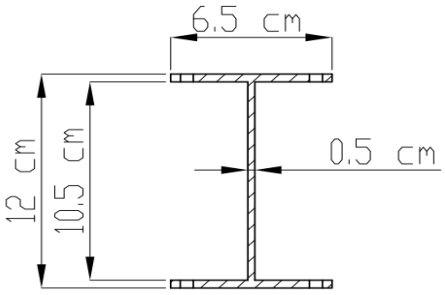

Figure 4.3: Modified Wide Flanged shape of drop tower

Impactor assembly

Additional masses inserted to vary impactor mass. The work uses twelve (12) additional masses with weight of 0.45 kg (three pairs) and 0.5 kg (the other three pairs). The impactor housing has a mass of 2.0 kg, totally the impactor assembly has a mass of 5.0 kg. Added masses fix in position using M10 bolt in order to prevent upward motion while the impactor moves downward.

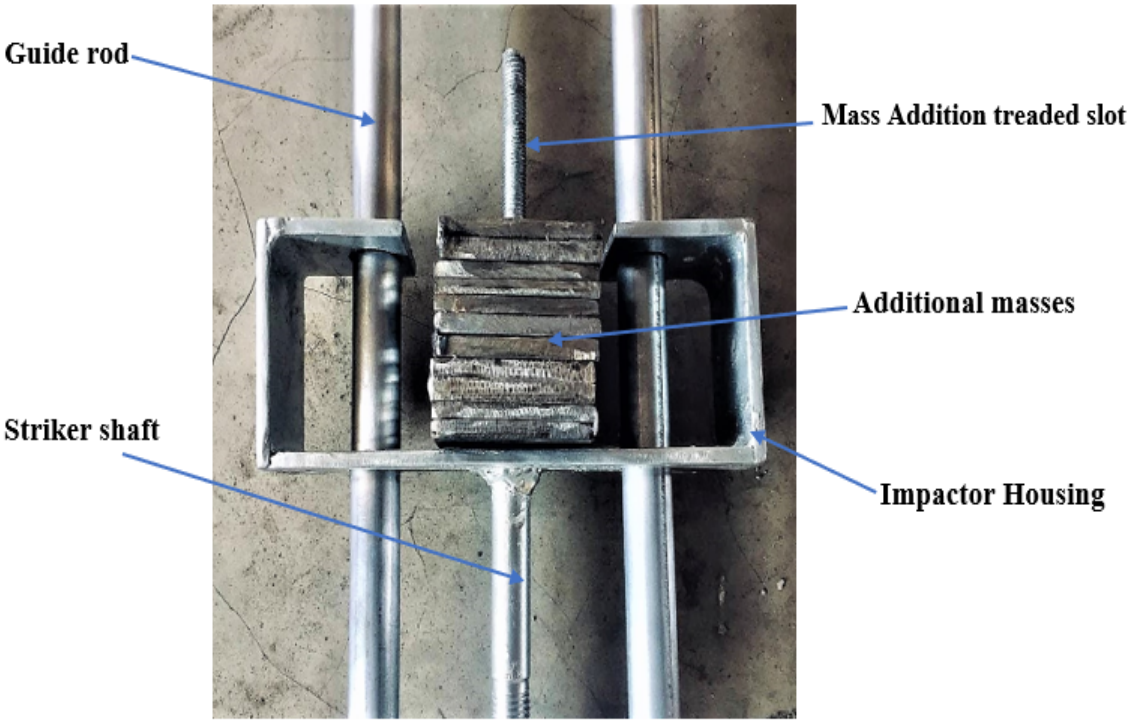

Figure 4.4: Impactor assembly with added masses

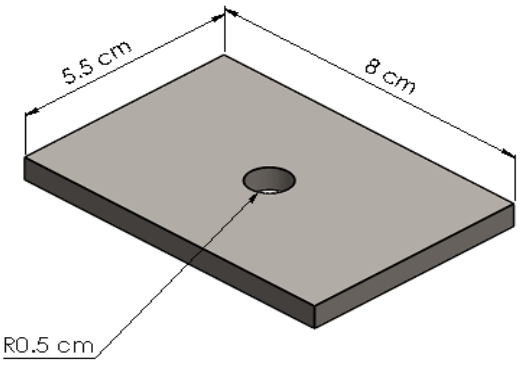

Figure 4.5: Additional Rectangular Mass

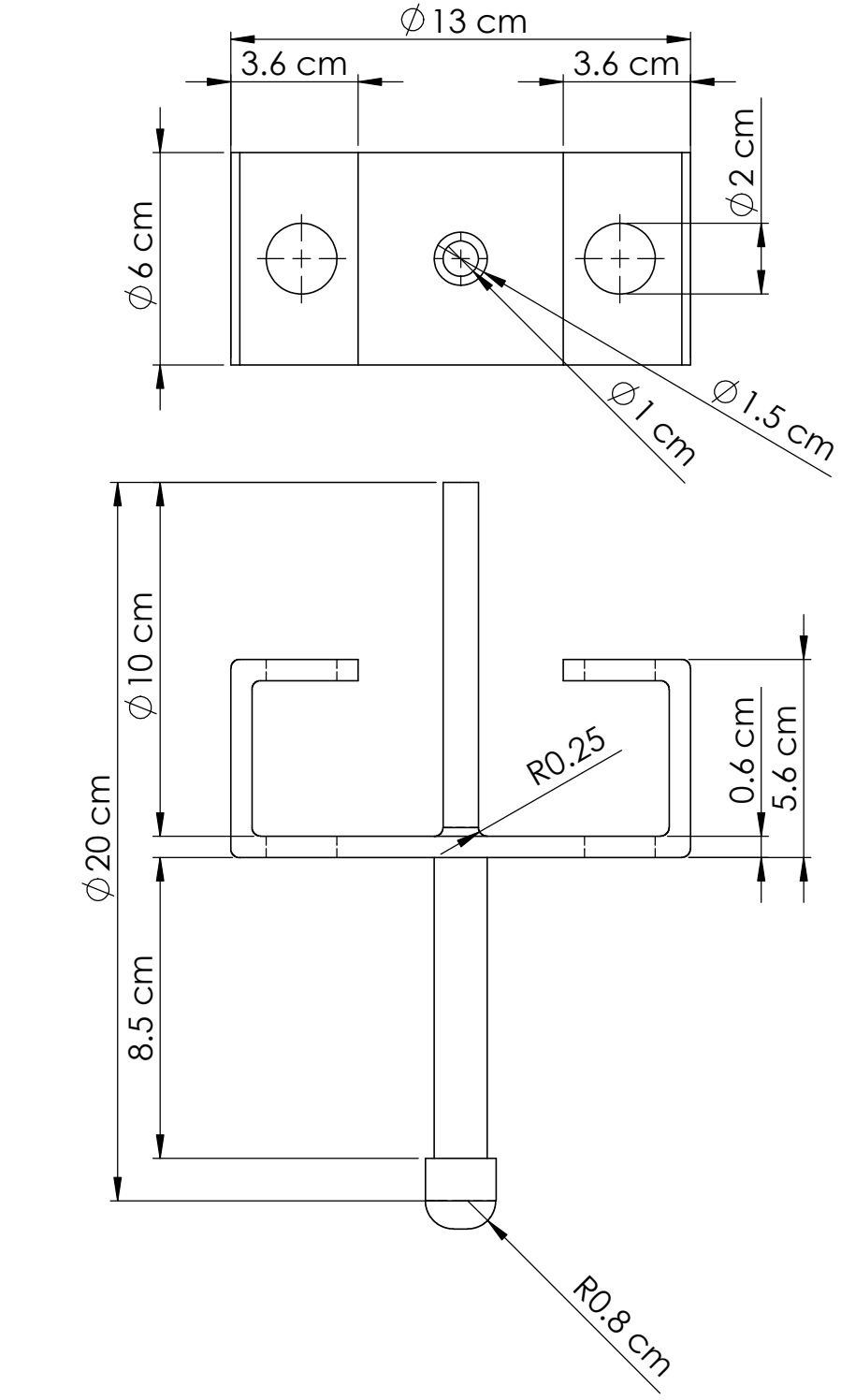
∅13 cm
3.6 cm
3.6 cm
∅2 cm
∅6 cm
∅1 cm
∅1.5 cm
∅10 cm
∅20 cm
R0.25
0.6 cm
5.6 cm
8.5 cm
R0.8 cm

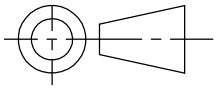

Support bracket

The proposed support bracket in the final concept fits in the area of the drop tower, i.e. on the flanges of the section beam. Now, the size of the drop tower changed which inter affects the conceptual design of support bracket which is L-shaped and assembled to the drop tower and guide rods using M6 bolt. Finally the following support bracket shown in figure 4.6 used for prototyping,

Figure 4.6: Modified support bracket

Figure 4.7: Assembly of support bracket on the drop tower (wide flanged support)

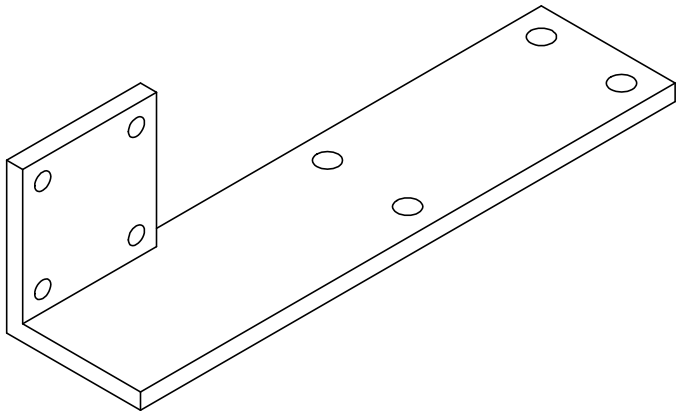

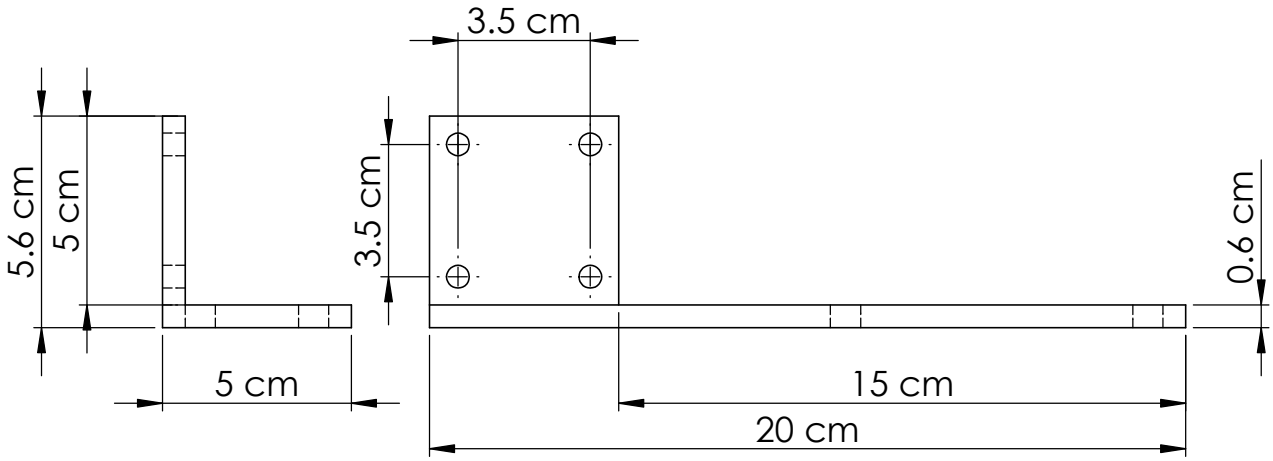
3.5 cm
5.6 cm
5 cm
3.5 cm
0.6 cm
5 cm
15 cm
20 cm

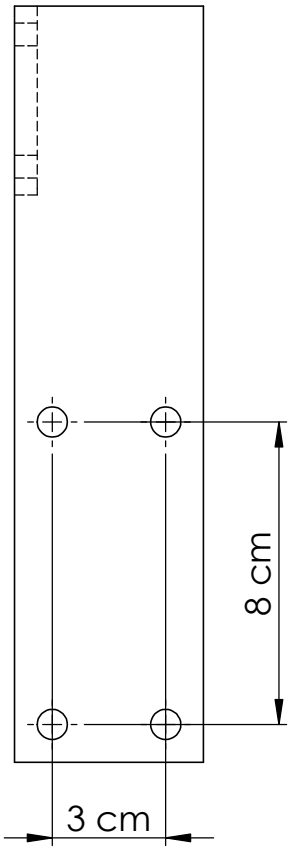
8 cm
3 cm

Bolt strength at the Support bracket

Bolts which fits support bracket to the drop tower shown in figure 4.8 are critically loaded (support the whole weight except the drop tower) when compared to the other bolt, which need analysis for shear stress on each bolt, bearing stress and critical bending stress on support bracket.

Weights on the bolts $F = 90\ N$ (i.e. weight of impactor assembly + weight of guide rods assembly + weight of M8×16 bolts). Therefor, point O, the centroid of the bolt group in figure 4.8, is found by symmetry. If a free-body diagram of the beam were constructed, the shear reaction V would pass through O and the moment reactions M would be about O. These reactions are,

$$V = 45N, M = 45(17.5) = 7.875N.m \tag{4.1}$$

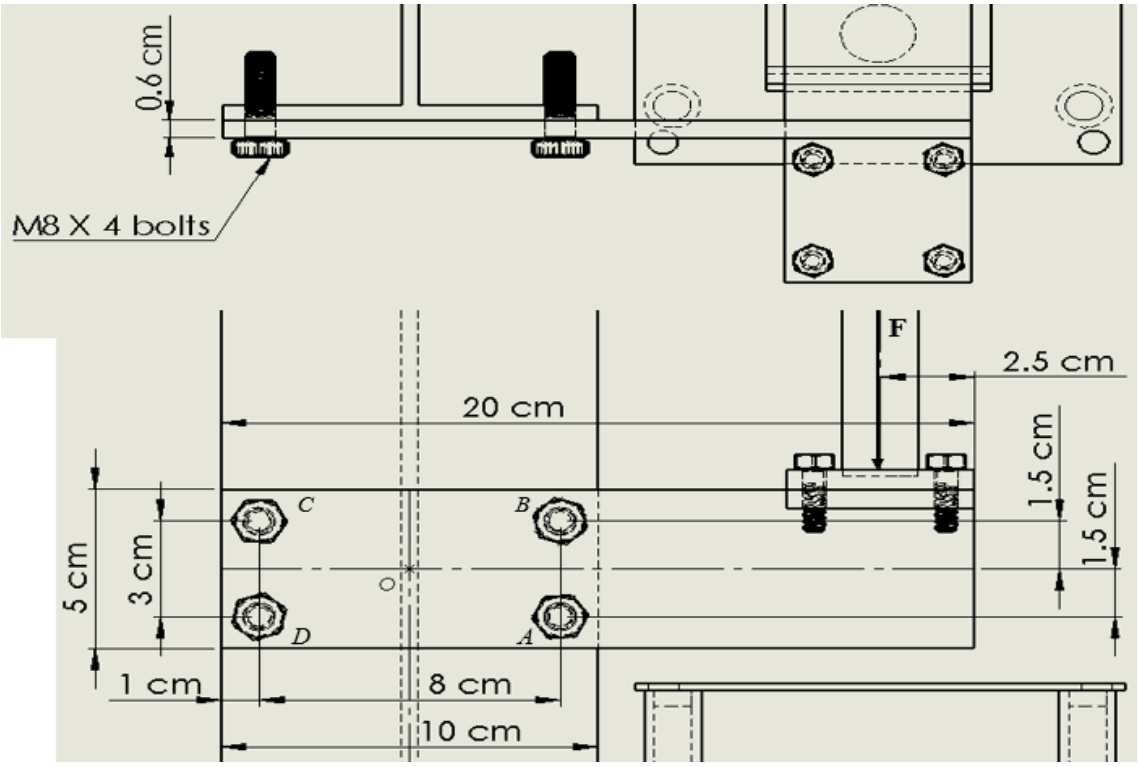

Figure 4.8: Cantilevered support bracket on drop tower using four tightly fitted location

- The resultant load on each bolt

  In figure 4.1.2, the bolt group has been drawn to a larger scale and the reactions are shown. The distance from the centroid to the center of each bolt is,

$$r = \sqrt{(1.5)^2 + (4)^2} = 4.27cm \tag{4.2}$$

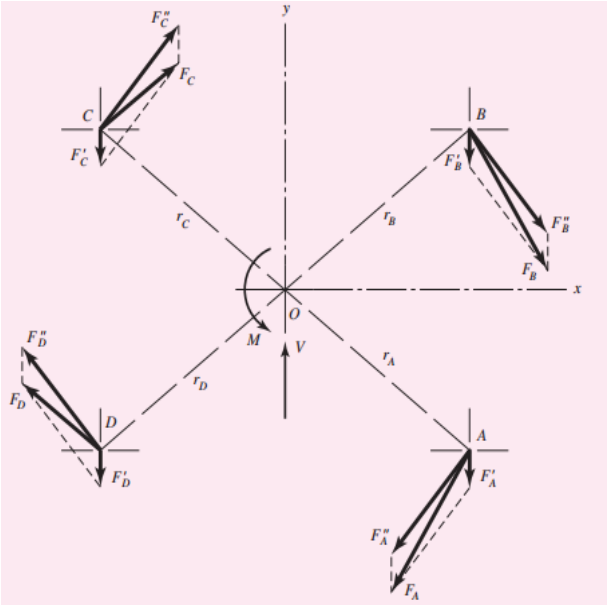

  The primary shear load per bolt is,

$$F' = \frac{V}{n} = \frac{45}{4} = 11.25N \tag{4.3}$$

  The secondary shear forces are equal to,

$$F"_n = \frac{M_1 r_n}{(r^2)_A + (r^2)_B + (r^2)_C + ...} = \frac{Mr}{4r^2} = \frac{M}{4r} = \frac{7.875N.m}{4(0.0427m)} = 46.1N \tag{4.4}$$

  the resultants obtained by using the parallelogram rule ($R = \sqrt{F'^2 + F"^2 \pm 2F'F" \cos\theta}$). The magnitudes are found by measurement (or analysis) to be

$$F_A = F_B = 53.3N, F_c = F_D = 39.6N \tag{4.5}$$

- The maximum shear stress in each bolt

Bolts A and B are critical because they carry the largest shear load. Does this shear act on the threaded portion of the bolt, or on the unthreaded portion? The bolt length will be sum of bracket thickness (6 mm) plus drop tower thickness (5 mm) plus 2 mm for washer. From appendix A Table A-31, gives the nut height is 6.8 mm, including two threads beyond the nut, this adds up to a length of 21.8 mm. So a bolt of 24 mm needed.

for metric bolts is

$$L_T = \begin{cases} 2d+6 & L \le 125 \quad d \le 48 \\ 2d+12 & 125 < L \le 200 \\ 2d+25 & L > 200 \end{cases}$$

The thread length $L_T = 2d + 6 = 22mm$. Thus the unthreaded portion of the bolt is $24 - 22 = 2mm$. This is less than the 6 mm for the plate, so the bolt will tend to shear across its minor diameter. Therefor the shear-stress area is $A_s = 28.27mm^2$. This the shear stress is,

$$\tau = \frac{F}{A_s} = \frac{53.3N}{28.27mm^2} = 1.885MPa \tag{4.6}$$

- Maximum bear stress

  The wide flanged channel (drop tower) is thinner than the support bracket, and so the largest bearing stress is due to the pressing of the bolt against the tower thickness (web). The bearing area is $A_b = td = 5(8) = 40mm^2$. Thus the bearing stress is

$$\sigma = -\frac{F}{A_b} = -\frac{53.3N}{40mm^2} = -1.34MPa \tag{4.7}$$

Foundation

The foundation of the final concept explained in section 3.2.4 was using a plate filled with concrete. For simplicity and weight purpose, filling using a concrete avoided. 340 mm×340 mm×6mm, square flat mild steel plate which directly welded to the

drop tower is used for prototyping as shown in figure 4.9.

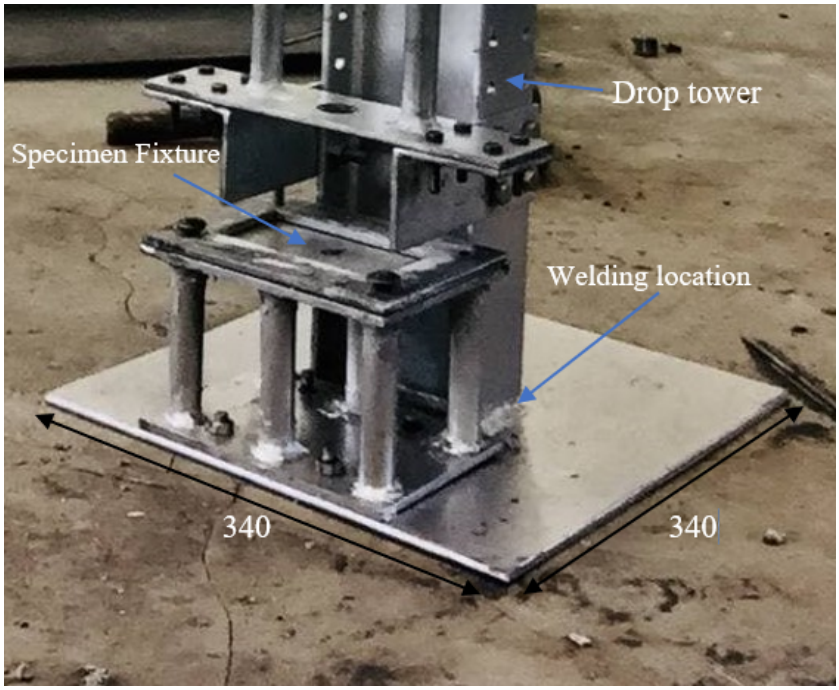

Figure 4.9: Modified Foundation

4.1.3 Design for weldment

A weld joint is a permanent joint which is obtained by the fusion of the two parts to be joined together, with or without the application pressure and a filler material [8]. In this work, electric arc welding, where the filler material is supplied by metal welding electrode as shown in figure 4.10. Critical welding components designed in the following sub-sections

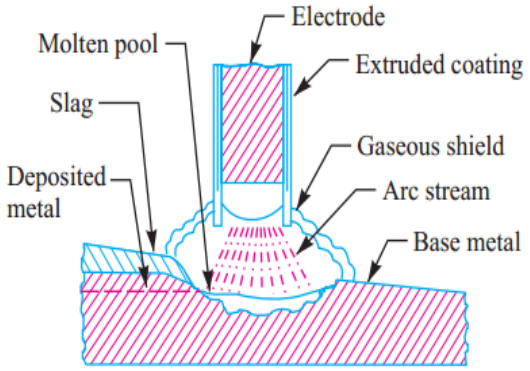

Figure 4.10: Shield electric arc welding

Basic welding symbols according to IS:813 - 1961 are shown in figure 4.11.

S. No.	*Form of weld*	*Sectional representation*	*Symbol*
1.	Fillet		
2.	Square butt		
3.	Single-*V* butt		
4.	Double-*V* butt		
5.	Single-*U* butt		
6.	Double-*U* butt		
7.	Single bevel butt		
8.	Double bevel butt		

Figure 4.11: Basic weld symbol [8]

Weld at support bracket

Welding at the bottom of support fixture is critical since it holds the components such as impactor assembly and guide rods.

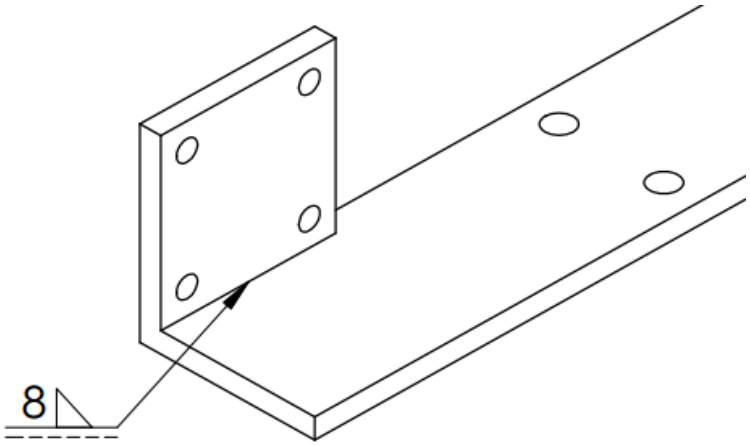

Figure 4.12: Fillet weld at the support bracket

The load imposed on the support bracket is eccentric. The stresses induced on

the joint may be of different nature or of the same nature. The induced stresses are combined depending upon the nature of stresses.

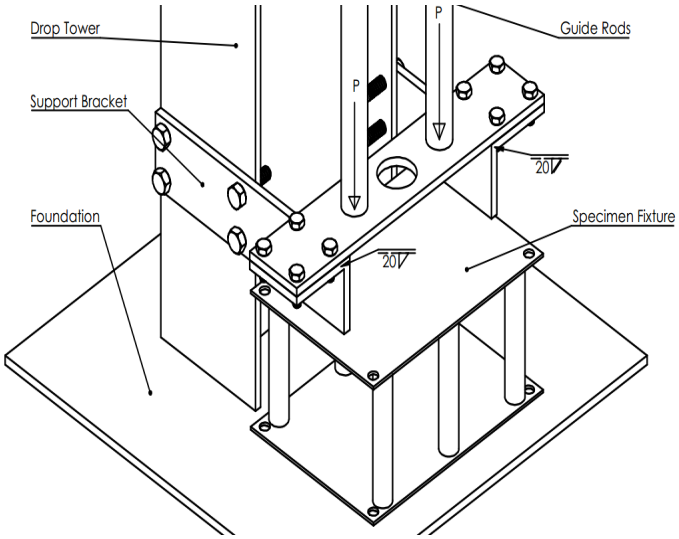

Figure 4.13: Welding location and application of load at the support bracket

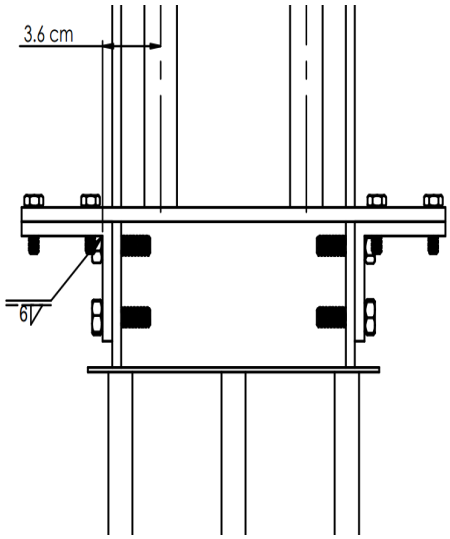

Figure 4.14: Front view of welding location at support bracket

When the bending and shear stresses are simultaneously present in a joint (see figure 4.13), the maximum stresses are as follows [8].

Maximum normal stress,

$$\sigma_{t(max)} = \frac{\sigma_b}{2} + \frac{1}{2}\sqrt{(\sigma_b)^2 + 4\tau^2} \tag{4.8}$$

and maximum shear stress,

$$\tau_{max} = \frac{1}{2}\sqrt{(\sigma_b)^2 + 4\tau^2} \tag{4.9}$$

Where

σ_b=bending stress and τ=shear stress Consider L-joint in figure 4.12 fixed at both ends and subjected to an eccentric load P at a distance $e = 60mm$ as shown in

figure 4.13.

The figure shows the values of polar moment of inertia of the throat area about the center of gravity 'G' and the section modulus for some important types of welds which may be used for eccentric loading.

Let

$s = Size\ of\ weld$, $l = Length\ of\ weld = 50$ mm, and $t = Throat\ thickness = s\cos\theta$

The joint will be subjected to the following two types of stresses:

1. Direct shear stress due to the shear force P acting at the welds, and
2. Bending stress due to the moment $P \times e$

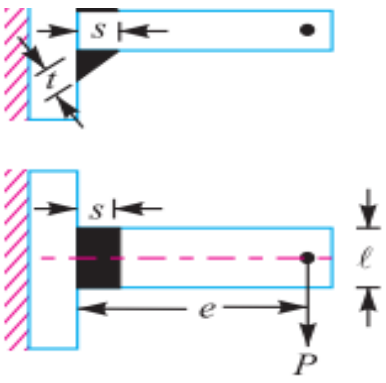

Figure 4.15: Eccentrically loaded L-joint

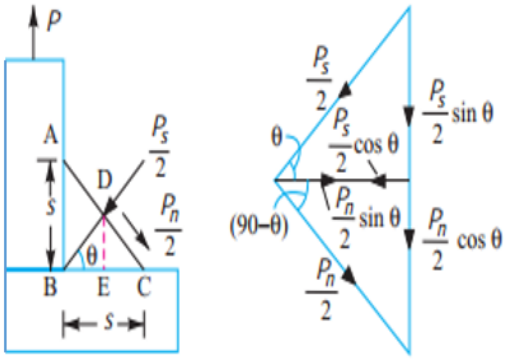

Figure 4.16: Plane of maximum shear stress when load acts at right angles to the weld

When the load acts at right angle to the weld (transverse load), then the shear force and the normal force will act on the weld. From figure 4.16,

$$P = \frac{P_s}{2}\sin\theta + \frac{P_n}{2}\cos\theta \tag{4.10}$$

Assuming that the resultants of $\frac{P_s}{2}$ and $\frac{P_n}{2}$ is vertical, then the horizontal components are equal and opposite,

$$\frac{P_2}{2}\cos\theta = \frac{P_n}{2}\sin\theta, P_n = \frac{P_s\cos\theta}{\sin\theta} \tag{4.11}$$

Substituting the value of P_n in equation 4.10,

$$P = \frac{P_s}{2}\sin\theta + \frac{P_s\cos^2\theta}{2\sin\theta} \tag{4.12}$$

Multiplying throughout by $2\sin\theta$,

$$P\sin\theta = P_s\sin^2\theta + P_s\cos^2\theta = P_s \tag{4.13}$$

From the geometry of Figure 4.16, ... $BC = BE + EC = BE + DE$ or $s = t\cos\theta + t\sin\theta$

Therefor, throat thickness,

$$t = \frac{s}{\cos\theta + \sin\theta} \tag{4.14}$$

Minimum area of weld or throat area,

$$A = t \times l = \frac{s}{\cos\theta + \sin\theta} \times l = \frac{s \times l}{\cos\theta + \sin\theta} \tag{4.15}$$

The load P is the sum of wight of guide rods which is 20 N and the impactor assembly at the point of impact, 50 N. Totally the Load P is 70 N.

Shear stress in the weld (assuming uniformly distributed),

$$\tau = \frac{P_s}{A} = \frac{P\sin\theta(\cos\theta + \sin\theta)}{s \times l} \tag{4.16}$$

For maximum shear stress, differentiating the above expression with respect to θ

and equate to zero.

$$\frac{d\tau}{d\theta} = \frac{P}{sl}\left[\sin\theta\left(-\sin\theta+\cos\theta\right)+\left(\cos\theta+\sin\theta\right)\cos\theta\right] \ldots\ldots\ldots \left(\frac{d(u.v)}{d\theta}u\frac{dv}{d\theta}+v\frac{du}{d\theta}\right) \tag{4.17}$$

From further simplification, the value of $\theta = 67.5$. Substituting the value of θ in equation 4.16, the maximum shear stress,

$$\tau_{max} = \frac{1.21P}{s\times l} and, P = \frac{s\times l\times\tau_{max}}{1.21} = 0.83s\times l\times\tau_{max} \tag{4.18}$$

Bending moment, $M = \mathrm{P}\times$ e $= 70\times 60mm = 4200N-mm$

From manufactured support bracket shown in figure 4.12, the size of weld s is 6 mm and length of weld is 50 mm.

Section modulus of the weld through the throat [8]

$$Z = \frac{s\times l^2}{4.242} = 3535.8mm^3 \tag{4.19}$$

Bending stress

$$\sigma_b = \frac{M}{Z} = 1.2N/mm^2 \tag{4.20}$$

• Maximum shear stress

$\tau_{max} = \frac{1.21(70)}{6\times 50} = 0.28$ MPa

Weld at guide rods

The 20 mm diameter guide rods which have 670 mm height, welded to the flat plate as shown in figure 4.17. The size of weld is 7 mm.

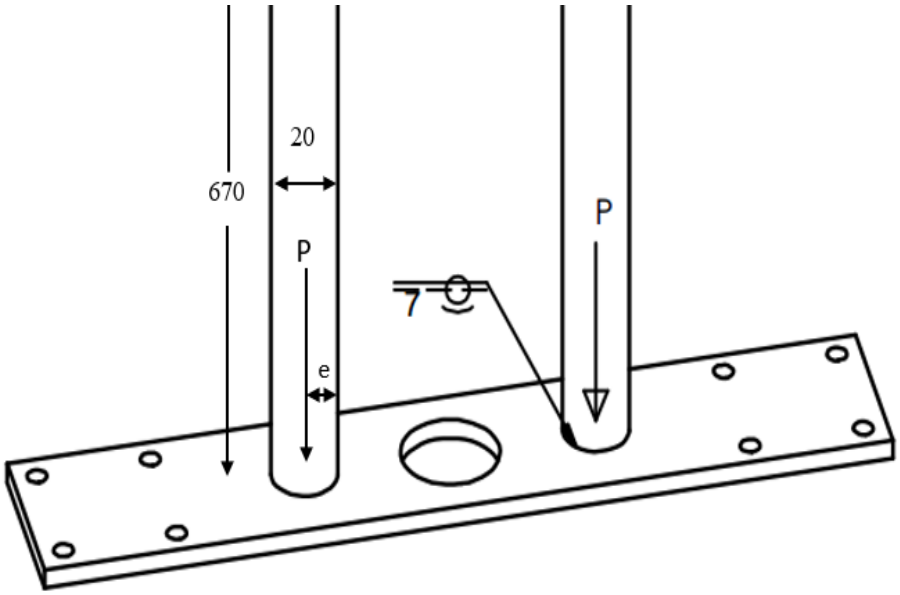

Figure 4.17: Fillet weld on circular guide rods (dimensions are in mm)

The throat area for circular fillet weld,

$$A = t \times \pi D = 0.707s \times \pi D.....(t = s \times \cos 45) \tag{4.21}$$

A=0.707× 7× π× 20=311 mm^2

Shear stress,

$$\tau = \frac{P}{A} = \frac{70}{311} = 0.225MPa \tag{4.22}$$

The bending moment,

$M = P \times e = 70 \times 10 = 700$ N-mm

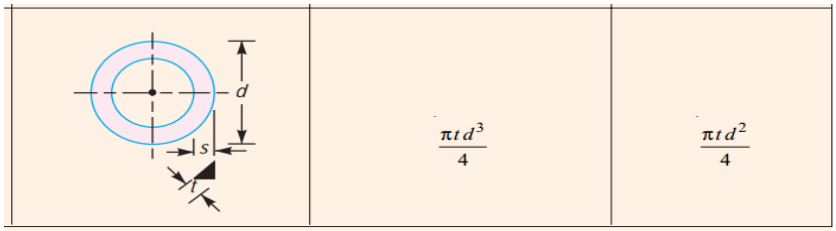

Figure 4.18: Polar moment of inertia and section modulus of circular weld [8]

For circular section, section modulus from figure 4.18,

$$Z = \frac{\pi t d^2}{4} = \frac{\pi 0.707 \times 7 \times (20)^2}{4} = 1554.8 mm^3 \tag{4.23}$$

Bending stress,

$\sigma_b = \frac{M}{Z} = \frac{700}{1554.8} = 0.45\ MPa$

Maximum shear stress, $\tau_{max} = \frac{1}{2}\sqrt{(\sigma_b)^2 + 4 \times \tau^2} = \frac{1}{2}\sqrt{0.45^2 + 4 \times 0.225^2} = 0.636\ MPa$

Weld at striker shaft

The striker shaft is welded to impactor housing using circular fillet weld shown in figure 4.19, which has weld size of 7 mm. The diameter of striker shaft D is 10 mm and the impact load, P (assuming proportional to impact weight) is 50 N.

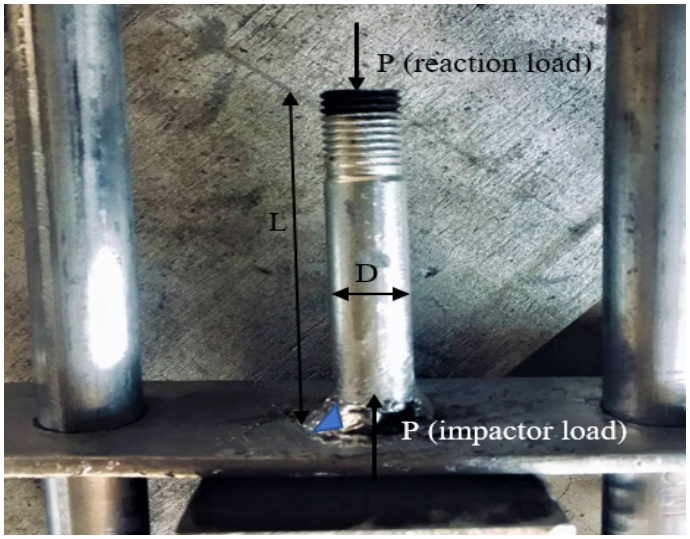

Figure 4.19: Circular fillet Weld at the striker shaft

Minimum area of weld or throat area,

$A = t \times \pi D = 0.707 \times 7 \times 10\pi = 155.5\ mm^2$

Shear stress,

$\tau = \frac{P}{A} = \frac{50}{155.5} = 0.32\ MPa$

The bending moment,

$M = P \times e = 50 \times 10 = 500\ N - mm$

Section modulus for circular section,

$Z = \frac{\pi \times 0.707 \times 7 \times (10)^2}{4} = 388.7\ mm^2$

Bending stress,

$\sigma_b = \frac{M}{Z} = \frac{500}{388.7} = 1.29\ MPa$

Maximum shear stress,

$\tau_{max} = 1.44\ MPa$

4.2 Final Concept

Finally, the concept used for prototyping is shown in figure below, which differs from the proposed final concept in components listed section 4.1.2.

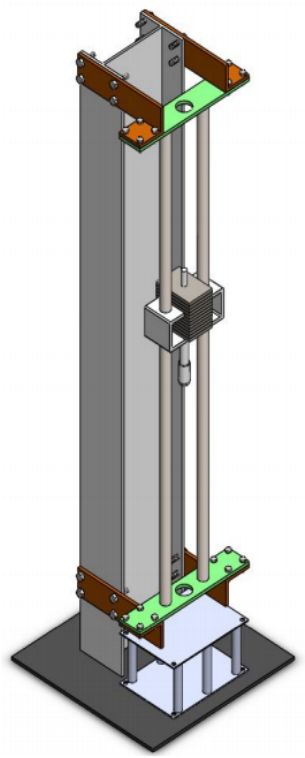

Figure 4.20: CAD model of modified DWITM

Figure 4.21: Prototype of modified DWITM

4.2.1 Assembly and disassembly

The procedures while assembling and disassembling the drop weight impact tester shown in figure 4.22 followed the following procedures listed below,

- Initially, the drop tower (1) welded (flat fillet weld) to the foundation (8) to attain verticality and strength.
- Second, the specimen fixture (5) attached to the foundation using 4×M8 bolts. The purpose of making the specimen fixture disassembled from the foundation is for preventing load transmitted directly to the drop tower.
- Third, the support brackets (2) assembled to the drop tower using 16×M8 bolts (10) in the provided locations.
- Fourth, the guide rod assembly (3) attached to the support brackets using 16×M6 bolts (9) in the provided holes. The impactor housing (4) can't be disassembled from the guide rods, when additional load needed the testing person can add additional masses (7).
- Finally, the tup assembled to the striker shaft when test is conducted when necessary instrumentation are incorporated.

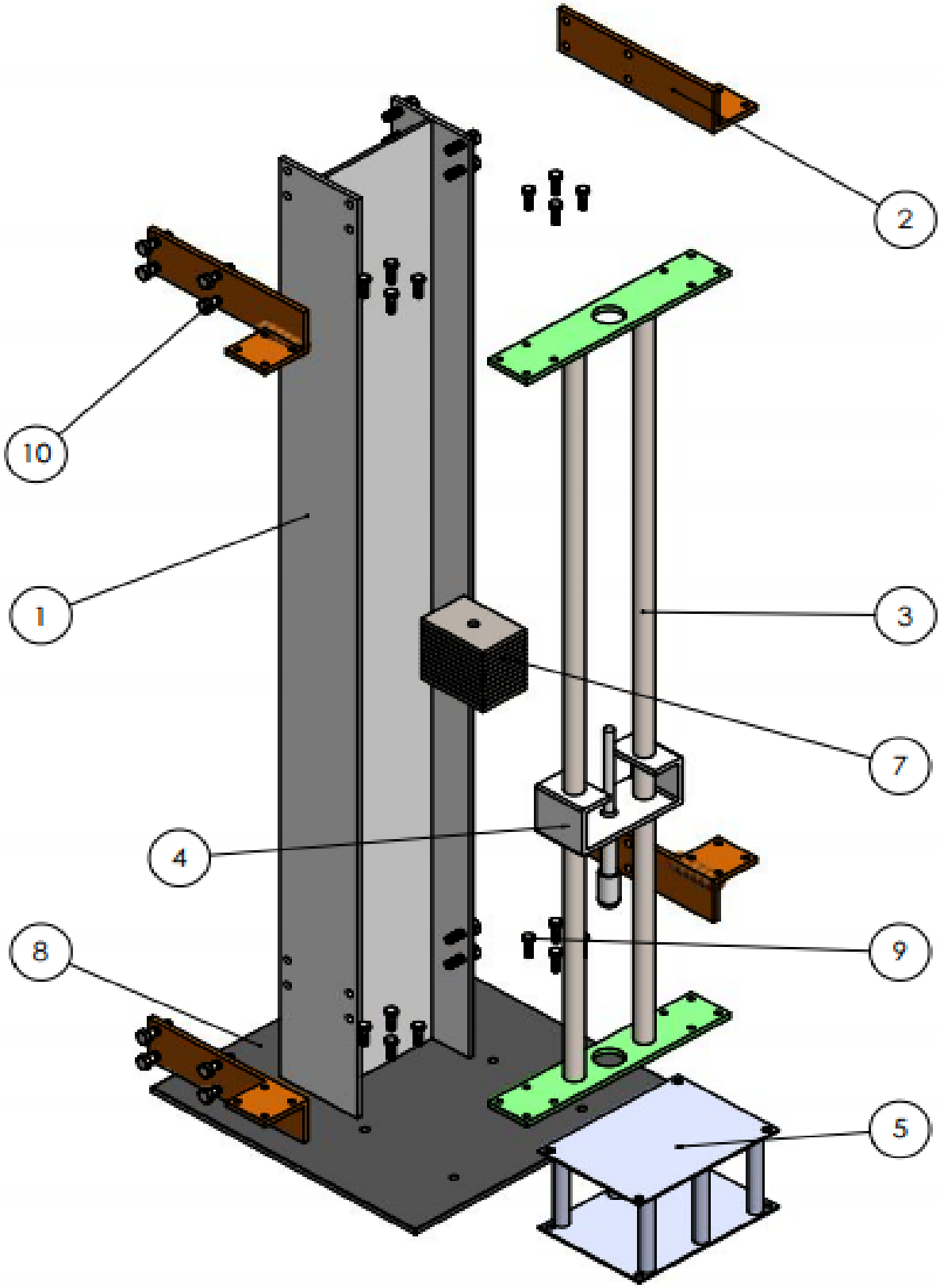

Figure 4.22: Exploded view of modified DWITM

Chapter 5

Experimental Investigation

In this chapter, the test methods used to impact the plats are presented. In particular this means each different type of impact is identified, and the impactor mass and drop height configuration used are described. The method for performing the simulated impact using a drop weight impact machine is presented. Then the typical results from an impact are presented, showing what information can be garnered from the data.

5.1 Test Specimen

This paper uses already prepared fibre reinforce composite material from the workshop of school of mechanical and industrial engineering. By properly and safely cutting three materials according to the design requirements, test conducted on those materials shown in Figure 5.1 & 5.2.

Figure 5.1: Prepared Test Specimen

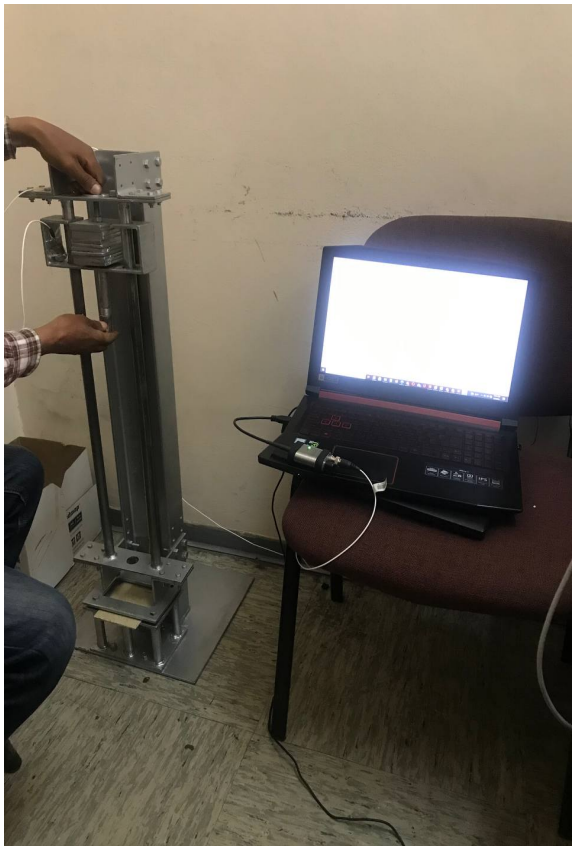

Figure 5.2: Test Setup

5.2 Impact Testing

It is known that in the low velocity impact of isotropic solids the softer body is permanently deformed. Although the softer body will always deform to a greater extent, the behavior of composite structures under impact is very much material dependent.

The main objective of the current research is to investigate the response of fibre reinforced composite laminates at perpendicular impacts. The design facilitated impact energies up to 33.5 Joules and impact velocities in the range 0 to 3.49 m/s. A 5.5 kg mass, with a 16 mm hemispherical impactor, was raised to specified level, released and caught manually at its maximum rebound height. The incident and rebound kinetic energies were evaluated, by accurately monitoring the striking and rebound velocities of the indenting mass.

The measurement system which described section 5.2.1 in details, consisted of piezoelectric accelerometer connected to the drop weight. The output of the sensor fed to Model $485B39$ digital ICP signal conditioner.

5.2.1 Impact Instrumentation

To fully characterize the impact behavior of the material under test and to determine the energy dissipated by the specimen, the following parameters should be measured at least: crushing force, specimen deflection under compressive load, initial and final linear impact velocity or initial impact energy (immediately before the impact) and energy dissipated by the specimen during the impact.

In addition, other important properties (i.e., fracture/damage propagation, extent of plastic strain, formation of plastic hinges, etc.) can be determined by a careful examination of the specimen after the test which will not be covered in this work.

This paper presents the design of an instrumented tester, using an accelerometer as the sole instrumentation, in which a PC computer is used for data acquisition, computations, and the reporting of results.

Sensor selection

In order to record relevant impact data such as the load/time history etc., some sensors selection needs to be necessary. The following sensors are widely used in impact assessment of composite materials, which are also reviewed in literature (see section 5.2.1):

1. **Load cell**: have been widely used in the past either mounted on the tup or in the sample support. This measured the loads experienced by the tup or those transmitted to the support. This approach to instrumentation was taken by several authors [21, 36, 44, 45, 53–55] as it provides a reliable method of analyzing the dynamic response of structures.

2. **Laser Doppler Velocimetery (LDV)**: originally developed to measure the velocity of fluids. Worrall [60] record velocity of the tup using LDV during impact.

3. **Accelerometer**: the device can be mounted on the tup, the support or even the test specimen itself as described in section 5.2.1 [17, 22]. Compared to the other types of sensors, piezoelectric accelerometers have important advantages [61]:

    - Extremely wide dynamic range, low output noise - suitable for shock measurement as well as for almost imperceptible vibration.
    - Excellent linearity over their dynamic range
    - Wide frequency range
    - Compact yet highly sensitive
    - No moving parts - no wear

- Self-generating - no external power required
- Great variety of models available for nearly any purpose
- Acceleration signal can be integrated to provide velocity and displacement - no need of additional velocity, displacement sensors.

Selection: Cessna et al[2]. seem to have been the first to realize that it is possible to obtain both kinematic information (deflections, velocities) and dynamic information (forces, energies) from a single accelerometer attached to the falling weight in a falling weight-plaque geometry. This minimizes the cost for force, velocity and deflection measurements independently. According to Newton's law, acceleration in the impact direction (measured by the accelerometer) immediately yields the total force on the striker in the impact direction. Since only the use of an accelerometer in situations in which all forces on the striker not related to its interaction with the sample are known is being proposed, the force between striker and sample can be obtained by subtraction. In addition, as long as the force between sample and striker is different from zero the sample and striker are in contact which means that the velocity of the sample at the contact point is equal to the velocity of the striker, and the deflection of the sample at the contact point is equal to the displacement of the striker (assuming the striker to be rigid in comparison with the sample). The velocity and displacement of the striker, in turn, may be obtained from the acceleration by successive integration[22].

Accelerometer: Piezoelectric Sensors

The solution to the transient response problems identified as a result of the introduction of the piezoelectric accelerometer into the transducer market place. The piezoelectric materials used had high moduli. In addition, their self-generating responses produced wide dynamic signal ranges. Both of these properties combined to enable the design of accelerometers with high resonant frequencies. These high resonant frequencies eliminated the need for damping to extend the accelerometer's usable flat frequency response. Phase shift over the usable frequency range of the

accelerometer also was eliminated. This large dynamic signal range also allowed size reduction of piezoelectric accelerometers relative to strain gauge accelerometers while providing much higher g (acceleration due to gravity) capability. None of the strain gauge accelerometers had flat frequency response above 200 Hz while the piezoelectric accelerometers provided flat response to 10,000 Hz.

In impact testing there is a need for accelerometer with a high resonant frequency and zero damping which responds accurately to fast rise time and short duration shock motion. The device selected also have frequency response down to dc, or steady state acceleration, so it can measure long duration transients.

This paper revised companies that produce and distribute accelerometer world-wide. The principal early corporate pioneers and their fist locations included Brüel and Kjær (Denmark), Columbia Research Laboratories (Woodlyn, PA), Endevco (Pasadena, CA), Gulton Manufacturing (Metuchen, NJ), and Kistler Instruments (Buffalo, NY). It is interesting to note that all of these companies are still in existence today.

Columbia Research Laboratories and Gulton Manufacturing (now Gulton-Statham) have become broad-based transducer houses so that piezoelectric accelerometer development is no longer their central focus. Brüel and Kjær is currently focused as a systems house, transducers being one part, with about half of its product line directed towards shock and vibration. Kistler Instruments has split since its initial founding with the portion maintaining the Kistler name having a broad piezoelectric accelerometer line and a historical focus on force and pressure measurement. The significant company emerging from Kistler was PCB Piezotronics. PCB is a rapidly growing company with an increasing focus on piezoelectric accelerometers, particularly in the modal and industrial areas. Endevco has maintained a consistent focus on shock and vibration measurements.

Table 5.1: Companies that produce and distribute accelerometer worldwide

Company	**Description and Models**
Brüel & Kjær	• Sound and vibration measurement instrumentation • B&K Model 4303, 5kHz (1950s) • B&K Model 8307 (shear mode, 1972) • $DeltaTron^R$ - Integrated circuit system • $Thetashear^R$ - Low cost for volume application • B&K's 100,000 g accelerometer model is the 8309.
Columbic Research Laboratories	• Shock and vibration instrumentation • Model 5004 - first shock accelerometer • Currently focused on industrial marketplace
Gulton Manufacturing	• AQB 4901 and other for engine vibration monitoring • Proprietary piezoceramic (G-1900) • Current focus on broad based applications
Kistler Instrument Company	• Quartz (linear piezoelectric) transducers for force and pressure measurement • Quartz for high temperature applications and not to zero shift as do some of soft ferroelectric ceramics • Kistler's 805A - (the first, 100,000 g, 1966) • Kistler's 805B - (100,000 g, single crystal quartz) • At present, Kistler's principally manufactures accelerometer types including quartz shear.
PCB Piezoelectronics	• PCB split from Kistler in 1967 for force and pressure measurements • Integrated circuit piezoelectric (ICP) • Created demand for low-cost accelerometers

	• Addressing sensor installation, orientation, cabling, signal conditioning and end-to-end calibration • Model 308A04 - 1973 • Model 963A Gravimetric calibrator - 1973 • Model 9090C Accelerometer Array Calibrator - 1986, enabled up to 128 modal accelerometer to be calibrated • At present focused on accelerometer design
Endevco	• Product (piezoelements) focused on shock and vibration • Radiation hardened 2266 series of accelerometers to evolve in ranges to 20,000 g (1968) • 7270A, weight = 1.5 gm) was marketed in 1983 in ranges to 200,000 g with a 1.2 MHz resonant frequency. • 6237M70 & 6240 were released with a temperature capability of 1400° F in 1988
Wilcoxon Research	• Developed to support studies of noise damping characteristics of vibration isolation mounts for shipboard machinery.

Decision: from listed suppliers, PCB Piezoelectronics sensors selected due to their demand for low-cost and ability of addressing sensor installation, orientation, cabling, signal conditioning and end-to-end calibration. Using this requirements and requesting on PCB official website (https://www.pcb.com/shop-sensors). A Model: 352B voltage mode accelerometer from PCB Piezoelectronics selected which meets all these requirements.

Table 5.2: Accelerometer specification Model:352B

Technical Data	**Value**	**Units**
Acceleration range	1000	g
Sensitivity	1000	mv/g
Frequency response (±5)	2 to 10,000	Hz
Operating temperature	-54 to +93	C^o
Weight	25	gm
Mounting torque	113 to 226	N-cm

Sensor Mounting

When choosing a mounting method, consideration both on advantages and disadvantages of each techniques. Characteristics like location, ruggedness, amplitude range, accessibility, temperature and portability are extremely critical. However, the most important and often overlooked consideration is the effect the mounting technique has on the high frequency performance of the accelerometer [62].

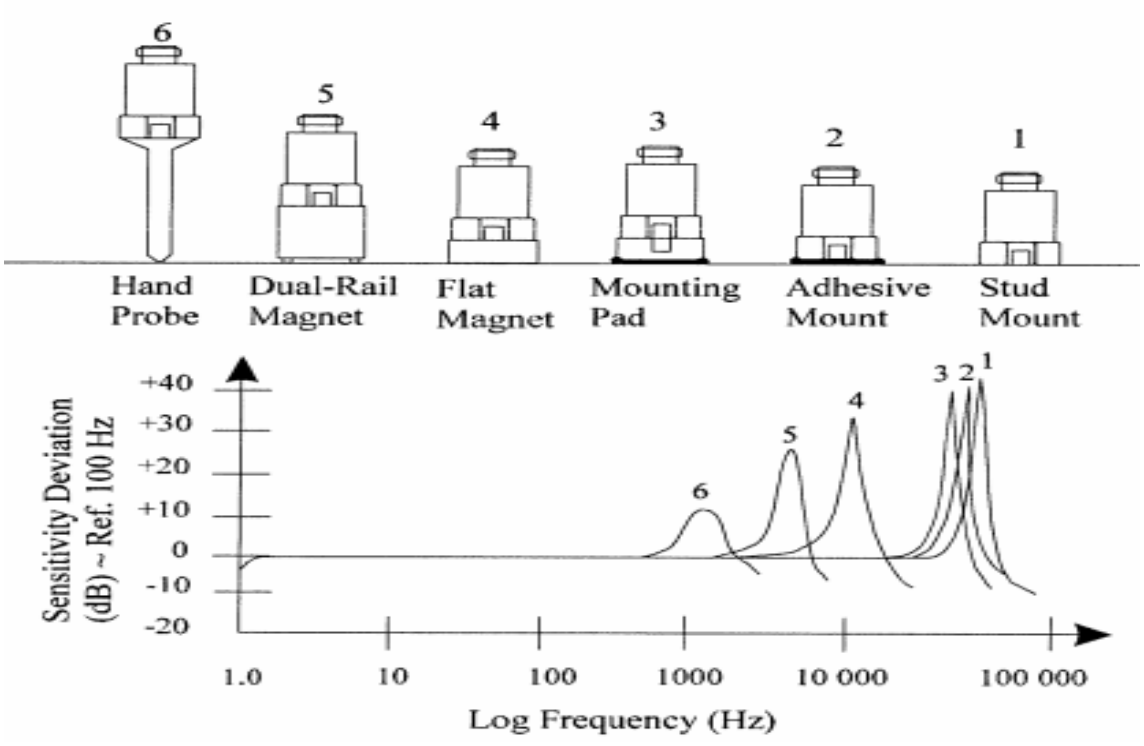

Figure 5.3: Assorted mounting configurations and their effects on high frequency

The accelerometer is positioned directly on the impactor mass, which needs permanent mounting technique in order to avoid misalignment of the accelerometer from the mass. Also hand probe, dual-rail magnet and flat magnet mounting are highly sensitive above 10,000 Hz, but the others sensitivity rise above 10,000 Hz. For these reasons stud mount is selected for long term measurement.

Data Acquisition and Manipulation

For simple drop-weight impact testing, no data acquisition equipment is required. According to ASTM D7136, if such equipment utilized, it shall be in accordance with Annex A1, Minimum Instrumentation Requirements, of Test Method D3763. The natural frequency of the transducer-impactor assembly shall be greater than 6 kHz, the analog-to-digital converter shall be 8-bit or greater, the minimum sampling rate shall be 100 kHz, and the data storage capacity shall be 1000 points or larger.

Table 5.3: Specification of Model 485B39 signal conditioner

Specifications	
Channel Count	2
Voltage Range (Nominal)	±10 V pk
ADC Resolution	24-bit
Frequency Range (± 5 %)	0.8 Hz to 20.7 kHz
Sample Rate	48, 44.1, 32, 22.05, 16, 11.025, 8 kHz
Anti-Aliasing Low-Pass Filter (-3 dB) at 48 kHz	22.9 kHz
Temperature Range (Operating)	14^oF to $+176^oF$ (-10^oC to $+80^oC$)
Housing Material	Stainless Steel
Size (length × width × height)	2.4” × 1.5” × 0.7” ($60mm \times 39mm \times 19mm$)
Weight	4.4 oz (125 grams)

The accelerometer puts out a voltage proportional to acceleration. The signal is recorded using the ICP signal conditioner. The 485B39 is a 2-channel ICP (IEPE) sensor signal conditioner featuring 2 BNC inputs and a USB digital signal output. Play & plug connectivity is achieved via USB without any cumbersome setup or driver installation. The 485B39 powers ICP sensors while digitizing their signals: simply plug the unit into a USB port of Lenovo E51 laptop computer to view, record, or process signal from the accelerometer. The data then plotted using SpectralPLUS-SC software as shown in the Figure 5.4.

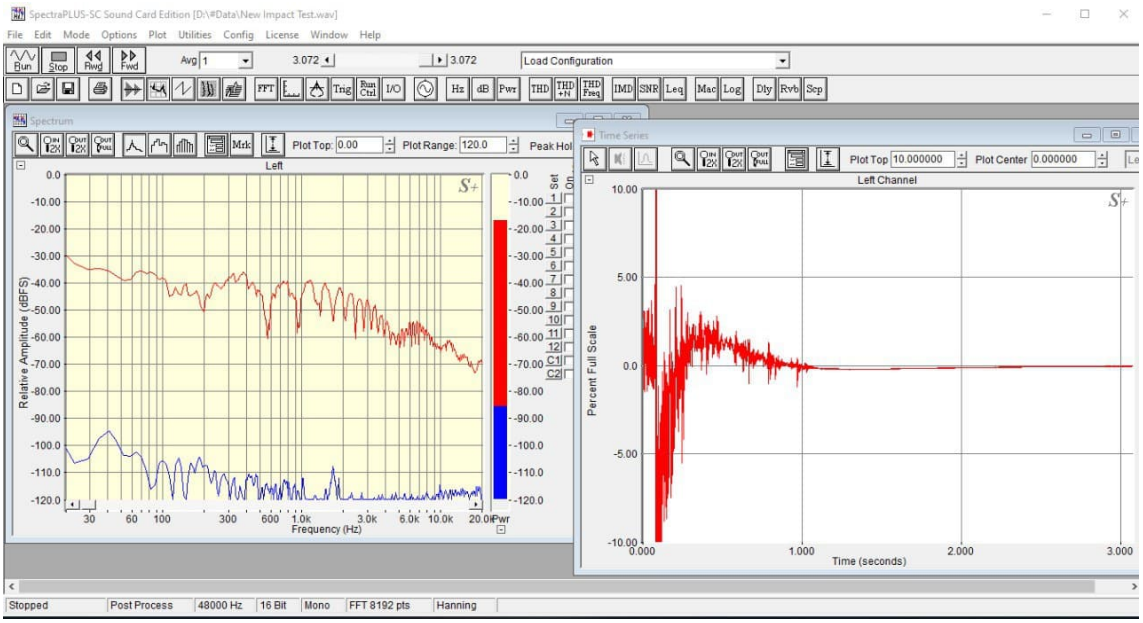

Figure 5.4: Spectral data from 352B accelerometer

Conversion of spectral data

Using Matlab software the result from spectral data plotted into force-time curve, energy-time curve, displacement-time curve, velocity-time curve, acceleration-time curve using free undamped vibration analysis. For conversion of spectral data from the accelerometer to the required velocity and acceleration, the paper used the following procedure.

Spectra are defined by the maximum response of a simple oscillator subjected to

base acceleration a(t). The equation of motion of the oscillator is given as [63];

$$x'' + 2\beta\omega\dot{x} + \omega^2 x = -a(t) \tag{5.1}$$

in which β = the fraction of critical damping and ω = the natural frequency of vibrations of the oscillator.

Assuming that a(t) may be approximated by a segmentally linear function, equation (5.1) may be written as

$$x'' + 2\beta\omega x' + \omega^2 x = -a_i - \frac{\Delta a_i}{\Delta t_i}(t - t_i); .....t_i \leq t \leq t_{i+1} \tag{5.2}$$

with

$$\Delta t_i = t_{i+1} - t_i, \Delta a_i = a_{i+1} - a \tag{5.3}$$

The solution of equation 5.2, for $t_i \leq t \leq t_{i+1}$ is given by

$$\begin{aligned} x = {} & e^{-\beta\omega(t-t_i)}\left[C_1 \sin\omega\sqrt{1-\beta^2}(t-t_i) + C_2\cos\omega\sqrt{1-\beta^2}(t-t_i)\right] \\ & - \frac{a_i}{\omega^2} + \frac{2\beta}{\omega^3}\frac{\Delta a_i}{\Delta t_i} - \frac{1}{\omega^2}\frac{\Delta a_i}{\Delta t_i}(t-t_i) \end{aligned} \tag{5.4}$$

in which C_1 and C_2 are constants of integration. Setting $x = x_i$ and $x' = x'_i$ at $t = t_i$ and solving for C_1 and C_2, it is found that

$$C_1 = \frac{1}{\omega\sqrt{1-\beta^2}}\left(\beta\omega x_i + x'_i - \frac{2\beta^2 - 1}{\omega^2}\frac{\Delta a_i}{\Delta t_i} + \frac{\beta}{\omega}a_i\right) \tag{5.5}$$

$$C_2 = x_i - \frac{2\beta}{\omega^3}\frac{\Delta a_i}{\Delta t_i} + \frac{a_i}{\omega^2} \tag{5.6}$$

Substitution of these values of C_1 and C_2 into equation 5.4 will show that x and x' at $t = t_{i+1}$ are given by

$$\bar{x}_{i+1} = A(\beta, \omega, \Delta t_i)\bar{x}_i + B(\beta, \omega, \Delta t_i)\bar{a}_i \tag{5.7}$$

in which

$$\bar{x_i} = \begin{pmatrix} x_i \\ \dot{x_i} \end{pmatrix} \qquad \text{and} \qquad \bar{a_i} = \begin{pmatrix} a_i \\ a_{i+1} \end{pmatrix} \tag{5.8}$$

$$A = \begin{bmatrix} a_{11} & a_{12} \\ a_{21} & a_{22} \end{bmatrix} \qquad \text{and} \qquad B = \begin{bmatrix} b_{11} & b_{12} \\ b_{21} & b_{22} \end{bmatrix} \tag{5.9}$$

The elements of the matrices A and B are given by

$$\begin{aligned}
a_{11} &= e^{-\beta\omega\Delta t_i}\left(\frac{\beta}{\sqrt{1-\beta^2}}\sin\omega\sqrt{1-\beta^2}\Delta t_1 + \cos\omega\sqrt{1-\beta^2}\Delta t_i\right) \\
a_{12} &= \frac{e^{-\beta\omega\Delta t_i}}{\omega\sqrt{1-\beta^2}}\sin\omega\sqrt{1-\beta^2}\Delta t_i \\
a_{21} &= -\frac{\omega}{\sqrt{1-\beta^2}}e^{-\beta\omega\Delta t_i}\sin\omega\sqrt{1-\beta^2}\Delta t_i \\
a_{22} &= e^{-\beta\omega\Delta t_i}\left(\cos\omega\sqrt{1-\beta^2}\Delta t_i - \frac{\beta}{\sqrt{1-\beta^2}}\sin\omega\sqrt{1-\beta^2}\Delta t_i\right)
\end{aligned} \tag{5.10}$$

$$\begin{aligned}
b_{11} &= e^{-\beta\omega\Delta t_i}\left[\left(\frac{2\beta^2-1}{\omega^2\Delta t_i + \frac{\beta}{\omega}}\right)\frac{\sin\omega\sqrt{1-\beta^2}\Delta t_i}{\omega\sqrt{1-\beta^2}} + \left(\frac{2\beta}{\omega^3\Delta t_i} + \frac{1}{\omega^2}\right)\cos\omega\sqrt{1-\beta^2}\Delta t_i\right] \\
&\quad - \frac{2\beta}{\omega^3\Delta t_i} \\
b_{12} &= -e^{-\beta\omega\Delta t_i}\left[\left(\frac{2\beta^2-1}{\omega^2\Delta t_i + \frac{\beta}{\omega}}\right)\frac{\sin\omega\sqrt{1-\beta^2}\Delta t_i}{\omega\sqrt{1-\beta^2}} + \frac{2\beta}{\omega^3\Delta t_i}\cos\omega\sqrt{1-\beta^2}\Delta t_i\right] \\
&\quad - \frac{1}{\omega^2} + \frac{2\beta}{\omega^3\Delta t_i} \\
b_{21} &= e^{-\beta\omega\Delta t_i}\left[\left(\frac{2\beta^2-1}{\omega^2\Delta t_i} + \frac{\beta}{\omega}\right)\left(\cos\omega\sqrt{1-\beta^2}\Delta t_i - \frac{\beta}{1-\beta^2}\sin\omega\sqrt{1-\beta^2}\Delta t_i\right)\right. \\
&\quad \left. - \left(\frac{2\beta}{\omega^2\Delta t_i} + \frac{1}{\omega^2}\right)\left(\omega\sqrt{1-\beta^2}\sin\omega\sqrt{1-\beta^2}\Delta t_i + \beta\omega\cos\omega\sqrt{1-\beta^2}\Delta t_i\right)\right] \\
&\quad + \frac{1}{\omega^2\delta t_i} \\
b_{22} &= -e^{-\beta\omega\Delta t_i}\left[\frac{2\beta^2-1}{\omega^2\Delta t_i}\left(\cos\omega\sqrt{1-\beta^2}\Delta t_i - \frac{\beta}{\sqrt{1-\beta^2}}\sin\omega\sqrt{1-\beta^2}\Delta t_i\right)\right. \\
&\quad \left. -\frac{2\beta}{\omega^3\Delta t_i}\left(\omega\sqrt{1-\beta^2}\sin\omega\sqrt{1-\beta^2}\Delta t_i + \beta\omega\cos\omega\sqrt{1-\beta^2}\Delta t_i\right)\right] \\
&\quad - \frac{1}{\omega^2\Delta t_i}
\end{aligned} \tag{5.11}$$

All equations from equation 5.8–5.11 imported to Matlab code listed in Appendix C.

Chapter 6

Result and Discussion

The aim of this paper, as mentioned earlier, is to study the behavior of composite plates, subjected to low velocity impact vertically. The influence of impact height and imparted energy, is shown to be of great importance with respect to induced damage and associated residual properties.

It is realistic to assume that composite structures will be subjected to some form of low velocity impact damage within their design lifetime. Thus it is pertinent to consider the effects of such damage on overall structure integrity (damage tolerance).

The precise form of damage will clearly depend on many factors e.g. type of composite materials (resin/matrix), structural form, impactor velocity and geometry, etc. Whatever the impacting conditions it is universally accepted that present levels of mathematical or numerical modelling are wholly unable to predict the resulting damage mechanisms which take place in the composite material. Accepting this fact it is therefore desirable to attempt to gain a greater insight into the many complex processes which contribute to damage within the composite.

In this chapter the experimental results from the test program are presented. These are characterized in terms of impact force, impact energy, impact velocity and impact displacement. Using the measured impact acceleration other impact properties

assessed.

6.1 Experimental Results

The experiment itself contains three stages; i) Four (4) tests taken during the impact event from the accelerometer at constant drop weight (5.5 kg) and different drop heights. ii) Recording the result using SpectralPLUS software. iii) Conversion of spectral data to dynamic data using matlab 2018b software using equation listed in section 5.2.1. These test programs are as follows

- 1^{st} test conducted from drop height of 200 mm,
- 2^{nd} test conducted from drop height of 400 mm,
- 3^{rd} test conducted from drop height of 500 mm,
- 4^{th} test conducted from drop height of 600 mm,

Results obtained from Matlab software and shown in details below.

6.1.1 Spectral curves

Indicates the impact amplitude which is proportional to acceleration. Pick points in four plots are rebound during the impact event, two picks indicate two rebound. Considerable noise is suddenly seen on the signal. This noise is due to vibrations in the body of the falling weight caused by sudden changes in the force as the sample impacted.

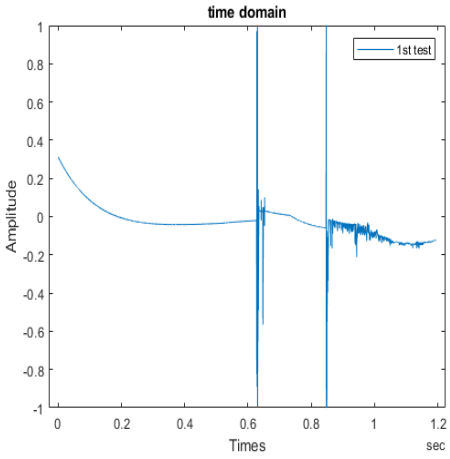

Figure 6.1: Spectral plot (test-1)

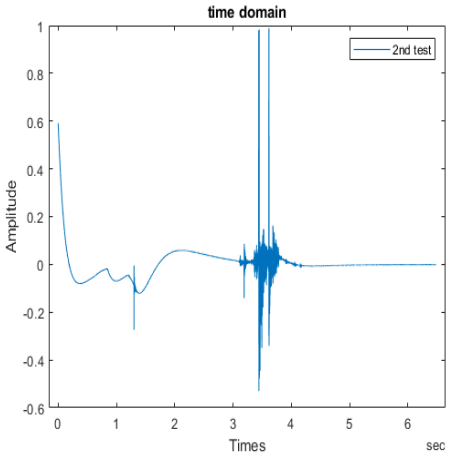

Figure 6.2: Spectral plot (test-2)

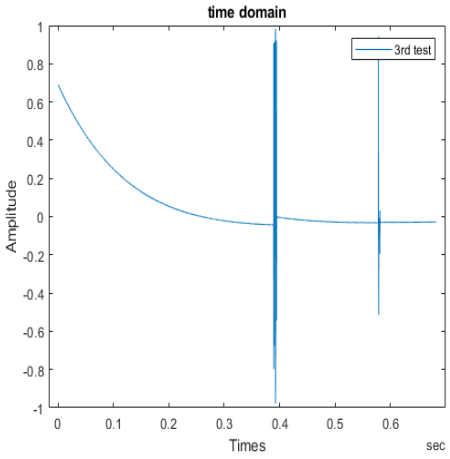

Figure 6.3: Spectral plot (test-3)

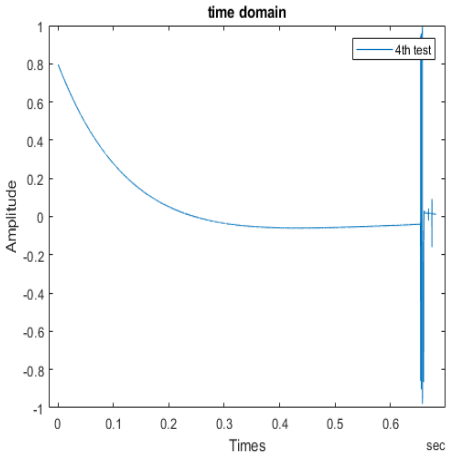

Figure 6.4: Spectral plot (test-4)

6.1.2 Force-time curve

The signal measured by accelerometers during impact can be regarded as the sum of several terms [17].

- the actual specimen reaction;
- the inertial load on the tup caused by the acceleration of the specimen;
- ringing of impactor and specimen

To highlight the relative influence of the various components of the load signal, a first step was to determine the natural frequencies of the impactor; the accelerometer

signal, in fact, represents the local dynamics of a complex system (many dynamic models of impact, for example, represent the system as an assemblage of mass and springs), and the estimate of the tup-specimen contact force from accelerometer signals can therefore be affected by significant errors.

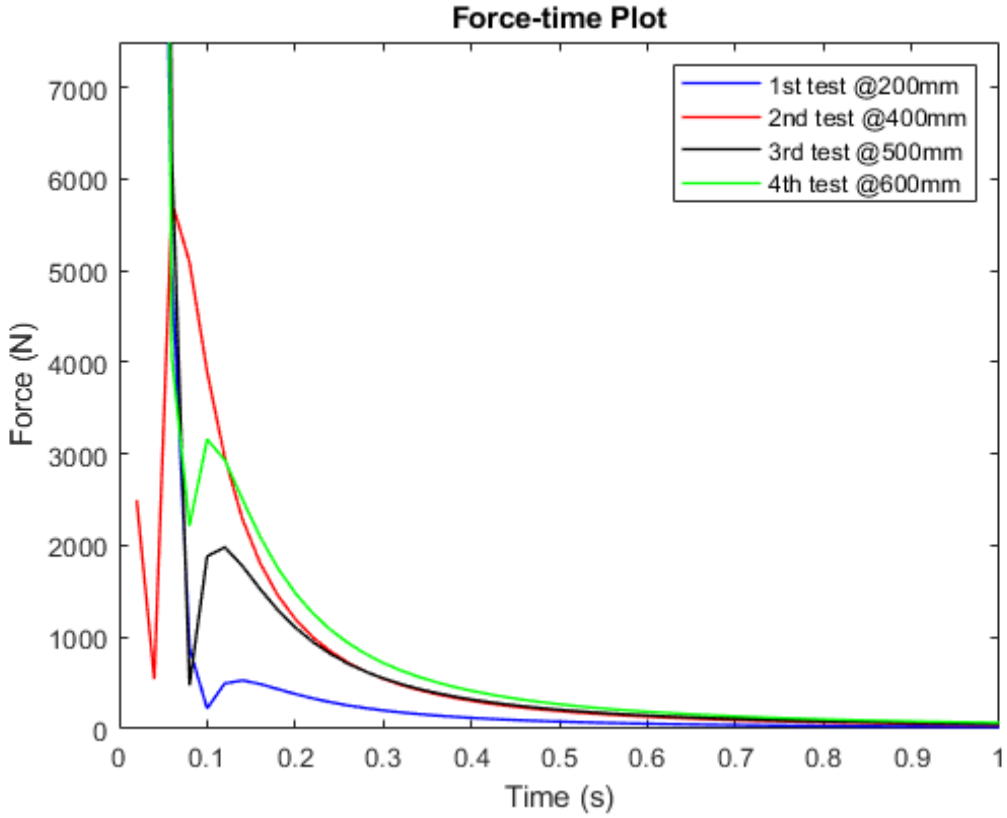

Figure 6.5: Force-time curve

From figure 6.5, after 0.1 seconds contact between impactor tup and test specimen occurred. The rise and fall of the curves after 0.1 second is the moment where the impactor rebounds from the test specimen, the maximum force measured at this point. Because of their high frequency, these oscillations disappear when the force is integrated to obtain the energy absorbed by the specimen, but their high amplitude most of the time makes it difficult to identify the actual contact force as a function of time. It is important to notice that in several applications the force is the impact controlling parameter and proves, in any case, an indicator that is more sensitive than energy to the various phases of damage progression.

- the sharp drop suspected to be caused by the initiation of delaminations, which also cause a significant loss of stiffness.

6.1.3 Energy-time curves

From figure 6.6 steadily increasing energy transfer up to the moment of impact with in 0.1 sec, and becoming essentially level during the rebound interval of the falling weight. If crack occurred on the specimen additional increase in energy could be noticed on the curve. As seen in the figure maximum and minimum energy absorbed by the specimen at 600 mm and 200 mm respectively.

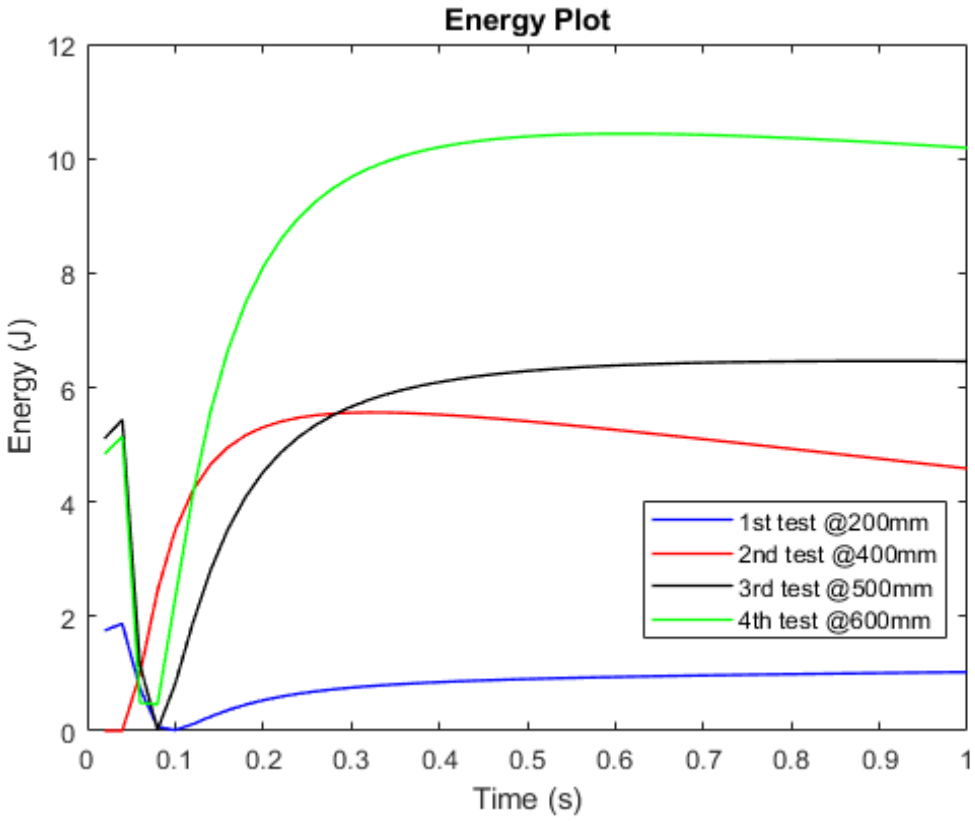

Figure 6.6: Energy-time curve

6.1.4 Velocity-time curves

The velocity trace (Fig. 6.7) increases suddenly for about 0.1 seconds and reaches maximum for all test programs . Then decreases up to 0.6 seconds in all test programs which indicates the moment of cracking before becoming essentially constant

relatively for the next seconds. The nearly constant velocity is due to the weight falling freely after cracking the sample.

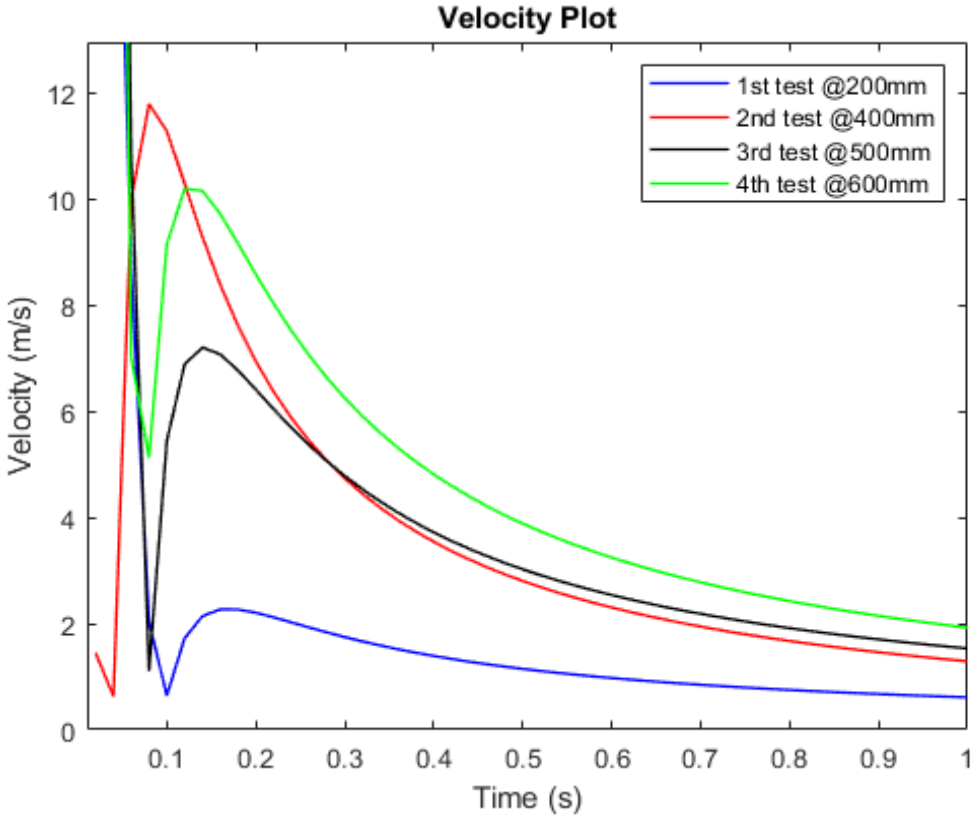

Figure 6.7: Velocity-time curve

6.1.5 Displacement-time curves

The deflection plot (Fig. 6.8), for this case shows a maximum of no maximum–it simply keeps decreasing until 0.1 seconds and steadily increase up to 0.25 seconds, finally reaches constant for the rest of the test. The point where the graph starts falling in all test programs indicate the location of the impactor (i.e. it stops after the impactor completely looses it's energy).

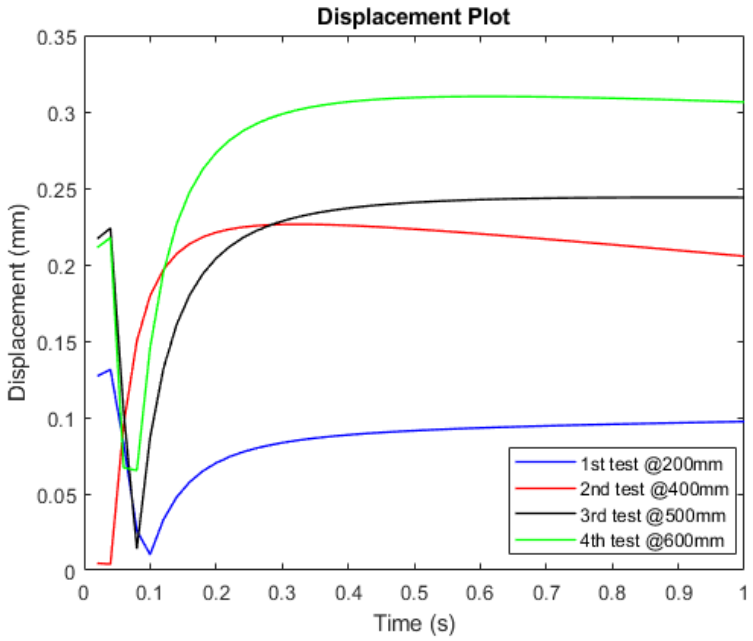

Figure 6.8: Displacement-time curve

In all cases there was crack formation with out penetration. The parameters at crack onset (force, deflection and energy transfer) were found to be independent of drop height or impact energy, as long as the impact was severe enough to cause cracking. The work concludes from this test apparatus that close results obtained when compared to conventional test apparatus like CEAST Drop Weight Machine (see Figure 2.7). The following maximum impact values obtained from four test programs

Table 6.1: Maximum absorbed energy, impact force, impact velocity and deformation from the test programs

Values (maximum)	**Test 1**	**Test 2**	**Test 3**	**Test 4**
Energy (J)	1.873	5.564	6.462	10.44
Force (N)	528.34	1.98×10^3	3.16×10^3	5.75×10^3
Velocity (m/s)	2.268	7.205	10.20	11.79
Displacement (mm)	0.1313	0.2264	0.2440	0.3100

Chapter 7

Conclusions and Further work

This chapter is divided into two sections. The conclusions of the work and ideas on future work to further study the drop weight impact test machine by properly selecting instrumentation and data manipulation systems.

7.1 Conclusion

Following the work, a number of conclusions drawn and these are outlined as follows;

- Portable and lightweight (23.8 Kg) drop weight impact tester designed and prototyped. The DWITM used to test fibre reinforced composite materials according to ASTM D7136 standard testing method.

- The thickness of the test specimen is 5 mm. The tester uses a standard mass of 5.5 Kg which outputs a total energy absorbed by the specimen during four test programs as shown in table 6.1 is 10.44 J in test 4, the corresponding velocity of 11.79 m/s, if the impactor released from a height of 600 mm.

- Both drop weight and height can be varied independently by adding additional mass (0.5 and 0.45 kg) to the impactor housing and moving the impactor assembly to the desired height respectively. The results (impact force or energy) from the tester by releasing large mass impactor from small drop height and releasing lighter mass impactor from large height are proportional. The test-

ing personnel can vary the impact energy by simply adding additional mass by keeping the drop height constant or vice versa.

- In designing the drop two, the work shows it's ability to support load (the whole components except the specimen fixture) without experiencing excessive stress; and the ability of the drop tower to support specified load without undergoing unacceptable deformation.

- The striker's tup of 16 mm hemispherical can be disassembled from the shaft which makes it interchangeable (when damage occurred to the tup due to repeated test).

- The designed drop weight impactor can easily be assembled and disassembled and can also be transported by a single person.

- At high drop heights, with increase in imparted energy with respect to impact force, part perforation of the specimen resulted. This indicates that the associated failure mechanisms absorb more energy and explains the increase in imparted energy resulting in fibre pull out and fibre fracture.

7.2 Further work

The author recommends the following points as areas as a future study

1. Using different specimen materials, such as unidirectional glass fibre composite laminates, carbon fibre laminates. Assessing the influence of varying the laminates stacking sequence.

2. Employing different impactor heads with various shapes and sizes. It is evident from other researchers that the size of impactor head contribute greatly in producing damage. Larger the head of the impactor will produce bigger contact area and therefore bigger damage area.

3. The instrumentation system can be varied. In this work accelerometer used as a sole instrumentation system for cost and minimizing additional instruments, but different researchers used different mechanism i.e directly measuring the impact force using load cell; or measuring velocity using infrared detector or velocimeter.

4. It can finally be mentioned that one of the problems in measuring an accurate impacting energy (or velocity) was the drop height method and a lubricating mechanism. It very important to install a self-lubricating on the drop guide system, or developing a mechanism that allows the guide rods to be consistently lubricated.

Bibliography

[1] M. W. Money, "Instrumented falling weight impact testing of polymethylmethacrylate and high density polyethylene," Ph.D. dissertation, University of London, 1988.

[2] L. C. Cessna, J. P. Lehane, R. H. Ralston, and T. Prindle, "The development of an instrumented projectile impact test: data glass-reinforced and impact-modified polypropylene," *Polymer Engineering & Science*, vol. 16, no. 6, pp. 419–425, 1976.

[3] A. S. T. M. D7136/D7136M-15, "Standard test method for measuring the damage resistance of a fiber-reinforced polymer matrix composite to a drop-weight impact event," 2015.

[4] R. L. Sierakowski and S. K. Chaturvedi, "Dynamic loading and characterization of fiber-reinforced composites," *Dynamic Loading and Characterization of Fiber-Reinforced Composites, by Robert L. Sierakowski, Shive K. Chaturvedi, pp. 252. ISBN 0-471-13824-X. Wiley-VCH, February 1997.*, p. 252, 1997.

[5] F. Ehrich, "Low velocity impact on pre-loaded composite structures," Ph.D. dissertation, Imperial College London, 2013.

[6] F. P. Beer, *Statics and mechanics of materials*. by The McGraw-Hill Companies, Inc, 2011.

[7] J. E. Shigley, *Shigley's mechanical engineering design*. Tata McGraw-Hill Education, 2011.

[8] R. S. Khurmi and J. K. Gupta, *A textbook of machine design*. Eurasia, 2005.

[9] D. Roylance, "Mechanical properties of materials," *Massachusetts Institute of Technology*, pp. 51–78, 2008.

[10] S. P. Timoshenko and S. Woinowsky-Krieger, *Theory of plates and shells*. McGraw-hill, 1959.

[11] J. Mabry, J. M. Skibo, M. B. Schiffer, and K. Kvamme, "Use of a falling-weight tester for assessing ceramic impact strength," *American Antiquity*, vol. 53, no. 4, pp. 829–839, 1988.

[12] U. Farooq and P. Myler, "Finite element simulation of damage and failure predictions of relatively thick carbon fibre-reinforced laminated composite panels subjected to flat and round noses low velocity drop-weight impact," *Thin-Walled Structures*, vol. 104, pp. 82–105, 2016.

[13] S. W. J. H. Khoo, "Low velocity impact of composite structures." 1991.

[14] E. McMenamin, *Impact testing: understanding impact test methods and standards*. Quality Magazine, 2019.

[15] S. Abrate, *Impact on composite structures*. Cambridge university press, 2005.

[16] A. Ahmadnia, "Energy absorption of macrocomposite laminates," Ph.D. dissertation, 2000.

[17] F. Aymerich, P. Marcialis, S. Meili, and P. Priolo, "An instrumented drop-weight machine for low-velocity impact testing," *WIT Transactions on The Built Environment*, vol. 25, 1970.

[18] H. Bayer, A. von Bohlen, R. Klockenkämper, and D. Klockow, "Choice of a suitable material for construction of a Battelle type impactor to minimize systematic errors in sampling of airborne dust," *Microchimica Acta*, vol. 119, no. 1-2, pp. 167–176, 1995.

[19] M. Wisheart, "Impact properties and finite element analysis of a pultruded composite system," Ph.D. dissertation, © M. Wisheart, 1996.

[20] B. Aryal, E. V. Morozov, H. Wang, K. Shankar, P. J. Hazell, and J. P. Escobedo-Diaz, "Effects of impact energy, velocity, and impactor mass on the damage induced in composite laminates and sandwich panels," *Composite Structures*, vol. 226, p. 111284, 2019.

[21] M. S. Rajput, M. Burman, A. Segalini, and S. Hallström, "Design and evaluation of a novel instrumented drop-weight rig for controlled impact testing of polymer composites," *Polymer Testing*, vol. 68, pp. 446–455, 2018.

[22] P. Zoller, "Instrumentation for impact testing of plastics," *Polymer Testing*, vol. 3, no. 3, pp. 197–208, 1983.

[23] J. Williams, "An assessment of low velocity impact damage of composite structures." Ph.D. dissertation, Paisley College of Technology, 1987.

[24] G. Tsigkourakos, "Experimental and numerical analysis of damage in crfc laminates under static and impact loading conditions," Ph.D. dissertation, Loughborough University, 2013.

[25] A. P. Paran, "The low-velocity impact response of thin, stiffened cfrp panels." Ph.D. dissertation, University of Sheffield, 1999.

[26] F. Taheri-Behrooz, M. Shokrieh, and H. Abdolvand, "Designing and manufacturing of a drop weight impact test machine," *Engineering Solid Mechanics*, vol. 1, no. 2, pp. 69–76, 2013.

[27] Hodgkinson, *Mechanical testing of advanced fibre composites*. Elsevier, 2000.

[28] J. D. Winkel and D. F. Adams, "Instrumented drop weight impact testing of cross-ply and fabric composites," *Composites*, vol. 16, no. 4, pp. 268–278, 1985.

[29] W. Zhang, S. Chen, and Y. Liu, "Effect of weight and drop height of hammer on the flexural impact performance of fiber-reinforced concrete," *Construction and Building Materials*, vol. 140, pp. 31–35, 2017.

[30] S. Madjidi, "Low velocity impact of obliquely inclined composite plates," Ph.D. dissertation, University of the West of Scotland, 1994.

[31] T. Mitrevski, I. H. Marshall, R. Thomson, R. Jones, and B. Whittingham, "The effect of impactor shape on the impact response of composite laminates," *Composite Structures*, vol. 67, no. 2, pp. 139–148, 2005.

[32] S. N. A. Safri, M. T. H. Sultan, N. Yidris, and F. Mustapha, "Low velocity and high velocity impact test on composite materials–a review," *Int. J. Eng. Sci*, vol. 3, no. 9, pp. 50–60, 2014.

[33] W. J. Cantwell, "Geometrical effects in the low velocity impact response of GFRP," *Composites science and technology*, 2007.

[34] Z. Shen, "Characterisation of low velocity impact response in composite laminate," 2015.

[35] P. Robinson and G. A. O. Davies, "Impactor mass and specimen geometry effects in low velocity impact of laminated composites," *International journal of impact engineering*, vol. 12, no. 2, pp. 189–207, 1992.

[36] F. Yang, "Geometrical effects in the impact response of composite structures," Ph.D. dissertation, University of Liverpool, 2010.

[37] J. C. Lloyd, "Impact damage and damage tolerance of fibre reinforced advanced composite laminate structures," Ph.D. dissertation, © James Lloyd, 2002.

[38] K. Sofocleous, "Controlled impact tests on composite materials: damage development and energy analysis," Ph.D. dissertation, University of Surrey (United Kingdom), 2008.

[39] Y. Liu and B. Liaw, "Drop-weight impact tests and finite element modeling of cast acrylic/aluminum plates," *Polymer Testing*, vol. 28, no. 8, pp. 808–823, 2009.

[40] Q. Abessalam, "Investigation into the modes of damage and failure in natural fibre reinforced epoxy composite materials," Ph.D. dissertation, University of East London, 2011.

[41] X. Gong, "Investigation of different geometric structure parameter for honeycomb textile composites on their mechanical performance," Ph.D. dissertation, The University of Manchester (United Kingdom), 2011.

[42] Z. Mouti, "Localised low velocity impact performance of short glass fibre reinforced polyamide 66 oil pans," 2012.

[43] E. Sevkat, B. Liaw, and F. Delale, "Drop-weight impact response of hybrid composites impacted by impactor of various geometries," *Materials & Design (1980-2015)*, vol. 52, pp. 67–77, 2013.

[44] A. Malhotra, "Low velocity edge impact on composite laminates: damage tolerance and numerical simulations," Ph.D. dissertation, Queen Mary University of London, 2014.

[45] P. Nash, "Experimental impact damage resistance and tolerance study of symmetrical and unsymmetrical composite sandwich panels," Ph.D. dissertation, Loughborough University, 2016.

[46] K. T. Ulrich, *Product design and development*. Tata McGraw-Hill Education, 2003.

[47] Y. Haik, S. Sivaloganathan, and T. M. Shahin, *Engineering design process*. Nelson Education, 2018.

[48] S. Fukushima and S. Kurahara, "Drop test apparatus," Feb. 5 2009, uS Patent App. 11/832,739.

[49] R. B. Lewis, "Drop testing machine," Mar. 14 1933, uS Patent 1,901,460.

[50] L. M. Nazar, "Drop weight type impact testing machine," Oct. 22 1996, uS Patent 5,567,867.

[51] L. G. Freedy, "Drop testing machine," Feb. 11 1958, uS Patent 2,822,687.

[52] P. V. Brown, "Impact testing machine," Jul. 24 1956, uS Patent 2,755,658.

[53] L. Gunawan, T. Dirgantara, and I. S. Putra, "Development of a dropped weight impact testing machine," *International Journal of Engineering & Technology*, vol. 11, no. 6, pp. 120–126, 2011.

[54] X. X. Zhang, G. Ruiz, and R. C. Yu, "A new drop weight impact machine for studying the fracture behaviour of structural concrete," in *10 th International Conference on Structures Under Shock and Impact*, 2008, pp. 251–261.

[55] J. L. Ruiz-Herrero, M. A. Rodriguez-Perez, and J. A. De Saja, "Design and construction of an instrumented falling weight impact tester to characterise polymer-based foams," *Polymer testing*, vol. 24, no. 5, pp. 641–647, 2005.

[56] D. R. Ambur, C. B. Prasad, and W. A. Waters, "A dropped-weight apparatus for low-speed impact testing of composite structures," *Experimental Mechanics*, vol. 35, no. 1, pp. 77–82, 1995.

[57] B. Lawrence, "Low velocity impact assessment of flax and kevlar-flax fibre reinforced polymer laminates using experimental and numerical methods," Ph.D. dissertation, Ryerson University, 2012.

[58] P. L. Walter, "The history of the accelerometer: 1920s-1996-prologue and epilogue, 2006," *Sound & vibration*, vol. 41, no. 1, pp. 84–90, 2007.

[59] N. J. Mills and A. S. I. Moosa, "Impacts of hemispherical strikers on polystyrene bead foam," *Journal of cellular plastics*, vol. 35, no. 4, pp. 289–310, 1999.

[60] C. M. Worrall, "The behaviour of composite sandwich beams and panels under low velocity impact conditions." Ph.D. dissertation, University of Liverpool, 1990.

[61] M. M.-u. Frequenztechnik, "Piezoelectric Accelerometers: Theory and Application," *Available from Internet: http://www. gracey. co. uk/downloads/accelerometers. pdf*, 2001.

[62] J. Lally, "ACCELEROMETER SELECTION CONSIDERATIONS Charge and ICP® Integrated Circuit Piezoelectric," 2005.

[63] N. C. Nigam and P. C. Jennings, "Calculation of response spectra from strong-motion earthquake records," *Bulletin of the Seismological Society of America*, vol. 59, no. 2, pp. 909–922, 1969.

[64] E. T. Camponeschi, "Compression of composite materials: a review," in *Composite Materials: Fatigue and Fracture (Third Volume)*. ASTM International, 1991.

Appendix A

Charts and Table

Strain Gauge Tups and Inserts

CEAST 9350 Strain Gauge (Type 1) Tups

Catalog Number	Capacity		Minimum Insert Diameter (For Puncturing Test)	
	kN	lbs	mm	in
7529.301	22	5,000	10	0.394
7529.302	45	10,000	20	0.787
7529.303	90	20,000	20	0.787
7529.304	222	50,000	20	0.787

CEAST 9340 Strain Gauge (Type 1) Tups

Catalog Number	Capacity		Minimum Insert Diameter (For Puncturing Test)	
	kN	lbs	mm	in
7519.301	22	5,000	10	0.394
7519.302	45	10,000	20	0.787
7519.303	90	20,000	20	0.787

Tup Inserts for Strain Gauge (Type 1) Tups

Catalog Number	Description	Testing Standards	Tup Compatibility
7529.310	10 mm (0.394 in) Ø Hemispherical	ISO 6603-1,-2, ISO 7765-1,-2	7529.301
7519.310			7519.301
7529.311	12.7 mm (1/2 in) Ø Hemispherical	ASTM D3763, ASTM D7192, ASTM D5628 Method FD	7529.301
7519.311			7519.301
7529.313	20 mm (0.787 in) Ø Hemispherical	ISO 6603-1,-2, ISO 7765-1,-2 ASTM D5628 Method FE	All Strain Gauge (Type 1) Tups
7529.320	10 mm (0.394 in) Ø Hemispherical (For Non-Puncturing Test)	ISO 6603-1,-2, ISO 7765-1,-2	
7529.321	12.7 mm (1/2 in) Ø Hemispherical (For Non-Puncturing Test)	ASTM D3763, ASTM D7192, ASTM D5628 Method FD	
7529.322	16 mm (5/8 in) Ø Hemispherical (For Non-Puncturing Test)	ASTM D7136/7136M, Airbus AITM 1.0010, PR-EN 6038, ISO 18352, Boeing BSS 7260, SACMA 2R-94	
7529.324	25.4 mm (1 in) Ø Hemispherical	-	
7529.325	38.1 mm (1 1/2 in) Ø Hemispherical	ASTM D5628 Method FC	
7529.329	6.35 mm (1/4 in) Radius Conical, 25.4 mm Ø (1 in) Base	ASTM D5628 Method FB	
7529.330	Plastics Charpy Insert	ISO 179-2	
7529.331	Plastics Charpy Insert	ASTM D6110	
7529.332	Plastics Charpy Insert	ISO 180, ASTM D256	
7529.335	Metals Charpy Insert, 8 mm Tip Radius	ASTM E23, ISO 148	
7529.336	Metals Charpy Insert, 2 mm Tip Radius	ISO 148, DIN 50115, EN 10045	
7529.337	Metals IZOD Insert	ASTM E23	
7529.340	Metals DWTT Insert	ASTM E208	
7529.350	50 mm Ø Flat Faced	-	
7529.360	12.7 mm (1/2 in) Radius Conical, 50.8 mm Ø (2 in) Base	ASTM D2444 - Type A	
7529.361	50.8 mm (2 in) Radius Conical, 50.8 mm Ø (2 in) Base	ASTM D2444 - Type B	
7529.362	12.7 mm (1/4 in) Radius Conical, 50.8 mm Ø (2 in) Base	ASTM D2444 - Type C	

Table A–22

Results of Tensile Tests of Some Metals* *Source:* J. Datsko, "Solid Materials," chap. 32 in Joseph E. Shigley, Charles R. Mischke, and Thomas H. Brown, Jr. (eds.-in-chief), *Standard Handbook of Machine Design,* 3rd ed., McGraw-Hill, New York, 2004, pp. 32.49–32.52.

			Strength (Tensile)					
Number	Material	Condition	Yield S_y, MPa (kpsi)	Ultimate S_u, MPa (kpsi)	Fracture, σ_f, MPa (kpsi)	Coefficient σ_0, MPa (kpsi)	Strain Strength, Exponent m	Fracture Strain ϵ_f
1018	Steel	Annealed	220 (32.0)	341 (49.5)	628 (91.1)†	620 (90.0)	0.25	1.05
1144	Steel	Annealed	358 (52.0)	646 (93.7)	898 (130)†	992 (144)	0.14	0.49
1212	Steel	HR	193 (28.0)	424 (61.5)	729 (106)†	758 (110)	0.24	0.85
1045	Steel	Q&T 600°F	1520 (220)	1580 (230)	2380 (345)	1880 (273)†	0.041	0.81
4142	Steel	Q&T 600°F	1720 (250)	1930 (210)	2340 (340)	1760 (255)†	0.048	0.43
303	Stainless steel	Annealed	241 (35.0)	601 (87.3)	1520 (221)†	1410 (205)	0.51	1.16
304	Stainless steel	Annealed	276 (40.0)	568 (82.4)	1600 (233)†	1270 (185)	0.45	1.67
2011	Aluminum alloy	T6	169 (24.5)	324 (47.0)	325 (47.2)†	620 (90)	0.28	0.10
2024	Aluminum alloy	T4	296 (43.0)	446 (64.8)	533 (77.3)†	689 (100)	0.15	0.18
7075	Aluminum alloy	T6	542 (78.6)	593 (86.0)	706 (102)†	882 (128)	0.13	0.18

*Values from one or two heats and believed to be attainable using proper purchase specifications. The fracture strain may vary as much as 100 percent.

†Derived value.

Table A–20

Deterministic ASTM Minimum Tensile and Yield Strengths for Some Hot-Rolled (HR) and Cold-Drawn (CD) Steels [The strengths listed are estimated ASTM minimum values in the size range 18 to 32 mm ($\frac{3}{4}$ to $1\frac{1}{4}$ in). These strengths are suitable for use with the design factor defined in Sec. 1–10, provided the materials conform to ASTM A6 or A568 requirements or are required in the purchase specifications. Remember that a numbering system is not a specification.] *Source:* 1986 SAE Handbook, p. 2.15.

1	2	3	4	5	6	7	8
UNS No.	SAE and/or AISI No.	Process-ing	Tensile Strength, MPa (kpsi)	Yield Strength, MPa (kpsi)	Elongation in 2 in, %	Reduction in Area, %	Brinell Hardness
G10060	1006	HR	300 (43)	170 (24)	30	55	86
		CD	330 (48)	280 (41)	20	45	95
G10100	1010	HR	320 (47)	180 (26)	28	50	95
		CD	370 (53)	300 (44)	20	40	105
G10150	1015	HR	340 (50)	190 (27.5)	28	50	101
		CD	390 (56)	320 (47)	18	40	111
G10180	1018	HR	400 (58)	220 (32)	25	50	116
		CD	440 (64)	370 (54)	15	40	126
G10200	1020	HR	380 (55)	210 (30)	25	50	111
		CD	470 (68)	390 (57)	15	40	131
G10300	1030	HR	470 (68)	260 (37.5)	20	42	137
		CD	520 (76)	440 (64)	12	35	149
G10350	1035	HR	500 (72)	270 (39.5)	18	40	143
		CD	550 (80)	460 (67)	12	35	163
G10400	1040	HR	520 (76)	290 (42)	18	40	149
		CD	590 (85)	490 (71)	12	35	170
G10450	1045	HR	570 (82)	310 (45)	16	40	163
		CD	630 (91)	530 (77)	12	35	179
G10500	1050	HR	620 (90)	340 (49.5)	15	35	179
		CD	690 (100)	580 (84)	10	30	197
G10600	1060	HR	680 (98)	370 (54)	12	30	201
G10800	1080	HR	770 (112)	420 (61.5)	10	25	229
G10950	1095	HR	830 (120)	460 (66)	10	25	248

Model Number
485B39

DIGITAL ICP® - USB SIGNAL CONDITIONER

Revision: A
ECN #:

	ENGLISH	SI
PERFORMANCE		
Channel Count	2	2
Voltage Range (nominal[1])	± 10 V pk	± 10 V pk
ADC Resolution	24-bit[2]	24-bit[2]
Frequency Range (± 5 %)	0.8 Hz to 20.7 kHz	0.8 Hz to 20.7 kHz
Sample Rate	48, 44.1, 32, 22.05, 16, 11.025, 8 kHz	48, 44.1, 32, 22.05, 16, 11.025, 8 kHz
Antialiasing Lowpass Filter (-3dB) at 48 kHz	22.9 kHz[3]	22.9 kHz[3]
AC High Pass Filter (-3dB)	1 Hz to 0.5 Hz[4]	1 Hz to 0.5 Hz[4]
Digital Output Interface	USB class 1 audio	USB class 1 audio
ENVIRONMENTAL		
Temperature Range (Operating)	14 °F to +176 °F	-10 °C to +80 °C
Temperature Range (Storage)	-40 °F to +176 °F	-40 °C to +80 °C
ELECTRICAL		
Excitation Voltage (to sensor: ± 5 %)	24 V DC	24 V DC
Constant Current Excitation (± 5 %)	4 mA	4 mA
DC Power (USB)	< 500 mW (5 V at 100 mA)	< 500 mW (5 V at 100 mA)
Settling Time	1.5 seconds	1.5 seconds
Electrical Isolation (case)	Grounded	Grounded
MECHANICAL		
Housing Material	Stainless steel	Stainless steel
Size (length x width x height)	2.36 in x 1.54 in x 0.75 in	60 mm x 39 mm x 19 mm
Weight	4.4 oz	125 gram
Sensor Inputs	2 BNC jacks	2 BNC jacks
Digital Output	9 in integral USB cable	23 cm integral USB cable
USB Connector	Type A	Type A

NOTES:
[1] ± 8 V pk, guaranteed
[2] 16-bit selectable by software
[3] Proportional to sample rate
[4] Sample rate dependent (48 kHz to 8 kHz)

OPTIONAL ACCESSORIES:
MD821AM/A USB A to Lightning camera adaptor
USB A to USB OTG adaptor

PRODUCT DRAWING

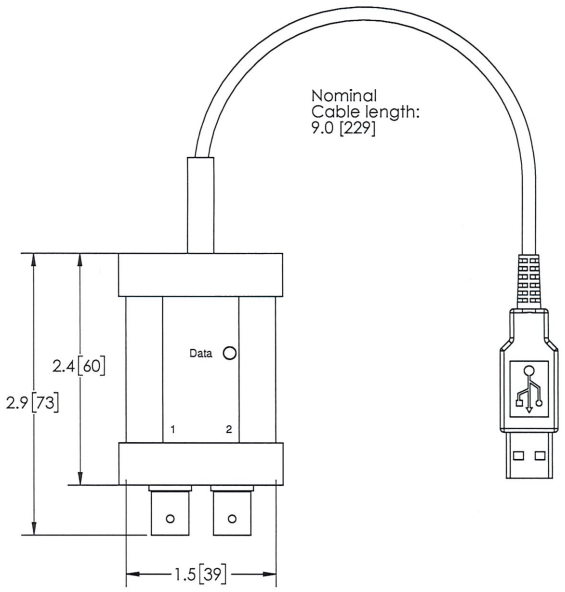

Dimensions in inches [mm]

In the interest of constant product improvement, specifications may change without notice.

CE

All specifications are at room temperature unless otherwise specified.

Project Engineer:	Product Manager:	Mkt Team Leader:	Spec Number:
tec	MAP		PS-0149
Date: 6/28/18	Date: 6/28/18	Date: 6/29/18	

THE MODAL SHOP
MTS SYSTEMS CORPORATION

3149 East Kemper Road
Cincinnati, OH 45241

800-860-4867 Fax (513) 458-2172
+1 513-351-9919

info@modalshop.com

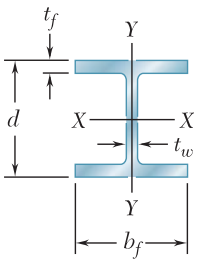

APPENDIX C Properties of Rolled-Steel Shapes

(SI Units)

Continued from page A18

W Shapes

(Wide-Flange Shapes)

Designation†	Area A, mm^2	Depth d, mm	Flange Width b_f, mm	Flange Thickness t_f, mm	Web Thickness t_w, mm	Axis X-X I_x 10^6 mm^4	Axis X-X S_x 10^3 mm^3	Axis X-X r_x mm	Axis Y-Y I_y 10^6 mm^4	Axis Y-Y S_y 10^3 mm^3	Axis Y-Y r_y mm
W310 × 143	18200	323	310	22.9	14.0	347	2150	138	112	728	78.5
107	13600	312	305	17.0	10.9	248	1600	135	81.2	531	77.2
74	9420	310	205	16.3	9.40	163	1050	132	23.4	228	49.8
60	7550	302	203	13.1	7.49	128	844	130	18.4	180	49.3
52	6650	318	167	13.2	7.62	119	747	133	10.2	122	39.1
44.5	5670	312	166	11.2	6.60	99.1	633	132	8.45	102	38.6
38.7	4940	310	165	9.65	5.84	84.9	547	131	7.20	87.5	38.4
32.7	4180	312	102	10.8	6.60	64.9	416	125	1.94	37.9	21.5
23.8	3040	305	101	6.73	5.59	42.9	280	119	1.17	23.1	19.6
W250 × 167	21200	290	264	31.8	19.2	298	2060	118	98.2	742	68.1
101	12900	264	257	19.6	11.9	164	1240	113	55.8	433	65.8
80	10200	257	254	15.6	9.4	126	983	111	42.9	338	65.0
67	8580	257	204	15.7	8.89	103	805	110	22.2	218	51.1
58	7420	252	203	13.5	8.00	87.0	690	108	18.7	185	50.3
49.1	6260	247	202	11.0	7.37	71.2	574	106	15.2	151	49.3
44.8	5700	267	148	13.0	7.62	70.8	531	111	6.95	94.2	34.8
32.7	4190	259	146	9.14	6.10	49.1	380	108	4.75	65.1	33.8
28.4	3630	259	102	10.0	6.35	40.1	308	105	1.79	35.1	22.2
22.3	2850	254	102	6.86	5.84	28.7	226	100	1.20	23.8	20.6
W200 × 86	11000	222	209	20.6	13.0	94.9	852	92.7	31.3	300	53.3
71	9100	216	206	17.4	10.2	76.6	708	91.7	25.3	246	52.8
59	7550	210	205	14.2	9.14	60.8	582	89.7	20.4	200	51.8
52	6650	206	204	12.6	7.87	52.9	511	89.2	17.7	174	51.6
46.1	5880	203	203	11.0	7.24	45.8	451	88.1	15.4	152	51.3
41.7	5320	205	166	11.8	7.24	40.8	398	87.6	9.03	109	41.1
35.9	4570	201	165	10.2	6.22	34.4	342	86.9	7.62	92.3	40.9
31.3	3970	210	134	10.2	6.35	31.3	298	88.6	4.07	60.8	32.0
26.6	3390	207	133	8.38	5.84	25.8	249	87.1	3.32	49.8	31.2
22.5	2860	206	102	8.00	6.22	20.0	193	83.6	1.42	27.9	22.3
19.3	2480	203	102	6.48	5.84	16.5	162	81.5	1.14	22.5	21.4
W150 × 37.1	4740	162	154	11.6	8.13	22.2	274	68.6	7.12	91.9	38.6
29.8	3790	157	153	9.27	6.60	17.2	220	67.6	5.54	72.3	38.1
24	3060	160	102	10.3	6.60	13.4	167	66.0	1.84	36.1	24.6
18	2290	153	102	7.11	5.84	9.20	120	63.2	1.24	24.6	23.3
13.5	1730	150	100	5.46	4.32	6.83	91.1	62.7	0.916	18.2	23.0
W130 × 28.1	3590	131	128	10.9	6.86	10.9	167	55.1	3.80	59.5	32.5
23.8	3040	127	127	9.14	6.10	8.91	140	54.1	3.13	49.2	32.0
W100 × 19.3	2470	106	103	8.76	7.11	4.70	89.5	43.7	1.61	31.1	25.4

†A wide-flange shape is designated by the letter W followed by the nominal depth in millimeters and the mass in kilograms per meter.

Table A–31

Dimensions of Hexagonal Nuts

Nominal Size, in	Width W	Height H: Regular Hexagonal	Height H: Thick or Slotted	Height H: JAM
$\frac{1}{4}$	$\frac{7}{16}$	$\frac{7}{32}$	$\frac{9}{32}$	$\frac{5}{32}$
$\frac{5}{16}$	$\frac{1}{2}$	$\frac{17}{64}$	$\frac{21}{64}$	$\frac{3}{16}$
$\frac{3}{8}$	$\frac{9}{16}$	$\frac{21}{64}$	$\frac{13}{32}$	$\frac{7}{32}$
$\frac{7}{16}$	$\frac{11}{16}$	$\frac{3}{8}$	$\frac{29}{64}$	$\frac{1}{4}$
$\frac{1}{2}$	$\frac{3}{4}$	$\frac{7}{16}$	$\frac{9}{16}$	$\frac{5}{16}$
$\frac{9}{16}$	$\frac{7}{8}$	$\frac{31}{64}$	$\frac{39}{64}$	$\frac{5}{16}$
$\frac{5}{8}$	$\frac{15}{16}$	$\frac{35}{64}$	$\frac{23}{32}$	$\frac{3}{8}$
$\frac{3}{4}$	$1\frac{1}{8}$	$\frac{41}{64}$	$\frac{13}{16}$	$\frac{27}{64}$
$\frac{7}{8}$	$1\frac{5}{16}$	$\frac{3}{4}$	$\frac{29}{32}$	$\frac{31}{64}$
1	$1\frac{1}{2}$	$\frac{55}{64}$	1	$\frac{35}{64}$
$1\frac{1}{8}$	$1\frac{11}{16}$	$\frac{31}{32}$	$1\frac{5}{32}$	$\frac{39}{64}$
$1\frac{1}{4}$	$1\frac{7}{8}$	$1\frac{1}{16}$	$1\frac{1}{4}$	$\frac{23}{32}$
$1\frac{3}{8}$	$2\frac{1}{16}$	$1\frac{11}{64}$	$1\frac{3}{8}$	$\frac{25}{32}$
$1\frac{1}{2}$	$2\frac{1}{4}$	$1\frac{9}{32}$	$1\frac{1}{2}$	$\frac{27}{32}$
Nominal Size, mm				
M5	8	4.7	5.1	2.7
M6	10	5.2	5.7	3.2
M8	13	6.8	7.5	4.0
M10	16	8.4	9.3	5.0
M12	18	10.8	12.0	6.0
M14	21	12.8	14.1	7.0
M16	24	14.8	16.4	8.0
M20	30	18.0	20.3	10.0
M24	36	21.5	23.9	12.0
M30	46	25.6	28.6	15.0
M36	55	31.0	34.7	18.0

Table A.1: Physical and mechanical property values for representative ply and core materials widely used in fiber-reinforced composite laminates[9].

	S-glass/ epoxy	**Kevlar/ epoxy**	**HM Graphite/ epoxy**	**Pine**	**Rohacell 51 rigid foam**
Elastic Properties					
E_1, GPa	55	80	230	13.4	0.07
E_2, GPa	16	5.5	6.6	0.55	0.07
G_{12}, GPa	7.6	2.1	4.8	0.83	0.021
v_{12}	0.26	0.31	0.25	0.3	-
Tensile strengths					
σ_1, MPa	1800	2000	1100	78	1.9
σ_2, MPa	40	20	21	2.1	1.9
σ_{12}, MPa	80	40	65	6.2	0.8
Compressive Strengths					
σ_1, MPa	690	280	620	33	0.9
σ_2, MPa	140	140	170	3.0	0.9
Physical Properties					
α_1, 10^{-6}/degC	2.1	-4.0	-0.7		33
α_2, 10^{-6}/degC	6.3	60	28		33
Volume fraction	0.7	0.54	0.7		
Thickness, mm	0.15	0.13	0.13		
Density, Mg/m^3	2.0	1.38	1.63	0.55	0.05

Appendix B

CAD Drawing

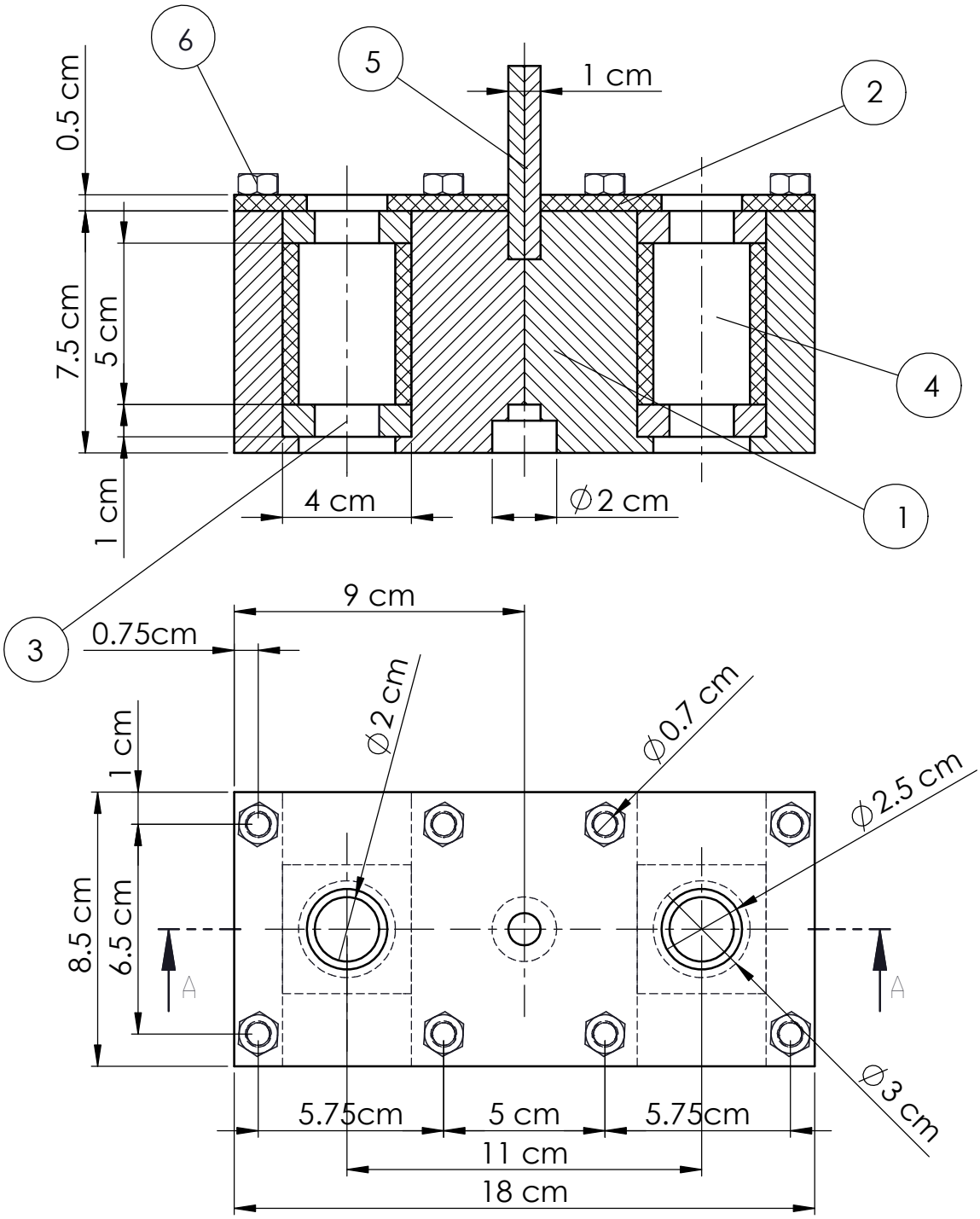

ITEM NO.	PART NAME	MATERIAL	QUANTITY
6	IMPACTOR FIXING BOLT	GRADE 2 STANDARD STEEL	8
5	IMPACTOR HOLDER	AISI 1006 LOW CARBON STEEL	1
4	CYLINDERICAL SUPPORT	AISI 1020 LOW CARBON STEEL	2
3	GUIDE ROD SUPPORT	AISI 1020 LOW CARBON STEEL	4
2	PLATE	AISI 1006 LOW CARBON STEEL	1
1	IMPACT MASS	AISI 1006 LOW CARBON STEEL	1

DR. BY: DAGMAWE TADESSE	ADDIS ABABA INSTITUTE OF TECHNOLOGY	DR. NO.
CH. BY: DR. DANIEL & MR. ARAYA	SCHOOL OF MECHANICAL AND INDUSTRIAL ENG.	01
SCALE	TITLE	DATE
1:2	IMPACTOR ASSEMBLY	24 - 10 - 2020

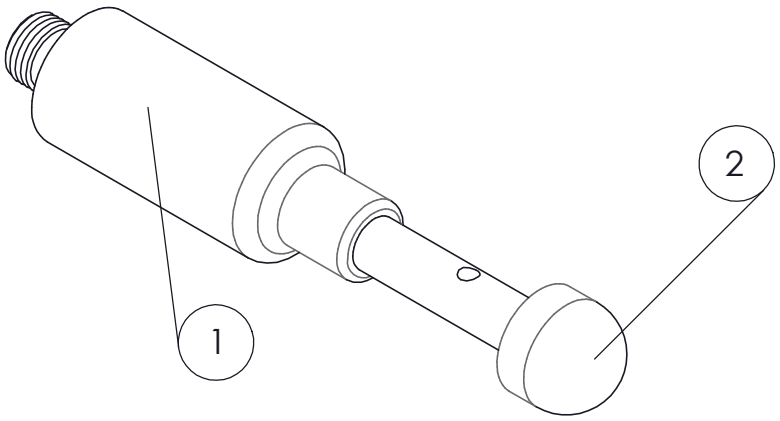

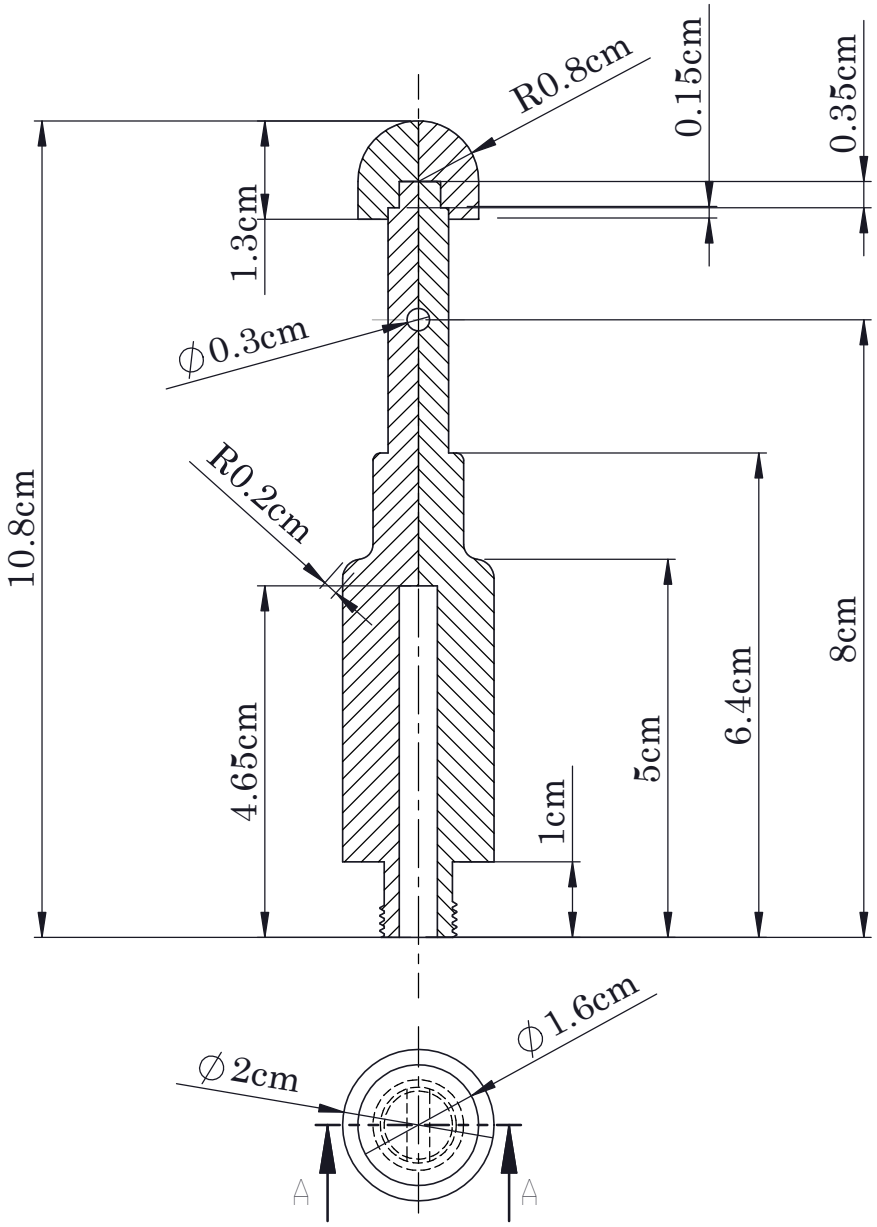

ITEM NO.	PART NAME	MATERIAL	QUANTITY
1	STRIKER SHAFT	AISI 1020 STEEL	1
2	TUP	A2 TOOL STEEL	1

DR. BY: DAGMAWE TADESSE	ADDIS ABABA INSTITUTE OF TECHNOLOGY	DR. NO.
CH. BY: DR. DANIEL & MR. ARAYA	SCHOOL OF MECHANICAL AND INDUSTRIAL ENG.	02
SCALE	TITLE	DATE
1:1	SECTIONAL VIEW OF STRIKER ASSEMBLY	24-10-2020

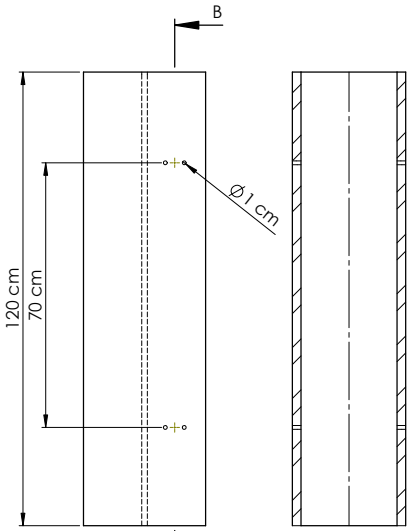

SECTION B-B

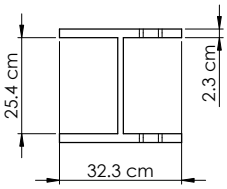

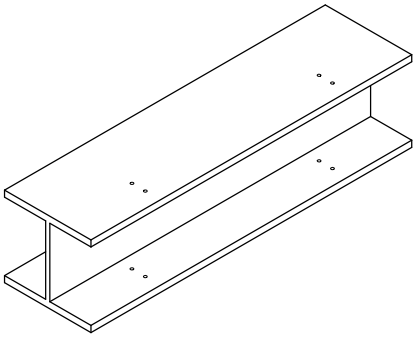

DR. BY: DAGMAWE TADESSE		ADDIS ABABA INSTITUTE OF TECHNOLOGY	DR. NO.
CHK BY: Dr. DANIEL & Mr. ARAYA B.		SCHOOL OF MECHANICAL AND INDUSTRIAL ENGINEERING	03
SCALE		TITLE	DATE
1:10		WIDE - FLANGED W310X143 STEEL DROP TOWER	24 - 10 - 2020

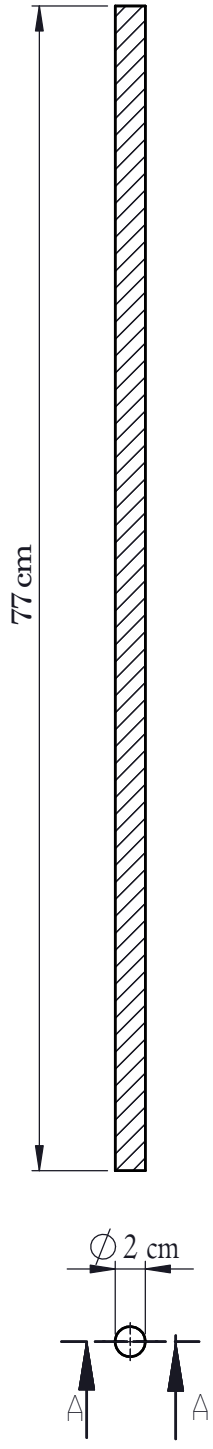

DR. BY: DAGMAWE TADESSE	ADDIS ABABA INSTITUTE OF TECHNOLOGY	DR. NO.
CH. BY: DR. DANIEL & MR. ARAYA	SCHOOL OF MECHANICAL AND INDUSTRIAL ENG.	04
SCALE	TITLE	DATE
1:2	GUIDE ROD	24 - 10 - 2020

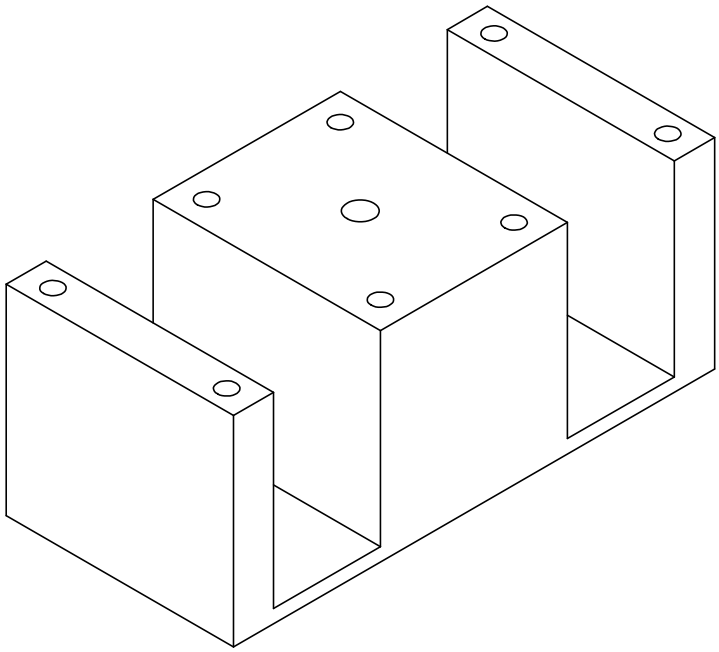

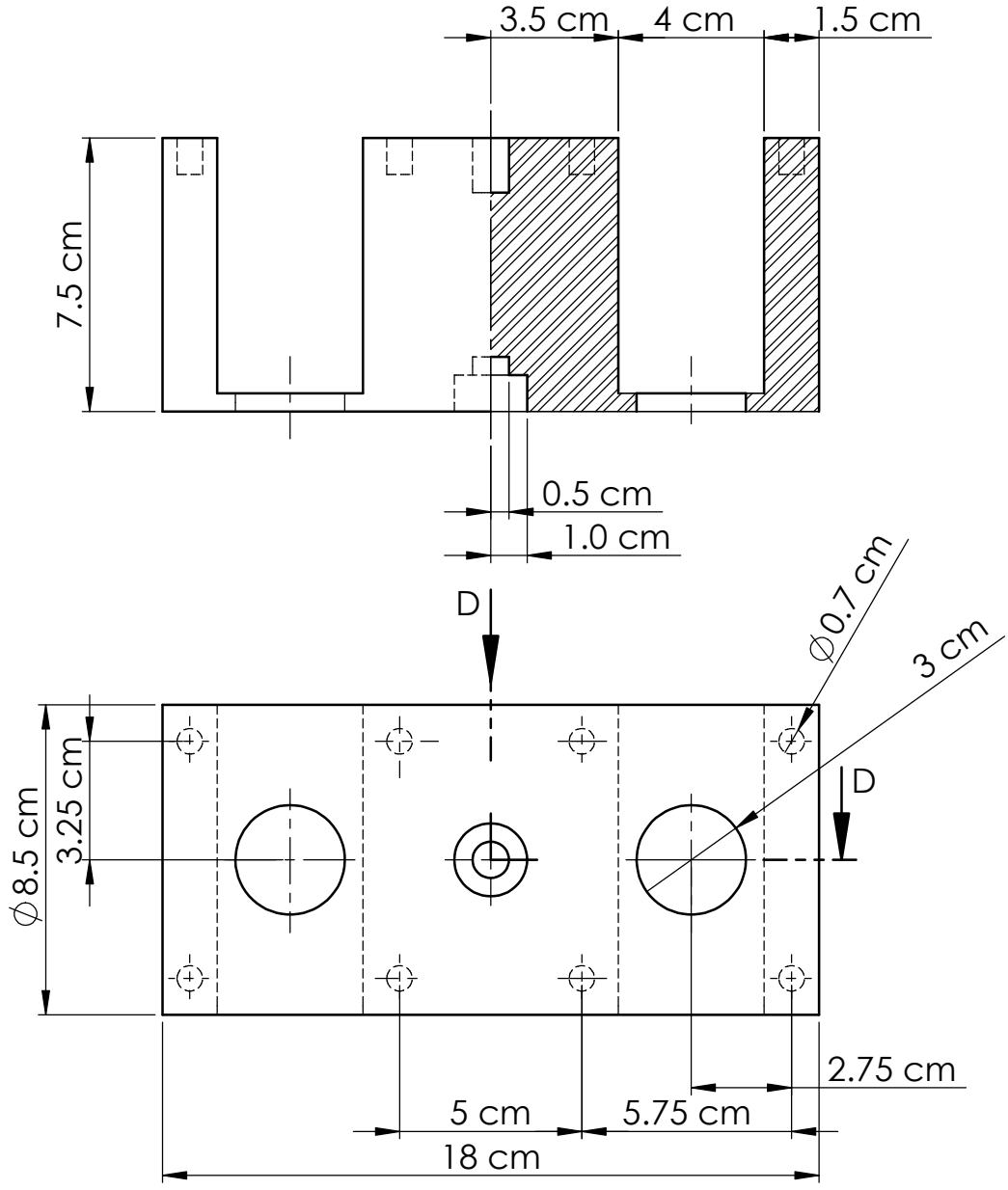

DR. BY: DAGMAWE TADESSE	ADDIS ABABA INSTITUTE OF TECHNOLOGY	DR. NO.
CH. BY: DR. DANIEL & MR. ARAYA	SCHOOL OF MECHANICAL AND INDUSTRIAL ENG.	05
SCALE	TITLE	DATE
1:1	IMPACTING MASS	24 - 10 - 2020

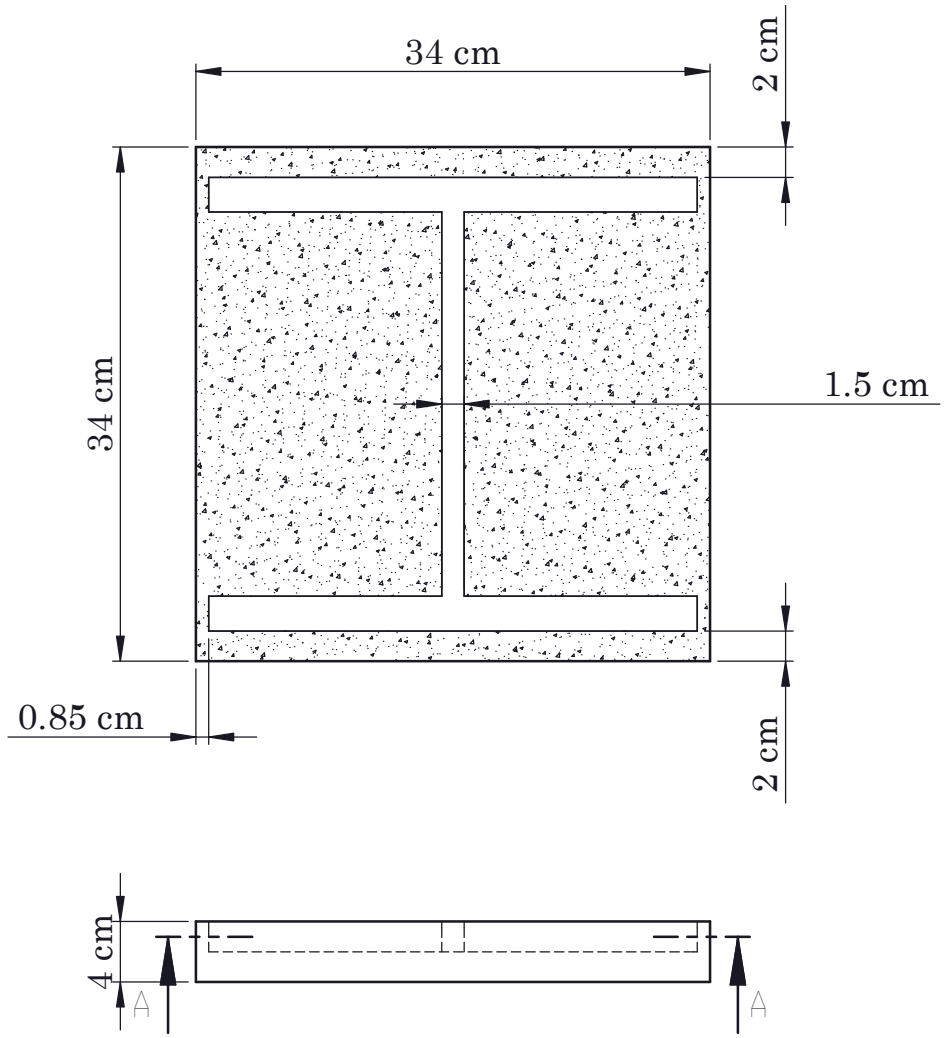

DR. BY: DAGMAWE TADESSE		ADDIS ABABA INSTITUTE OF TECHNOLOGY	DR. NO.
CH. BY: DR. DANIEL & MR. ARAYA		SCHOOL OF MECHANICAL AND INDUSTRIAL ENG.	06
SCALE		TITLE	DATE
1:5		FOUNDATION	24 - 10 - 2020

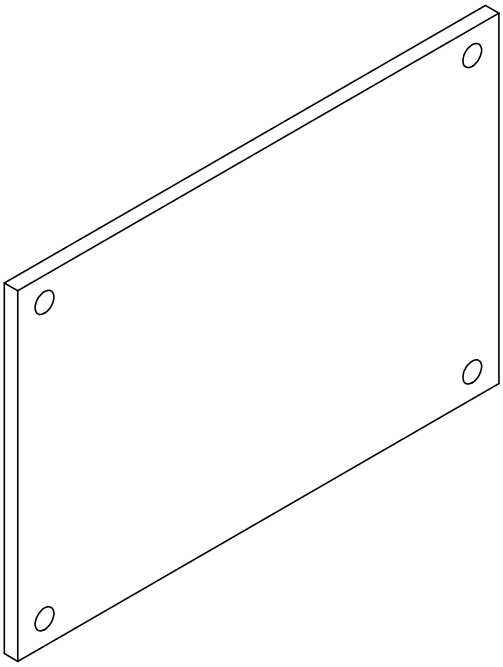

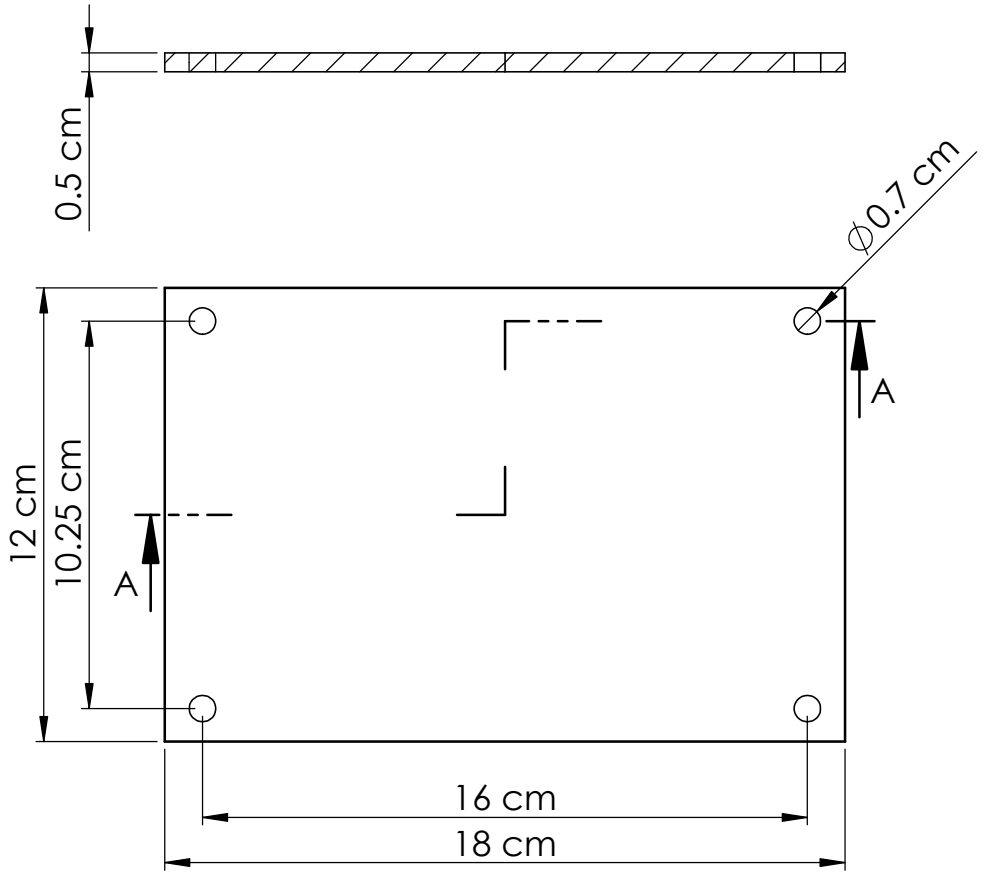

DR. BY: DAGMAWE TADESSE		ADDIS ABABA INSTITUTE OF TECHNOLOGY	DR. NO.
CH. BY: DR. DANIEL & MR. ARAYA		SCHOOL OF MECHANICAL AND INDUSTRIAL ENG.	07
SCALE		TITLE	DATE
1:2		SPECIMEN FIXTURE BOTTOM PLATE	24 - 10 - 2020

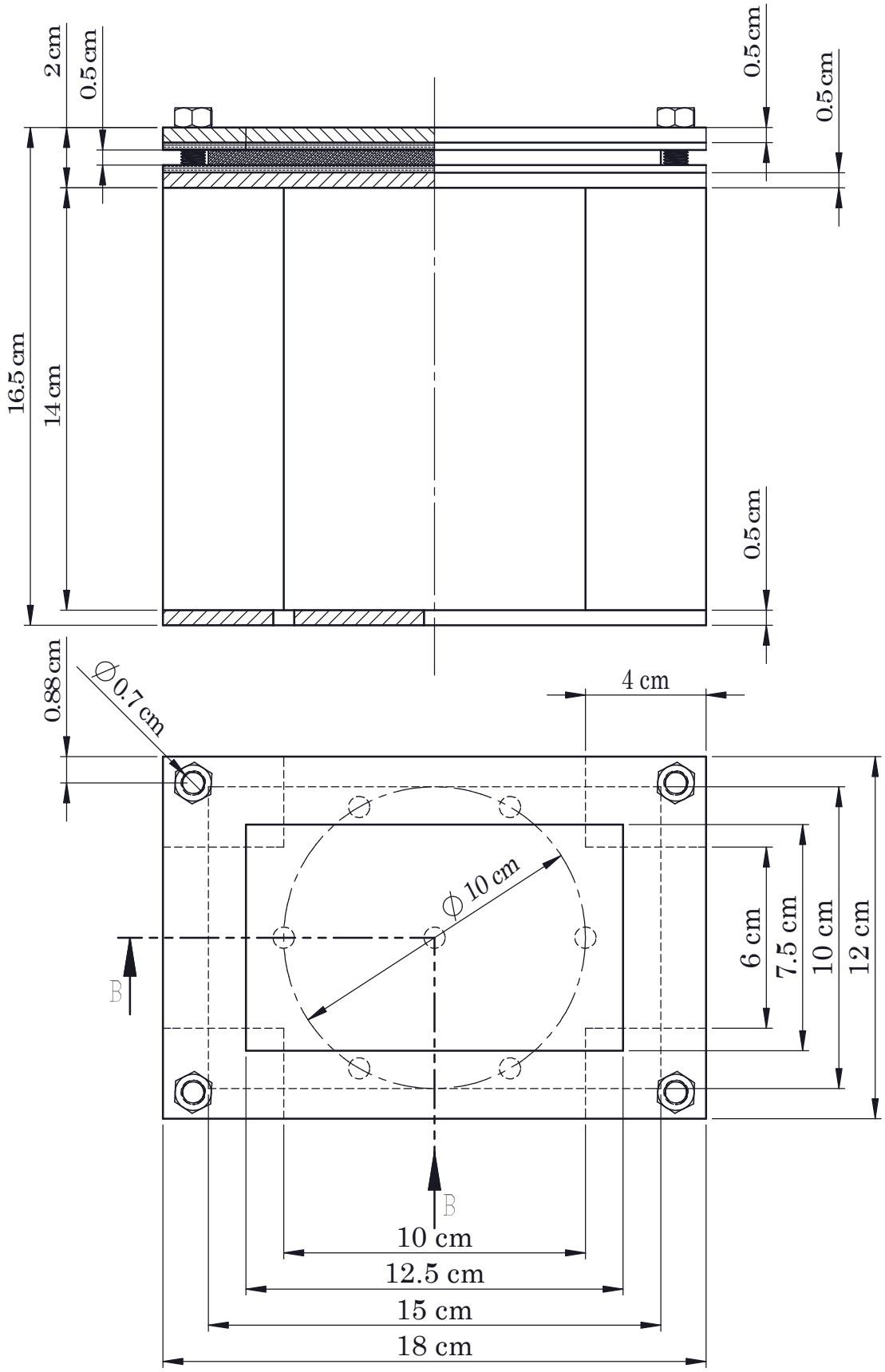

DR. BY: DAGMAWE TADESSE		ADDIS ABABA INSTITUTE OF TECHNOLOGY	DR. NO.
CH. BY: DR. DANIEL & MR. ARAYA		SCHOOL OF MECHANICAL AND INDUSTRIAL ENG.	08
SCALE		TITLE	DATE
1:2		SPECIMEN FIXTURE ASSEMBLY	24 - 10 - 2020

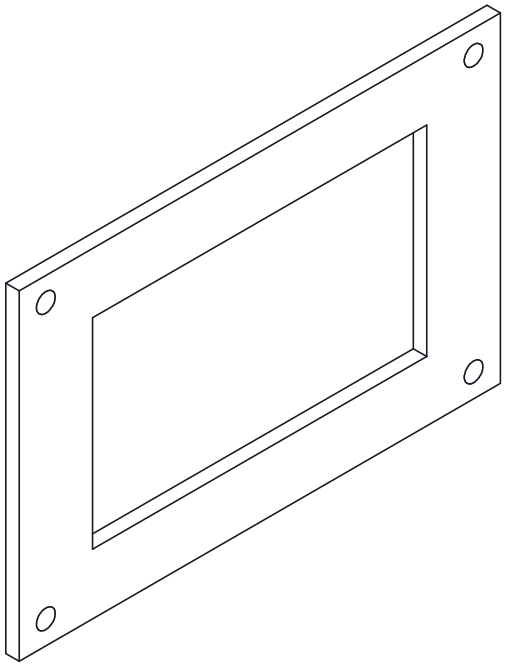

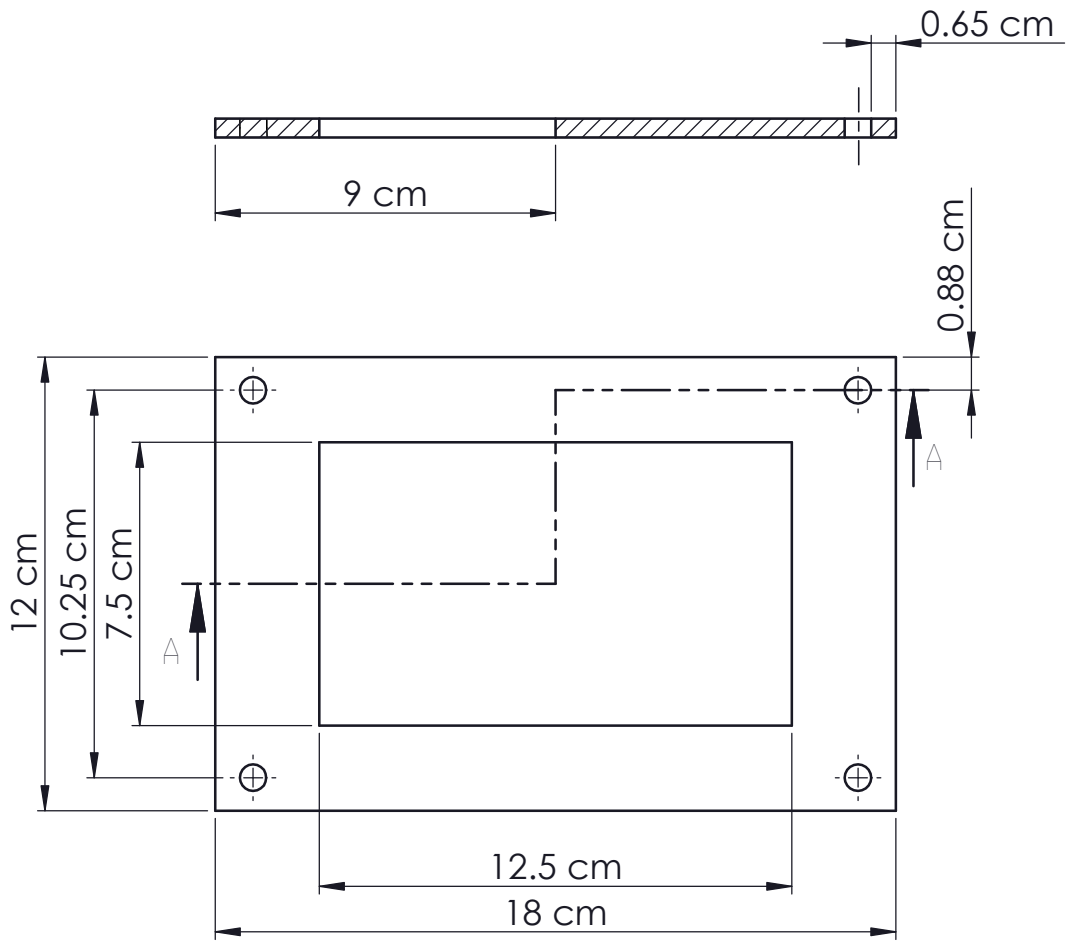

DR. BY: DAGMAWE TADESSE	ADDIS ABABA INSTITUTE OF TECHNOLOGY	DR. NO.
CH. BY: DR. DANIEL & MR. ARAYA	SCHOOL OF MECHANICAL AND INDUSTRIAL ENG.	09
SCALE	TITLE	DATE
1:5	SPECIMEN FIXTURE UPPER PLATE	24 - 10 - 2020

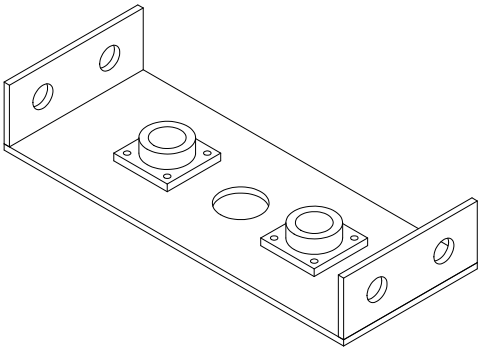

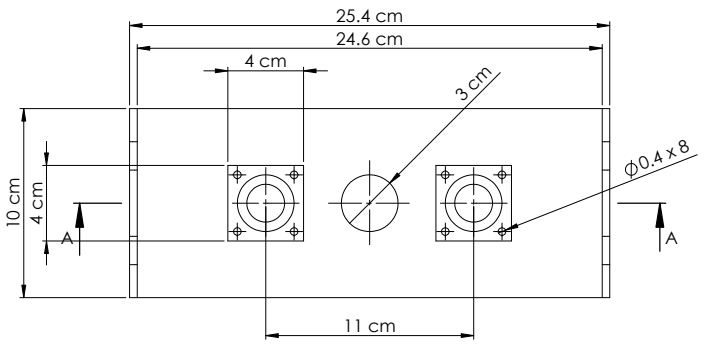

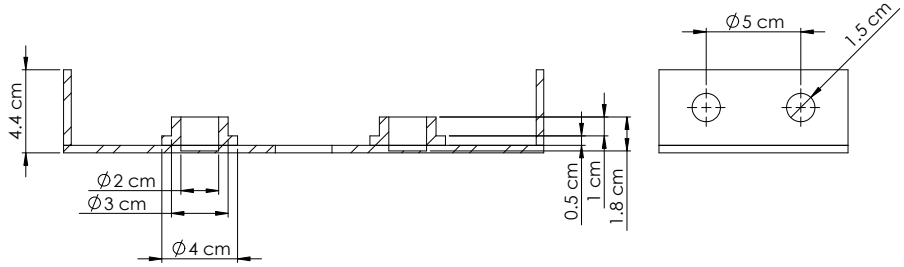

SECTION A-A

DR. BY: DAGMAWE TADESSE		ADDIS ABABA INSTITUTE OF TECHNOLOGY	DR. NO.
CHK BY: Dr. DANIEL & Mr. ARAYA B.		SCHOOL OF MECHANICAL AND INDUSTRIAL ENGINEERING	10
SCALE		TITLE	DATE
1: 2		SUPPORT BRACKET	24 - 10 - 2020

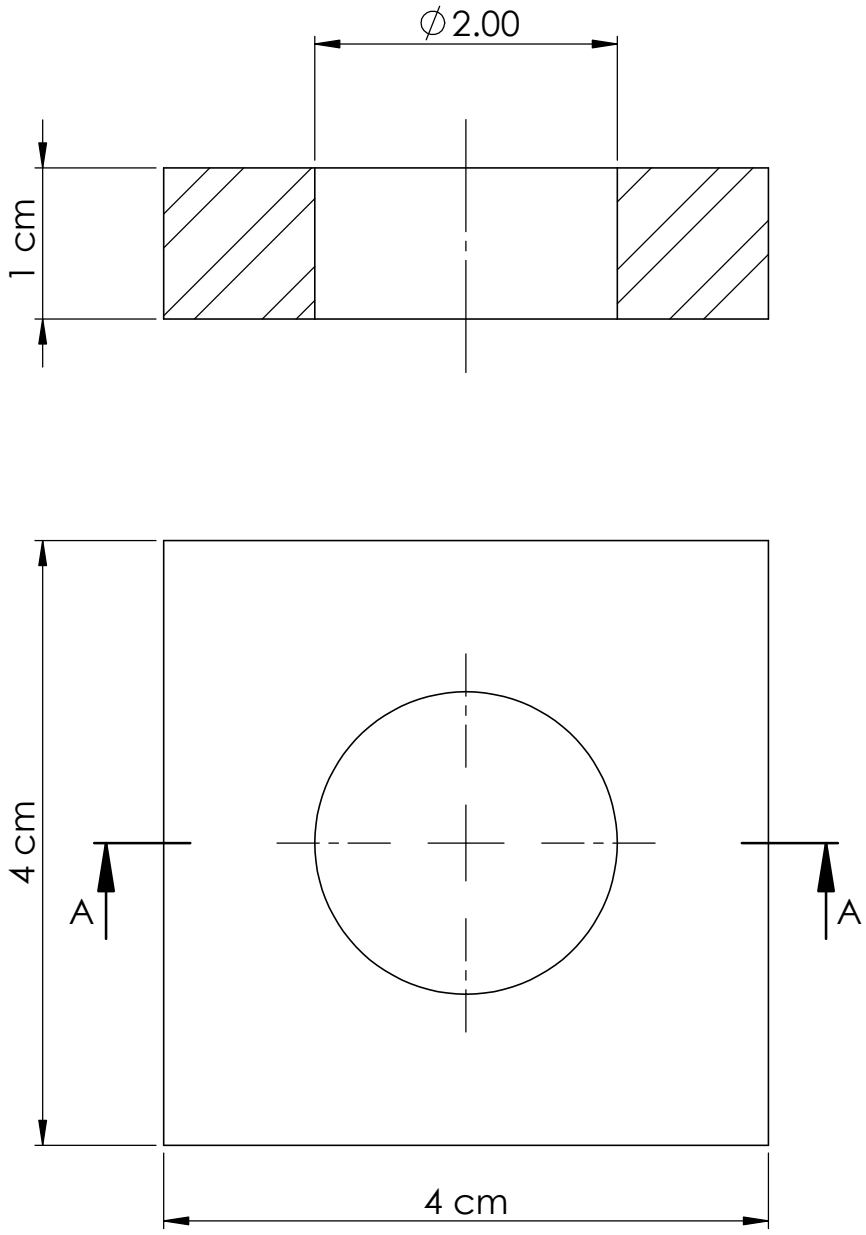

DR. BY: DAGMAWE TADESSE	ADDIS ABABA INSTITUTE OF TECHNOLOGY	DR. NO.
CH. BY: DR. DANIEL & MR. ARAYA	SCHOOL OF MECHANICAL AND INDUSTRIAL ENG.	13
SCALE	TITLE	DATE
1:2	IMPACTOR-GUIDE ROD SUPPORT	24 - 10 - 2020

USED ON
485B39

PD-4420

REVISIONS			
REV	BY	DESCRIPTION	DATE
NR		-	

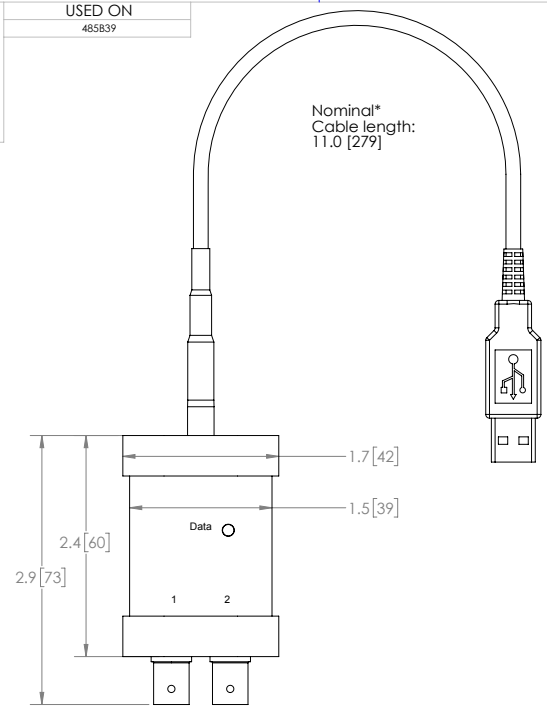

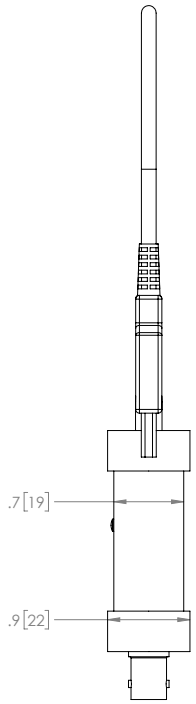

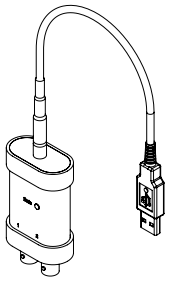

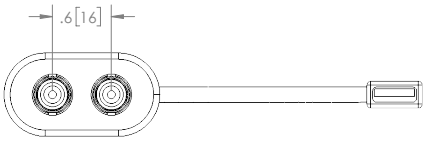

*Cable length minimum of 11.0 [279]

UNLESS OTHERWISE SPECIFIED		CREATED BY		CHECKED		PGM		PRODUCTION	
DIMENSIONS ARE IN INCHES	DIMENSIONS ARE IN mm [IN BRACKETS]	RA	10/17/18	NMA	02/14/19	N/A	-	N/A	-
DECIMALS : XX +/- .01 XXX +/- .005 ANGLES +/- 2 DEGREES	DECIMALS : X +/- .3 XX +/- .13 ANGLES +/- 2 DEGREES	MATERIAL:		HEAT TREAT:		FINISH:			
FILLETS AND RADII: .003-.005	FILLETS AND RADII: .07-.13	TITLE: ICPD OUTLINE DRAWING							
ENG-F004 REV.E 08/22/16									

Cincinnati OH, USA
www.modalshop.com
513.351.9919 VOICE
513.458.2172 FAX

THE MODAL SHOP
A PCB GROUP CO.

DWG. NO. PD-4420

SCALE: 1:1 | SHEET 1 OF 2

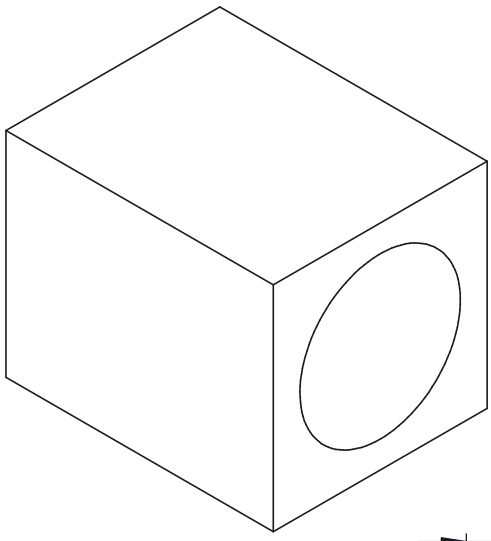

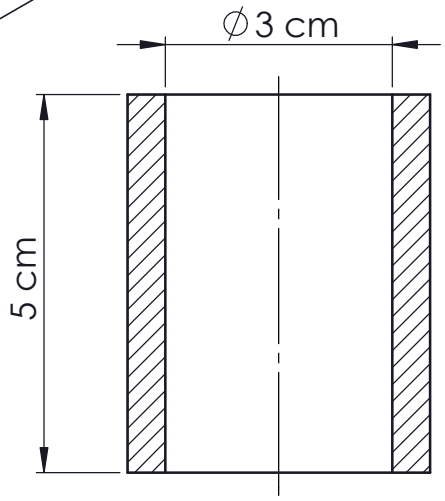

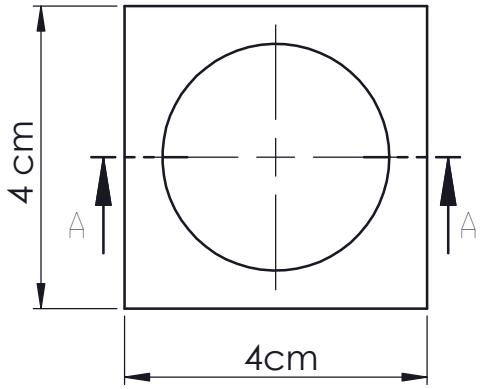

DR. BY: DAGMAWE TADESSE		ADDIS ABABA INSTITUTE OF TECHNOLOGY	DR. NO.
CH. BY: DR. DANIEL & MR. ARAYA		SCHOOL OF MECHANICAL AND INDUSTRIAL ENGINEERING	14
SCALE		TITLE	DATE
1:1		CYLINDERICAL SUPPORT (mass increment)	03 - 11 - 2020

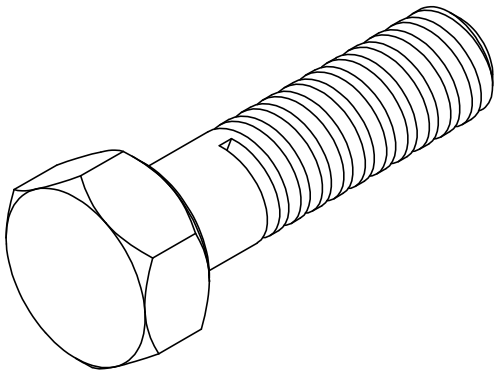

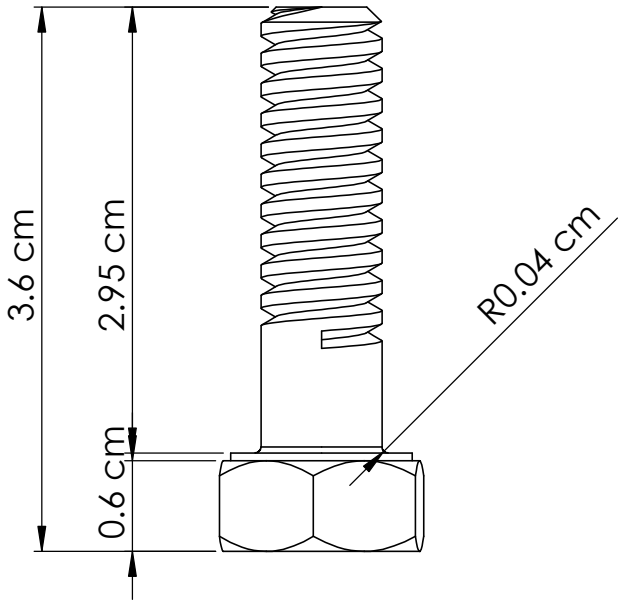

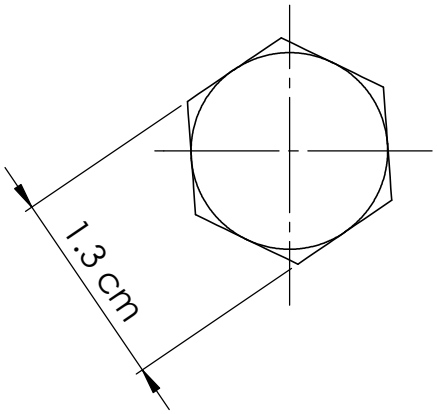

DR. BY: DAGMAWE TADESSE		ADDIS ABABA INSTITUTE OF TECHNOLOGY	DR. NO.
CH. BY: DR. DANIEL & MR. ARAYA		SCHOOL OF MECHANICAL AND INDUSTRIAL ENGINEERING	16
SCALE		TITLE	DATE
2:1		M8 BOLT	3 - 10 - 2020

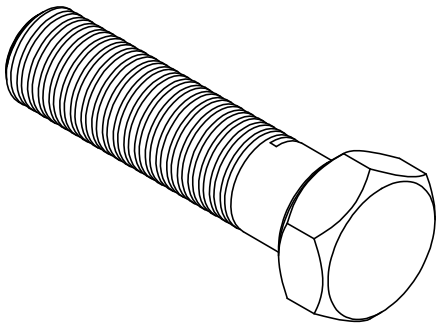

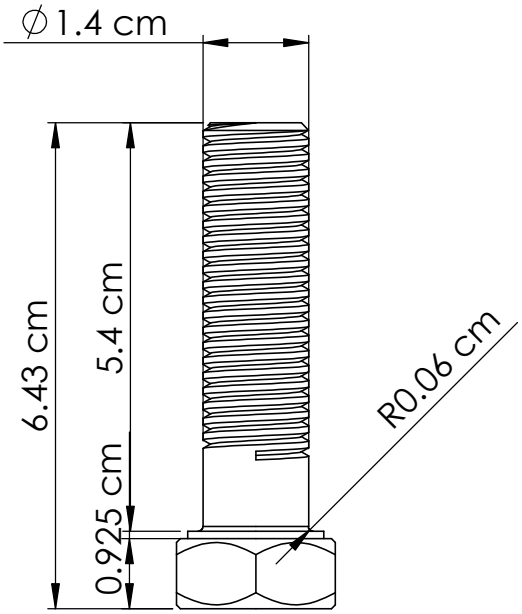

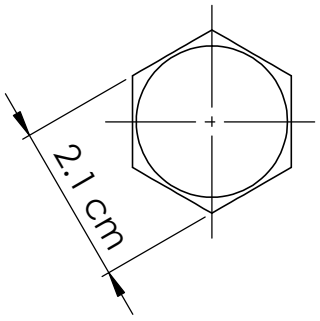

DR. BY: DAGMAWE TADESSE	ADDIS ABABA INSTITUTE OF TECHNOLOGY	DR. NO.
CH. BY: DR. DANIEL & MR. ARAYA	SCHOOL OF MECHANICAL AND INDUSTRIAL ENGINEERING	17
SCALE	TITLE	DATE
1:1	M14 BOLT	03 - 10 - 2020

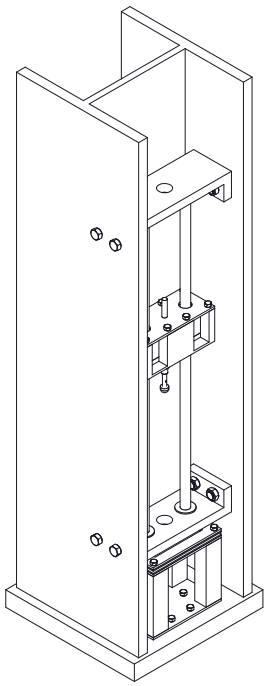

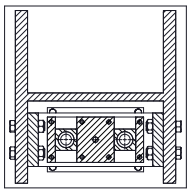

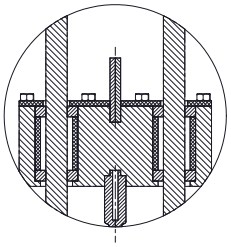

DETAIL B
SCALE 2 : 5

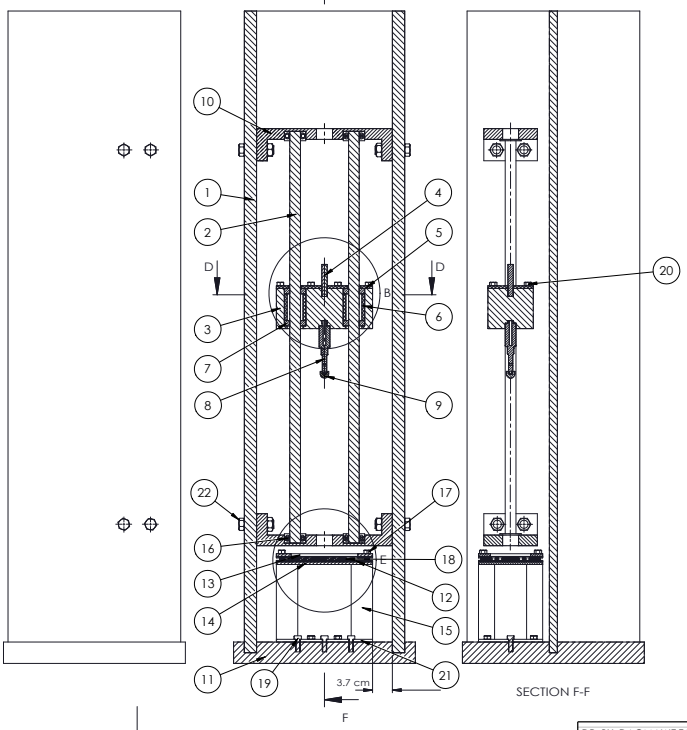

SECTION A-A

SECTION F-F

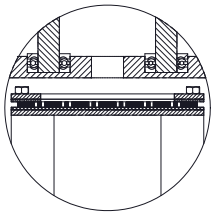

DETAIL E
SCALE 2 : 5

NOTE: LCS = LOW CABON STEEL

NO.	PART NAME	MATERIAL	QUANTITY
22	SUPPORT BRACKET BOLT (M14)	LOW OR MEDIUM CS	8
21	FIXTURE FOUNDATION PLATE	AISI 1006 LCS	1
20	IMPACTOR BOLT (M8)	LOW OR MEDIUM CS	8
19	FOUNDATION BOLT (M8)	LOW OR MEDIUM CS	6
18	SPECIMEN	ASTM D - 7136	1
17	SPECIMEN FIXTURE BOLT (M8)	LOW CARBON STEEL	4
16	RADIAL BALL BEARING	STAINLESS STEEL	4
15	FIXTURE SUPPORT ROD	AISI 1020 LCS	4
14	FIXTURE BOTTOM PLATE	AISI 1006 LCS	1
13	FIXTURE TOP PLATE	AISI 1006 LCS	1
12	FIXTURE RUBBER	NEOPRENE (CR)	2
11	FOUNDATION	M25 CONCRETE	1
10	SUPPORT BRACKET	AISI 1020 LCS	2
9	INTERCHANGABLE TUP	TYPE A2 TOOL STEEL	1
8	STRIKER SHAFT	AISI 1020 LCS	1
7	IMPACTOR - GUIDE ROD SUPPORT	AISI 1020 LCS	4
6	CYLINDERICAL SUPPORT	AISI 1020 LCS	2
5	IMPACTOR PLATE	AISI 1006 LCS	1
4	IMPACTOR HOLDER	AISI 1006 LCS	1
3	IMPACT MASS	AISI 1006 LCS	1
2	GUIDE ROD	AISI 304 STAINLESS STEEL	2
1	W310X143 SECTION DROP TOWER	ASTM A30 STEEL	1

DR. BY: DAGMAWE TADESSE	ADDIS ABABA INSTITUTE OF TECHNOLOGY	DR. NO.
CH. BY: DR. DANIEL & MR. ARAYA	SCHOOL OF MECHANICAL AND INDUSTRIAL ENGINEERING	12
SCALE 1:5	TITLE: DROP WEIGHT IMPACT TEST MACHINE - ASSEMBLY	DATE: 03 - 11 - 2020

Appendix C

Matlab code

Five test conducted with the designed drop weight impact test machine, data feed to the Matlab with the same code, here the only difference is in the audioread (data collected from the data acquisition element as audio file) command where;

1. For first data as $test1$ at $20cm.wav$,
2. For second data as *second test* at 40cm
3. For third data as $test3$ at 50cm
4. For fourth data as $test4$ at $60cm$

```
clc;
close all;

[y,fs]=audioread('test1 at 20cm.wav'); % reading the first data
info=audioinfo('test1 at 20cm.wav');
[y2,fs2]=audioread('Second Test.wav'); % reading the third data
info2=audioinfo('Second Test.wav');
[y3,fs3]=audioread('test3 at 40cm.wav'); % reading the second data
info3=audioinfo('test3 at 40cm.wav');
[y4,fs4]=audioread('test4 at 50cm.wav'); % reading the fourth data
info4=audioinfo('test4 at 50cm.wav');
%time domain
%-----------------------------------------------------
%spectral response of first data
t=0:seconds(1/fs):seconds(info.Duration);
t=t(1:end-1);
figure(1);
plot(t,y); %plotting spectral response as a function of time
title('time domain')
xlabel('Times')
ylabel('Amplitude')
legend('1st test')

%-----------------------------------------------------
%spectral response of second data
t2=0:seconds(1/fs2):seconds(info2.Duration);
t2=t2(1:end-1);
figure(2);
plot(t2,y2); %plotting spectral response as a function of time
title('time domain')
xlabel('Times')
ylabel('Amplitude')
legend('2nd test')
%-----------------------------------------------------
%spectral response of third data
t3=0:seconds(1/fs3):seconds(info3.Duration);
t3=t3(1:end-1);
figure(3);
plot(t3,y3); %plotting spectral response as a function of time
title('time domain')
xlabel('Times')
ylabel('Amplitude')
legend('3rd test')
%-----------------------------------------------------
%spectral response of fourth data
t4=0:seconds(1/fs4):seconds(info4.Duration);
t4=t4(1:end-1);
figure(4);
plot(t4,y4); %plotting spectral response as a function of time
title('time domain')
xlabel('Times')
ylabel('Amplitude')
legend('4th test')
%-----------------------------------------------------
%fourier transform of first data
```

```
Y=fft(y);
L=info.TotalSamples;
P2=abs(Y/L);
P1=P2(1:L/2+1);
P1(2:end-1)=2*P1(2:end-1);
f=fs*(0:(L/2))/L;

%------------------------------------------------------------
%fourier transfrom of second data
Y2=fft(y2);
L2=info.TotalSamples;
P4=abs(Y2/L2);
P3=P4(1:L2/2+1);
P3(2:end-1)=2*P3(2:end-1);
f2=fs2*(0:(L2/2))/L2;

%------------------------------------------------------------
%fourier transfrom of third data
Y3=fft(y3);
L3=info.TotalSamples;
P6=abs(Y3/L3);
P5=P6(1:L3/2+1);
P5(2:end-1)=2*P5(2:end-1);
f3=fs3*(0:(L3/2))/L3;

%------------------------------------------------------------
%fourier transfrom of fourth data
Y4=fft(y4);
L4=info.TotalSamples;
P8=abs(Y4/L4);
P7=P8(1:L4/2+1);
P7(2:end-1)=2*P7(2:end-1);
f4=fs4*(0:(L4/2))/L4;
%------------------------------------------------------------
%frequency domain
Time_history=(0:0.02:50);
t=Time_history;
t2=Time_history;
t3=Time_history;
t4=Time_history;

%------------------------------------------------------------
%input data
xi=0.01;
dt=t(2)-t(1);
dt2=t2(2)-t2(1);
dt3=t3(2)-t3(1);
dt4=t4(2)-t4(1);
T=(0.02:0.02:1);
m=5.5;
g=10;
omega_n=2.*pi./T;
K=m.*omega_n.*omega_n; %stiffness
for j=1:length(T)
    wn=omega_n(j);
    k=K(j);
    [u,v]=function2(xi,m,k,P2,dt,wn,t);
```

```
    D(j)=max(abs(u)); %spectral displacement of first data
end

V=omega_n.*D; % spectral velocity of second data
A=omega_n.*omega_n.*D; % spectral acceleration
F=m.*A; % spectral force
E=(1/2.*k.*D.*D); % spectral energy

for j2=1:length(T)
    wn=omega_n(j2);
    k=K(j2);
    [u2,v2]=function3(xi,m,k,P4,dt2,wn,t2);
    D2(j2)=max(abs(u2)); %spectral displacement of second data
end

V2=omega_n.*D2; %spectral velocity of second data
A2=omega_n.*omega_n.*D2;%second spectral acceleration
F2=m.*A2;
E2=(1/2.*k.*D2.*D2);%second spectral energy

for j3=1:length(T)
    wn=omega_n(j3);
    k=K(j3);
    [u3,v3]=function4(xi,m,k,P6,dt3,wn,t3);
    D3(j3)=max(abs(u3)); %spectral displacement of second data
end

V3=omega_n.*D3; %spectral velocity of third data
A3=omega_n.*omega_n.*D3;%third spectral acceleration
F3=m.*A3;
E3=(1/2.*k.*D3.*D3);%third spectral energy

for j4=1:length(T)
    wn=omega_n(j4);
    k=K(j4);
    [u4,v4]=function5(xi,m,k,P8,dt4,wn,t4);
    D4(j4)=max(abs(u4)); %spectral displacement of second data
end

V4=omega_n.*D4; %spectral velocity of third data
A4=omega_n.*omega_n.*D4;%third spectral acceleration
F4=m.*A4;
E4=(1/2.*k.*D4.*D4);%third spectral energy

%Plot response-----------------------------------------------
%------------------------------------------------------
%Energy plot-------------------------------------------------
figure(5);
plot(T,E,'b',T,E2,'r',T,E3,'k',T,E4,'g','linewidth',1)

%title and labels
title('Energy Plot')
xlabel('Time (s)')
ylabel('Energy (J)')

legend('1st test @200mm','2nd test @400mm','3rd test @500mm','4th test @600mm')
%Velocity plot-----------------------------------------
```

```
figure(6);
plot(T,V,'b',T,V2,'r',T,V3,'k',T,V4,'g','linewidth',1)
title('Velocity Plot')
xlabel('Time (s)')
ylabel('Velocity (m/s)')
legend('1st test @200mm','2nd test @400mm','3rd test @500mm','4th test @600mm')
%Force plot-------------------------------------------------
figure(7);
plot(T,F,'b',T,F2,'r',T,F3,'k',T,F4,'g','linewidth',1)
title('Force-time Plot')
xlabel('Time (s)')
ylabel('Force (N)')
legend('1st test @200mm','2nd test @400mm','3rd test @500mm','4th test @600mm')
%Displacement plot-----------------------------------------
figure(8);
plot(T,D,'b',T,D2,'r',T,D3,'k',T,D4,'g','linewidth',1)
title('Displacement Plot')
xlabel('Time (s)')
ylabel('Displacement (mm)')
legend('1st test @200mm','2nd test @400mm','3rd test @500mm','4th test @600mm')
%-------------------------Maximum values---------------------------------
%Maximum force values-----------------
[pkmax1,indmax1]=findpeaks(F,T);
[pkmax2,indmax2]=findpeaks(F2,T);
[pkmax3,indmax3]=findpeaks(F3,T);
[pkmax4,indmax4]=findpeaks(F4,T);
%Maximum Energy values--------------------------------
[pkmaxE,indmaxE]=findpeaks(E,T);
[pkmaxE2,indmaxE2]=findpeaks(E2,T);
[pkmaxE3,indmaxE3]=findpeaks(E3,T);
[pkmaxE4,indmaxE4]=findpeaks(E4,T);
%Maximum Velocity values-----------------------------
[pkmaxV,indmaxV]=findpeaks(V,T);
[pkmaxV2,indmaxV2]=findpeaks(V2,T);
[pkmaxV3,indmaxV3]=findpeaks(V3,T);
[pkmaxV4,indmaxV4]=findpeaks(V4,T);
%Maximum Displacement values---------------------------
[pkmaxD,indmaxD]=findpeaks(D,T);
[pkmaxD2,indmaxD2]=findpeaks(D2,T);
[pkmaxD3,indmaxD3]=findpeaks(D3,T);
[pkmaxD4,indmaxD4]=findpeaks(D4,T);
```


Published with MATLAB® R2018b

```
function[u,v]=function2(xi,m,k,P2,dt,wn,t)
wd=wn*sqrt(1-xi^2); %xi as beta, wn as natural frwquency
sq=sqrt(1-xi^2);
ep=exp(-xi*wn*dt);%dt as delta t_i
si=sin(wd*dt);
co=cos(wd*dt);
%si and co used as avervaiation of sine and cosine functions
A=ep*(xi/sq*si+co);%A = a_{11}
B=ep*(1/wd*si);    %B = a_{12}
C=1/k*(2*xi)/(wn*dt)+ep*(((1-2*xi^2)/(wd*dt)-xi/sq)*si-(1+2*xi/
(wn*dt))*co);%C = a_{21}
D=1/k*(1-2*xi/(wn*dt))+ep*((2*xi^2-1)/(wd*dt)*si+(2*xi/(wn*dt)*co));%D
 = a_{22}
Ap=-ep*(wn/sq*si); %Ap = b_{11}
Bp=ep*(co-xi/sq*si); %Bp = b_{12}
Cp=1/k*(-1/dt+ep*((wn/sq+xi/(dt*sq)))*si+1/dt*co); %Cp = b_{21}
Dp=1/(k*dt)*(1-ep*(xi/sq*si+co)); % Dp = b_{22}

u=zeros(length(P2),1);
v=zeros(length(P2),1);
%initial conditions
u0=0;v0=0;
u(1)=u0;
v(1)=v0;
for i=1;length(P2)-1;
    u(i+1)=A*u(i)+B*v(i)+C*(-m*P2(i))+D*(-m*P2(i+1));
    v(i+1)=Ap*u(i)+Bp*v(i)+Cp*(-m*P2(i))+Dp*(-m*P2(i+1));
end
end
```

Published with MATLAB® R2018b

```
function[u2,v2]=function3(xi,m,k,P4,dt2,wn,t2)
wd=wn*sqrt(1-xi^2); %xi as beta, wn as natural frwquency
sq=sqrt(1-xi^2);
ep=exp(-xi*wn*dt2);%dt as delta t_i
si=sin(wd*dt2);
co=cos(wd*dt2);
%si and co used as avervaiation of sine and cosine functions
A=ep*(xi/sq*si+co);%A = a_{11}
B=ep*(1/wd*si);    %B = a_{12}
C=1/k*(2*xi)/(wn*dt2)+ep*(((1-2*xi^2)/(wd*dt2)-xi/sq)*si-(1+2*xi/(wn*dt2))*co);%C = a_{21}
D=1/k*(1-2*xi/(wn*dt2))+ep*((2*xi^2-1)/(wd*dt2)*si+(2*xi/(wn*dt2)*co));%D = a_{22}
Ap=-ep*(wn/sq*si); %Ap = b_{11}
Bp=ep*(co-xi/sq*si); %Bp = b_{12}
Cp=1/k*(-1/dt2+ep*((wn/sq+xi/(dt2*sq)))*si+1/dt2*co); %Cp = b_{21}
Dp=1/(k*dt2)*(1-ep*(xi/sq*si+co)); % Dp = b_{22}

u2=zeros(length(P4),1);
v2=zeros(length(P4),1);
%initial conditions
u0=0;v0=0;
u2(1)=u0;
v2(1)=v0;
for i2=1;length(P4)-1;
    u2(i2+1)=A*u2(i2)+B*v2(i2)+C*(-m*P4(i2))+D*(-m*P4(i2+1));
    v2(i2+1)=Ap*u2(i2)+Bp*v2(i2)+Cp*(-m*P4(i2))+Dp*(-m*P4(i2+1));
end
```

Published with MATLAB® R2018b

```
function[u3,v3]=function4(xi,m,k,P6,dt3,wn,t3)
wd=wn*sqrt(1-xi^2); %xi as beta, wn as natural frwquency
sq=sqrt(1-xi^2);
ep=exp(-xi*wn*dt3);%dt as delta t_i
si=sin(wd*dt3);
co=cos(wd*dt3);
%si and co used as avervaiation of sine and cosine functions
A=ep*(xi/sq*si+co);%A = a_{11}
B=ep*(1/wd*si);    %B = a_{12}
C=1/k*(2*xi)/(wn*dt3)+ep*(((1-2*xi^2)/(wd*dt3)-xi/sq)*si-(1+2*xi/(wn*dt3))*co);%C = a_{21}
D=1/k*(1-2*xi/(wn*dt3))+ep*((2*xi^2-1)/(wd*dt3)*si+(2*xi/(wn*dt3)*co));%D = a_{22}
Ap=-ep*(wn/sq*si); %Ap = b_{11}
Bp=ep*(co-xi/sq*si); %Bp = b_{12}
Cp=1/k*(-1/dt3+ep*((wn/sq+xi/(dt3*sq)))*si+1/dt3*co); %Cp = b_{21}
Dp=1/(k*dt3)*(1-ep*(xi/sq*si+co)); % Dp = b_{22}

u3=zeros(length(P6),1);
v3=zeros(length(P6),1);
%initial conditions
u0=0;v0=0;
u3(1)=u0;
v3(1)=v0;
for i3=1;length(P6)-1;
    u3(i3+1)=A*u3(i3)+B*v3(i3)+C*(-m*P6(i3))+D*(-m*P6(i3+1));
    v3(i3+1)=Ap*u3(i3)+Bp*v3(i3)+Cp*(-m*P6(i3))+Dp*(-m*P6(i3+1));
end
```

Published with MATLAB® R2018b

```
function[u4,v4]=function5(xi,m,k,Y8,dt4,wn,t4)
wd=wn*sqrt(1-xi^2); %xi as beta, wn as natural frwquency
sq=sqrt(1-xi^2);
ep=exp(-xi*wn*dt4);%dt as delta t_i
si=sin(wd*dt4);
co=cos(wd*dt4);
%si and co used as avervaiation of sine and cosine functions
A=ep*(xi/sq*si+co);%A = a_{11}
B=ep*(1/wd*si);    %B = a_{12}
C=1/k*(2*xi)/(wn*dt4)+ep*(((1-2*xi^2)/(wd*dt4)-xi/sq)*si-(1+2*xi/(wn*dt4))*co);%C = a_{21}
D=1/k*(1-2*xi/(wn*dt4))+ep*((2*xi^2-1)/(wd*dt4)*si+(2*xi/(wn*dt4)*co));%D = a_{22}
Ap=-ep*(wn/sq*si); %Ap = b_{11}
Bp=ep*(co-xi/sq*si); %Bp = b_{12}
Cp=1/k*(-1/dt4+ep*((wn/sq+xi/(dt4*sq)))*si+1/dt4*co); %Cp = b_{21}
Dp=1/(k*dt4)*(1-ep*(xi/sq*si+co)); % Dp = b_{22}

u4=zeros(length(Y8),1);
v4=zeros(length(Y8),1);
%initial conditions
u0=0;v0=0;
u4(1)=u0;
v4(1)=v0;
for i4=1;length(Y8)-1;
    u4(i4+1)=A*u4(i4)+B*v4(i4)+C*(-m*Y8(i4))+D*(-m*Y8(i4+1));
    v4(i4+1)=Ap*u4(i4)+Bp*v4(i4)+Cp*(-m*Y8(i4))+Dp*(-m*Y8(i4+1));
end
```

Published with MATLAB® R2018b

Appendix D

Derivation of Equations

D.1 Test specimen design calculations

Theoretical reduction in strength

In general, the total energy in the system is assumed to be expressed as;

$$E_I = W_1(D_e) + W_2(V_d) + W_{loss} \tag{D.1}$$

Where, $W_1(D_e)$ = Energy associated with the degree of damage. $W_2(V_d)$ = Energy associated with spreading the damaged zone. W_{loss} = Energy attributed to sound, heat and vibration.

Although W_{loss}, accounts for some energy, it cannot be easily determined and therefore has been taken to be negligible in this analysis.

It is reasonable to assume that:

$$W_{ds} = W_{us} - f(W1) \tag{D.2}$$

Where, W_{ds}, = Damaged Toughness Property, W_{us},= Undamaged Toughness Property

Because the toughness of the damaged specimen is recognized to be lower than that of the undamaged. Also, the mechanical properties of the material are assumed to be degraded with the damage caused by impact, and it must somehow relate to some kind of measure to characterize the degree of damage. Hence

$$W_1 = K_1(W_{us} - W_{ds}) \tag{D.3}$$

Where K_1 is a constant

Most assumptions inferred that the damage can be taken to be uniform through the thickness of the plate, then the volume, V_d, over which the damage is spread can reasonably be characterized by a damage area, A_d, in the plane of the specimen. The energy dissipation, W_2, can therefore be written as

$$W_2 = W_2(A_d) \tag{D.4}$$

As a result, by assuming $W_{loss} = 0$, and combining Equations (D.3) and (D.4) and substitute in (D.1), the new energy balance equation can be expressed as:

$$E_I = K_1(W_{us} - W_{de}) + W_2(A_d) \tag{D.5}$$

Equation (D.5) is the general dissipative equation, and the proportion that each of modes takes, is not necessarily constant over the entire range of the impact (striking) velocities.

Considering the limiting cases, i.e. V_S(striking velocity)=0 & V_S=V_P(perforation velocity);

@ $V_S = 0 \longrightarrow$ No damage $\longrightarrow A_d = 0$ hence $W_2(A_d) = 0$, and $W_{us} = W_{ds}$, since $E_1 = 0$

@ $V_S = V_P$ =Perforation velocity

hence a hole is produced with negligible surrounding damage. Therefore, a specimen

the same width as the damage would have no residual strength
Thus, $W_{us} = 0$ and Equation (D.5) becomes:

$$E_{IP} = K_1 (W_{ds}) + W_2 (A_{dp}) \tag{D.6}$$

where,E_{IP} = Imparted kinetic energy associated with the perforation velocity, $W_2(A_{dp})$= Energy dissipated over the damage area of the size A_{dp}

The two unknowns of Equation (D.5), K and $W_2(A_d)$, can be determined by firstly assuming that the impactor striking velocity is very low. Therefore the damage area size, A_d, is relatively small and comparable to the contact area.Thus, in comparison with the energy causing damage to the material, the associated energy, $W_2(A_d)$,can be neglected. The value of the constant K, for each material can then be evaluated by rearranging Equation(D.5):

$$K_1 = \frac{E_I}{W_{us} - W_{ds}} \tag{D.7}$$

Secondly, knowing K_1, rearrange Equation (D.5) to obtain $W_2(A_d)$;

$$W_2(A_d) = E_I - K_1(W_{us} - W_{ds}) \tag{D.8}$$

By loading the specimens up to failure, and measuring the corresponding areas under load extension curves, the values for toughness properties, W_{us} & W_{ds}, can be determined. The right hand side of Equation (D.8) can be acquired for each known striking velocity, that can be plotted against the damaged area measured at the corresponding V_s. Thus $W_2(A_d)$ can be evaluated. Equation(D.8) can therefore be rewritten as follows to predict the damaged specimen property, W_d:

$K_1(W_{us} - W_{ds}) = E_I - W_2(A_d)$

$W_{us} - W_{ds} = \frac{1}{K_1}(E_I - W_2(A_d))$, Therefore;

$$W_{us} = W_{ds} - \frac{1}{K_1}(E_I - W_2(A_d)) \tag{D.9}$$

The amount of energy absorbed increases so does the damage area and in turn so does the reduction in both strength and stiffness properties of the material. Hence the analysis will be tackled by utilising the principles of Linear Elastic Fracture Mechanics (LEFM).

In accordance to LEFM principles, let us consider a specimen of isotropic material with a slit of length 2b. The energy release rate, G_I maybe expressed as,

$$G_I = \frac{1 - v^2}{E}\pi {K_I}^2 \tag{D.10}$$

where K_I = Stress Intensity Factor and is given by:

$$K_I = \sigma\,(\pi a)^{1/2} \tag{D.11}$$

For critical energy release rate, G_{IC}, combine equations D.10 and D.11:

$$G_I = \frac{1 - v^2}{E}\pi\left(\sigma^2 \pi a\right) \longrightarrow G_{IC} = BaW_C \tag{D.12}$$

Where $B = Constant$, W_c =Strain energy stored in the material under the load-extension curve (work done to break the specimen at maximum load causing incipient crack growth)

An idealized undamaged specimen can be modeled by introducing a flaw of dimension $2a_o$ to the specimen such that the area under the Load-Extension curve for the unflawed specimen will be the same as the energy (or work done) to cause failure.

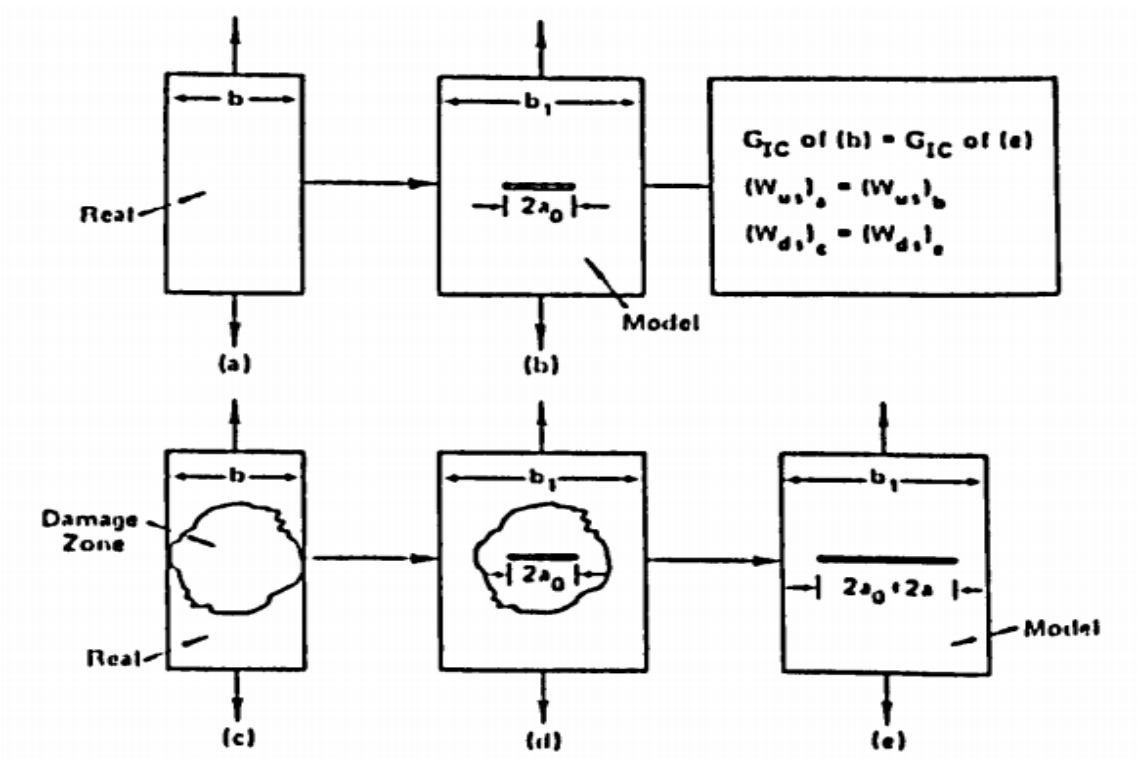

Figure D.1: Schematic Modelling in Accordance with the Principles of LEFM for Undamaged and Damaged Specimens.

$$G_{IC} = Ba_oW_{us} \tag{D.13}$$

Similarly, the impacted specimen may be presented by a crack (or flaw) of $2(a+a_o)$:

$$G_{IC} = B(a + a_o)W_{ds} \tag{D.14}$$

As schematically shown in Figure D.1, the microscopic effects of micro-flaws are therefore neglected and the problem is considered at the macroscopic level treating the damage as a continuum.

From Equation (D.11), the critical stress intensity factor, K_{IC}, for the above idealization and the associated concepts can be obtained as

$$K_{IC} = \sigma_{us} \left(\pi a_o\right)^{1/2} \tag{D.15}$$

and

$$K_{IC} = \sigma_{ds} \left[\pi(a_o + a)\right]^{1/2} \tag{D.16}$$

where, σ_{us} = Maximum applied stress in the undamaged specimen. And σ_{ds}= Maximum applied stress in the damaged specimen

Equate and simplify equations D.15 and D.16:

$$\frac{\sigma_{ds}}{\sigma_{us}} = \left(\frac{a_o}{a_o + a}\right)^{1/2} \tag{D.17}$$

Also equate equation D.13 and D.14 and simplify:

$$\left(\frac{W_{ds}}{W_{us}}\right)^{1/2} = \left(\frac{a_o}{a_o + a}\right)^{1/2} \tag{D.18}$$

Equating equations D.17 and D.18

$$\sigma_{ds} = \sigma_{us} \left(\frac{W_{ds}}{W_{us}}\right)^{1/2} \tag{D.19}$$

But from equation D.9

$$\frac{W_{ds}}{W_{us}} = 1 - \frac{1}{K_I W_{us}} \left[E_I - W_2(A_d)\right] \tag{D.20}$$

Substituting equation D.20 into D.19

$$\sigma_{ds} = \sigma_{us} \left[1 - \frac{1}{K_I W_{us}} \left[E_I - W_2(A_d)\right]\right]^{1/2} \tag{D.21}$$

Hence, knowing the imparted energy (E_I), tensile strength, constant K_1, and $W_2(A_d)$ the residual strength of an impacted specimen maybe evaluated.

Theoretical Reduction in Stiffness

It is important to distinguish *stiffness*, which is a measure of the load needed to induce a given deformation in the material, from the *strength*, which usually refers to the material's resistance to failure by fracture or excessive deformation[9].

Theoretically, the material stiffness (Young's Modulus) can also be evaluated provided a relationship for Load-Extension is obtained:

$$P = \Psi(x) \tag{D.22}$$

Converting equation D.22 to Stress-Strain relationship, where Ψ is the stiffness in N/m

$$\sigma = \Psi(\epsilon) \tag{D.23}$$

Differentiating equation (D.23) with respect to "E" and inserting zero strain into the resulting equation:

$$\frac{d\sigma}{d\epsilon} = \frac{d}{d\epsilon}\Psi(\epsilon) \longleftrightarrow \frac{d(E\epsilon)}{d\epsilon} = \frac{d}{d\epsilon}\Psi(\epsilon) \tag{D.24}$$

$$E = \frac{d\Psi(\epsilon)}{d\epsilon} = \frac{d\Psi(0)}{d\epsilon} \tag{D.25}$$

Experimentally, the following Load/Extension relationship[64] can be evaluated by:

$$P = P_m \left[1 - \left(1 - \frac{x}{x_m}\right)^{3/2}\right] \tag{D.26}$$

Equation(D.26) may also be presented as:

$$\sigma = \sigma_m \left[1 - \left(1 - \frac{\epsilon}{\epsilon_m}^{3/2}\right)\right] \tag{D.27}$$

But $E = \frac{d(\sigma)}{d\epsilon}$, and differentiating equation D.27

$$E = \frac{d(\sigma)}{d\epsilon} = 0 - \frac{3}{2}\left(1 - \frac{\epsilon}{\epsilon_m}\right)^{1/2} - \frac{1}{\epsilon_m} = \frac{3}{2}\frac{\sigma_m}{\epsilon_m}\left(1 - \frac{\epsilon}{\epsilon_m}\right)^{1/2} \tag{D.28}$$

At $\epsilon = 0$

$$\boxed{E = \tfrac{3}{2}\tfrac{\sigma_m}{\epsilon_m}} \tag{D.29}$$

where, P_m =maximum peak force, σ_m =maximum stress, ϵ_m =maximum strain The material toughness will be theoretically computed, if the area under the Load Extension curve is evaluated (provided the end points of the curve are known). Toughness of damaged specimen is given as:

$$W_{ds} = \int_0^{\epsilon_m} \left[\sigma_m - \sigma_m \left(1 - \frac{\epsilon}{\epsilon_m} \right)^{3/2} \right] d\epsilon \tag{D.30}$$

$$W_{ds} = \sigma_m \epsilon_m \left[\frac{2}{5} \left(1 - \frac{\epsilon_m}{\epsilon_m} \right)^{5/2} - \left(1 - \frac{\epsilon_m}{\epsilon_m} \right) - \frac{2}{5} + 1 \right] \tag{D.31}$$

$$W_{ds} = \sigma_m \epsilon_m \left[1 - \frac{2}{5} \right] \tag{D.32}$$

$$\Rightarrow \quad \boxed{W_{ds} = \tfrac{3}{5} \sigma_m \epsilon_m} \tag{D.33}$$

D.2 Specimen Support Plate Design Calculations

l The thickness of the plate used in manufacturing is 6 mm.

Givens: $m = 5.5kg, g = 9.81m/s^2, h = 0.62m, t = 6mm, E = 210GPa, v = 0.3$

$$e = \frac{1}{2} K y^2 = mgh \tag{D.34}$$

$$K = \frac{2mgh}{y^2} = \frac{2 \times 5.5kg \times 9.81m/s^2 \times 0.62m}{y^2} = \frac{66.91}{y^2} \tag{D.35}$$

Flexural rigidity of plate D, given as

$$D = \frac{Et^3}{12(1 - v^2)} = 4.153kNm \tag{D.36}$$

Where $m, e, E, K, y, h, D, t, v$ are impactor mass, energy, elastic modulus, spring constant, deflection, release height, plate rigidity, thickness of plate and poisson's ratio, respectively.

From Hooke's law and considering distributed force (q) per unit area;

$$F = Ky = qab \tag{D.37}$$

Where a and b are dimensions of the plate with $a = 120mm, b = 180mm$
The load q is due to the impacting mass dropped from a height of 0.62 m which is equal to the potential energy which is given as;

$$Force(F) \times thichness(t) = mgh \tag{D.38}$$

$$F = \frac{mgh}{t} = \frac{5.5kg \times 9.81m/s^2 \times 0.62m}{0.006m} = 5.6kN \tag{D.39}$$

The load q on the plate is then given as;

$$q = \frac{F}{ab} = \frac{5.6kN}{0.12 \times 0.18m^2} = 258kN \tag{D.40}$$

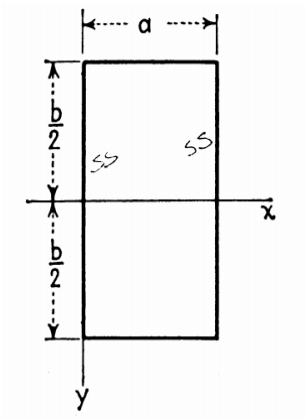

Figure D.2: Boundary condition of the plate

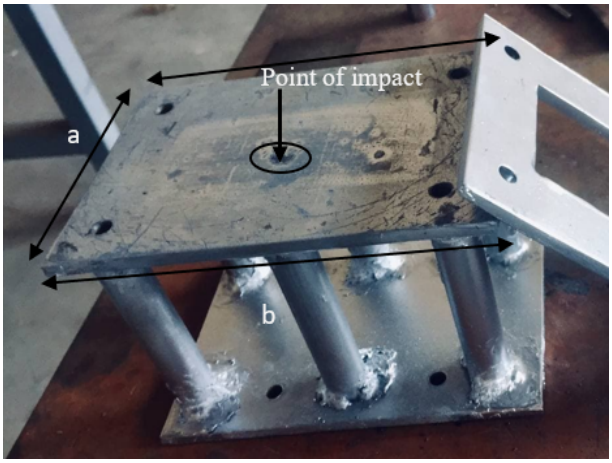

Figure D.3: Point of impact on fixed rectangular plate

For a fixed rectangular plate, bending moment, deflection and stress given in the reference of Timoshenko [10], theory of plates and shells;

Deflection on the surface of the plate is given as;

$$y = \frac{4qa^4}{\pi^5 D} \sum_{m=1,3,5...}^{\infty} \frac{1}{m^5}(1 - \frac{\alpha_m \tanh \alpha_m + 2}{2\cosh \alpha_m} \cosh \frac{2\alpha_m y}{b} + \frac{\alpha_m}{2\cosh \alpha_m} \frac{2y}{b} \sinh \frac{2\alpha_m y}{b}) \sin \frac{m\pi x}{a} \tag{D.41}$$

The maximum deflection is obtained at the middle of the plate $(x = \frac{a}{2}, y = 0)$,where

$$y_{max} = \frac{4qa^4}{\pi^5 D} \sum_{m=1,3,5..}^{\infty} \frac{(-1)^{(m-1)/2}}{m^5}(1 - \frac{\alpha_m \tanh \alpha_m + 2}{2\cosh \alpha_m}) \tag{D.42}$$

The maximum deflection of the expression D.42 can be represented in the form

$$y_{max} = \alpha \frac{qa^4}{D} \tag{D.43}$$

And the moments can be represented in the form [10];

$$(M_x)_{y=0} = \acute{\beta} qa^2, (M_y)_{y=0} = \acute{\beta_1} qa^2 \tag{D.44}$$

Where α is a numerical factor depending on the ratio b/a of the sides of the plate.

The bending moment acting along the middle line $x = a/2$ given as;

$$(M_x)_{x=a/2} = \beta'' qa^2, (M_y)_{x=a/2} = {\beta_1}'' qa^2 \tag{D.45}$$

The maximum values of these moments (equation D.44 and D.45);

$$(M_x)_{max} = \beta qa^2, (M_y)_{max} = \beta_1 qa^2 \tag{D.46}$$

at the center of the plate $(x = a/2, y = 0)$ and the corresponding factor α, β and β_1 are given in the Table below.

b/a	$w_{max} = \alpha \frac{qa^4}{D}$ α	$(M_x)_{max} = \beta qa^2$ β	$(M_y)_{max} = \beta_1 qa^2$ β_1	$(Q_x)_{max} = \gamma qa$ γ	$(Q_y)_{max} = \gamma_1 qa$ γ_1	$(V_x)_{max} = \delta qa$ δ	$(V_y)_{max} = \delta_1 qa$ δ_1	$R = nqa^2$ n
1.0	0.00406	0.0479	0.0479	0.338	0.338	0.420	0.420	0.065
1.1	0.00485	0.0554	0.0493	0.360	0.347	0.440	0.440	0.070
1.2	0.00564	0.0627	0.0501	0.380	0.353	0.455	0.453	0.074
1.3	0.00638	0.0694	0.0503	0.397	0.357	0.468	0.464	0.079
1.4	0.00705	0.0755	0.0502	0.411	0.361	0.478	0.471	0.083
1.5	0.00772	0.0812	0.0498	0.424	0.363	0.486	0.480	0.085
1.6	0.00830	0.0862	0.0492	0.435	0.365	0.491	0.485	0.086
1.7	0.00883	0.0908	0.0486	0.444	0.367	0.496	0.488	0.088
1.8	0.00931	0.0948	0.0479	0.452	0.368	0.499	0.491	0.090
1.9	0.00974	0.0985	0.0471	0.459	0.369	0.502	0.494	0.091
2.0	0.01013	0.1017	0.0464	0.465	0.370	0.503	0.496	0.092
3.0	0.01223	0.1189	0.0406	0.493	0.372	0.505	0.498	0.093
4.0	0.01282	0.1235	0.0384	0.498	0.372	0.502	0.500	0.094
5.0	0.01297	0.1246	0.0375	0.500	0.372	0.501	0.500	0.095
∞	0.01302	0.1250	0.0375	0.500	0.372	0.500	0.500	0.095

For our case $b/a = \frac{180}{120} = 1.5$, based on **b/a** value and numerical values given in Table D.1, the maximum deflection (y_{max}), maximum moments (($M_x)_{max}$ and $(M_y)_{max}$), maximum shear forces (($Q_x)_{max}$ and $(Q_y)_{max}$) and maximum reaction forces (($V_x)_{max}$ and $(V_y)_{max}$) can be calculated. Table D.1 shows the result of these values.

Table D.1: Results of uniformly loaded rectangular plate after Timoshenko and Woinowsky-Krieger[10]

b/a	y_{max}(mm)	$(M_x)_{max}$	$(M_y)_{max}$	$(Q_x)_{max}$	$(Q_y)_{max}$	$(V_x)_{max}$	$(V_y)_{max}$	R
1.5	0.0994	301.7	185	13,127	11,238	15,047	14,861	315.8

The maximum deflection expected on this rectangular plate is 0.0994 mm.

Stress on the plate for a concentrated force acting can be calculated as[10];

$$\sigma_x = \frac{6M_y}{at^2} = \frac{6 \times 185}{0.12 \times (0.006)^2} = 257MPa \tag{D.47}$$

$$\sigma_y = \frac{6M_x}{at^2} = \frac{6 \times 301.7}{0.12 \times (0.006)^2} = 419MPa \tag{D.48}$$

Let $\sigma_x = \sigma_A$, $\sigma_y = \sigma_B$ and $\sigma_3 = 0$, the von Mises stress ($\sigma^{'}$)

$$\sigma^{'} = \left(\sigma_A^2 - \sigma_A\sigma_B + \sigma_B^2\right)^{1/2} = \left(257^2 - 257 \times 419 + 419^2\right)^{1/2} = 366MPa \tag{D.49}$$